Interaction between p85 and Rab5 in the presence and absence of phosphorylated PDGFR peptide

A Thesis submitted to the College of Graduate Studies and Research in partial fulfillment of the requirements for a Masters of Science Degree in the Department of Biochemistry

University of Saskatchewan

Saskatoon

By:

Cody Nils Bergman

January, 2012

Permission to Use:

In presenting this thesis in partial fulfillment of the requirements for a Postgraduate degree from the University of Saskatchewan, I agree that the Libraries of this University may make it freely available for inspection. I further agree that permission for copying of this thesis in any manner, in whole or in part, for scholarly purposes may be granted by the professor or professors who supervised my thesis work or, in their absence, by the Head of the Department or the Dean of the College under which this thesis work was done. It is understood that any copying or publication or use of this thesis or parts thereof for financial gain shall not be allowed without my written permission. It is also understood that due recognition shall be given to me and to the University of Saskatchewan in any scholarly use which may be made of any materials in my thesis.

Requests for permission to copy or to make other use of materials in this thesis in whole or part should be addressed to:

Dr. Deborah H. Anderson
Cancer Research Unit
20 Campus Drive
University of Saskatchewan
Saskatoon, SK
S7N 4H4

Abstract

The adaptor subunit of phosphatidylinositol 3'-kinases (PI3K), p85, is involved in many different biological processes. Recent studies have shown that one of these functions is to serve as a GTPase activating protein (GAP) towards Rab5, a small monomeric G-protein. Rab5, like other G-proteins, can bind to either GDP or GTP *in vivo*, assuming its inactive and active form, respectively. The p85 protein has been shown to associate with both the nucleotide-bound and nucleotide-free states of Rab5. It has also been shown that p85 associates with activated, phosphorylated platelet-derived growth factor receptors (PDGFRs) via its two SH2 domains, and that upon binding there is a conformational change in the p85 protein which leads to a derepression of p110 kinase activity. The purpose of this study was to analyze if binding of the activated PDGFR peptides to p85 affects its Rab5GAP activity, as well as to measure the binding affinity of p85 towards Rab5 in each of its nucleotide-bound states. GAP assays were performed to measure the effect that peptide analogs of both the activated and inactivated PDGFR had on p85 Rab5GAP activity, while the binding affinity of p85 towards Rab5 was measured using surface plasmon resonance. The results of this study suggest that PDGFR peptides have no significant effect on p85 Rab5GAP activity. Furthermore, p85 appears to have a higher magnitude of binding to nucleotide-associated Rab5 proteins, than nucleotide-free Rab5 proteins. It also appears that p85 forms more stable complexes with Rab5-GTP than with Rab5-GDP. These results further support previous studies that show p85 to be an important regulator of Rab5-mediated endosomal fusion and show that this activity is not regulated by binding to the activated PDGFR itself.

Acknowledgements

I would like to thank my supervisor Dr. Anderson for her guidance, patience, and encouragement, and advice that she has provided for the past three years. I would also like to provide equal thanks to the members of my Advisory Committee, both past and present, Dr. Roesler, Dr. Khandelwal, Dr. Moore, and Dr. Pato. I would like to thank the College of Medicine and the Department of Biochemistry for financial support to myself as well as the Canadian Cancer Society for supporting this research within Dr. Anderson's laboratory. I would also like to thank all the members of the Anderson Lab, past and presence, and for the staff and students of the Saskatchewan Cancer Agency for their help, instruction, and friendship for these last three years. Finally, I would like to thank all my family and friends who, though they were incapable of staving off my eventual spiral into insanity, at least help mediate the process insofar as the consequences were not dire.

As per request of many friends and colleagues, I dedicate this work to all the brain cells lost in its making. They will surely be missed.

TABLE OF CONTENTS

LIST OF FIGURES

LIST OF ABBREVIATIONS

ABD	Adaptor binding domain, p85 binding domain
AEBSF	4-(2-Aminoethyl) benzenesulfonyl fluoride hydrochloride
BH	Breakpoint cluster region homology
BSA	Bovine serum albumin
DLS	Dynamic light scattering
DMEM	Dulbecco's Modified Eagle Medium
DTT	Dithiothreitol
EEA1	Early endosomal autoantigen 1
EDC	N-ethyl-N'-(dimethylaminopropyl) carbodiimide Hydrochloride
EDTA	Ethylenediaminetetraacetic acid
EGF	Epidermal growth factor
EGFR	Epidermal growth factor receptor
FBS	Fetal bovine serum
Fc1	Flowcell 1
Fc2	Flowcell 2
FPLC	Fast protein liquid chromatography
GAP	GTPase activating protein
GEF	Guanine nucleotide exchange factor
GDF	GDI-displacement factor
GDI	Guanosine nucleotide dissociation inhibitor
GDP	Guanosine diphosphate
GMP	Guanosine monophosphate
GNP	Guanine nucleotide phosphate
GST	Glutathione S-transferase
GTP	Guanosine triphosphate
HEPES	N-(d-hydroxyethyl) piperazine-N'-(2-ethanesulfonic acid)
HPLC	High-performance liquid chromatography
IPTG	Isopropyl β-D-thiogalactopyranoside
iSH2	InterSH2 Domain, p110 binding domain
LB	Luria-Bertani broth

LBA	Luria-Bertani broth plus ampicillin
MAP	Microtubule-associated proteins
NF	Nucleotide free
NHS	N-hydroxysuccinimide
NSF	N-ethylmaleimide sensitive factor
PBS	Phosphate buffered saline
PEI	Polyethylenimine
PDGF	Platelet-derived growth factor
PDGFR	Platelet-derived growth factor receptor
PDK1	Phosphoinositide-dependent protein kinase 1
PI3K	Phosphatidylinositol 3'-kinase
PI	Phosphatidylinositol
PI3P	Phosphatidylinositol 3'-phosphate
PI4P	Phosphatidylinositol 4-phosphate
$PI4,5P_2$	Phosphatidylinositol 4,5-bisphosphate
$PI3,4,5P_3$	Phosphatidylinositol 3,4,5-trisphosphate
RBD	Ras-binding domain
REP	Rab escort protein
RTK	Receptor tyrosine kinase
SDS	Sodium dodecyl sulfate
SDS-PAGE	SDS-polyacrylamide gel electrophoresis
SH2	Src homology 2
SH3	Src homology 3
SNARE	Soluble N-ethylmaleimide sensitive factor attachment receptor
SPR	Surface plasmon resonance
TEMED	N,N,N',N'-Tetra-methylethylenediamine
Tris-HCl	Tris(hydroxymethyl)aminomethane
TLC	Thin layer chromatography

1.0 Introduction

1.1 Signal Transduction Pathways

Signal transduction pathways are the primary means used by cells to respond to external stimuli and consist of numerous signalling molecules ranging from lipids to nucleic acids. These pathways allow cells to respond to a wide variety of signals, including hormones, ions, and gases (Schuller, 1991). Signal transduction pathways start at the plasma membrane, the interface between the cell and the outside world. On the membrane are a number of specialized receptors which respond to different extracellular stimuli. These receptors then transduce the information gathered from these external stimuli into the cell where they elicit a number of biochemical reactions to yield the appropriate cellular response.

In order to produce the strongest possible response to even a minimum stimulus, signal transduction pathways are typically amplified. This allows a small number of activated receptors to stimulate a sufficiently strong reaction from the cell. To this end, cells have evolved a means of having a relatively small number of signalling pathways activated by a wide variety of receptors. These form a complex system which can provide a number of unique signals from a limited number of signalling molecules (Citri and Yarden, 2006).

In order to yield such a wide range of responses from such a limited pool of signalling molecules, a means of differentiating external signals had to be developed in order to keep the cell responses clear. To this end, all cells have developed techniques to modify and sequester proteins in space and/or time as a means of regulating the cellular response. One of the most powerful methods cells use to specifically activate cell signalling molecules to specific tasks is through post-translational modifications. Post-translational modification occurs when proteins are chemically modified after the protein is translated from RNA. These modifications can alter the chemical properties, cellular localization, biological activity, or physical structure of the protein in question (Olsen *et al*., 2006; Yang and Seto, 2008).

One example of a post-translational modification used to regulate protein molecules is the phosphorylation amino acid residues by kinase enzymes. These phosphorylations can also be removed through the actions of phosphatase enzymes. (Burnett and Kennedy, 1954; Cozzone, 1988). These phosphorylations and dephosphorylations can either activate or deactivate the proteins in question or alter other properties such as binding functions or

localization (Olsen *et al*., 2006). Proteins are typically phosphorylated on one or more tyrosine, serine, or threonine residues. These phosphorylated residues can serve a number of roles including forming binding sites for specific protein binding domains. An example of this is the Src homology 2 (SH2) domain which binds to phosphorylated tyrosine and three to six additional amino acids adjacent to the phosphotyrosine residue (Bradshaw and Waksman, 2002; Grucza *et al*., 1999).

1.2 Receptor Tyrosine Kinases

Receptor tyrosine kinases (RTKs) are integral membrane cell surface receptors which are activated by extracellular signals. There are several subfamilies of RTKs which share many conserved domains, though with different affinities to different ligands (Zwick *et al*., 2001). What makes RTKs unique among cell surface receptors is that they, as the name suggests, have intrinsic protein tyrosine kinase activity when activated. All RTKs have a similar domain structure consisting of an extracellular ligand binding domain, a single α-helical transmembrane domain, and a cytoplasmic domain containing the intrinsic tyrosine kinase domain with enzymatic activity as well as phosphorylation sites (Ogiso *et al*., 2002; Pawson and Scott, 2005; Schlessinger, 2000) (Fig. 1.1). When a RTK binds its ligand, it undergoes a conformational change which allows it to dimerize (Biarc *et al*., 2011; Garrett *et al*., 1998; Ogiso *et al*., 2002). Once dimerized, the receptor undergoes an additional conformational change which induces the cross-phosphorylation (also known as *trans*-autophosphorylation**)** of the PDGFR monomers in their cytosolic domain (Ferguson, 2008). These phosphorylated tyrosine residues then serve as docking sites for proteins which are involved in further downstream signalling events.

There are many different types of RTKs expressed in human cells, two of which being the epidermal growth factor (EGF) receptor (EGFR) and the platelet-derived growth factor (PDGF) receptor (PDGFR) (Alvarez *et al*., 2006; Robinson *et al*., 2000). One of the signalling pathways that are activated by these receptors is the phosphatidylinositol 3'-kinase (PI3K)/Akt signalling pathway. This pathway is known to promote cell division and survival, as well as cell motility and invasion in cancer cells (Chin and Toker, 2009) (Fig. 1.2). The phosphorylated receptor recruits the PI3K complex via two of its phosphorylated tyrosine residues. Once bound to the activated receptor, PI3K can then phosphorylate phosphatidylino-

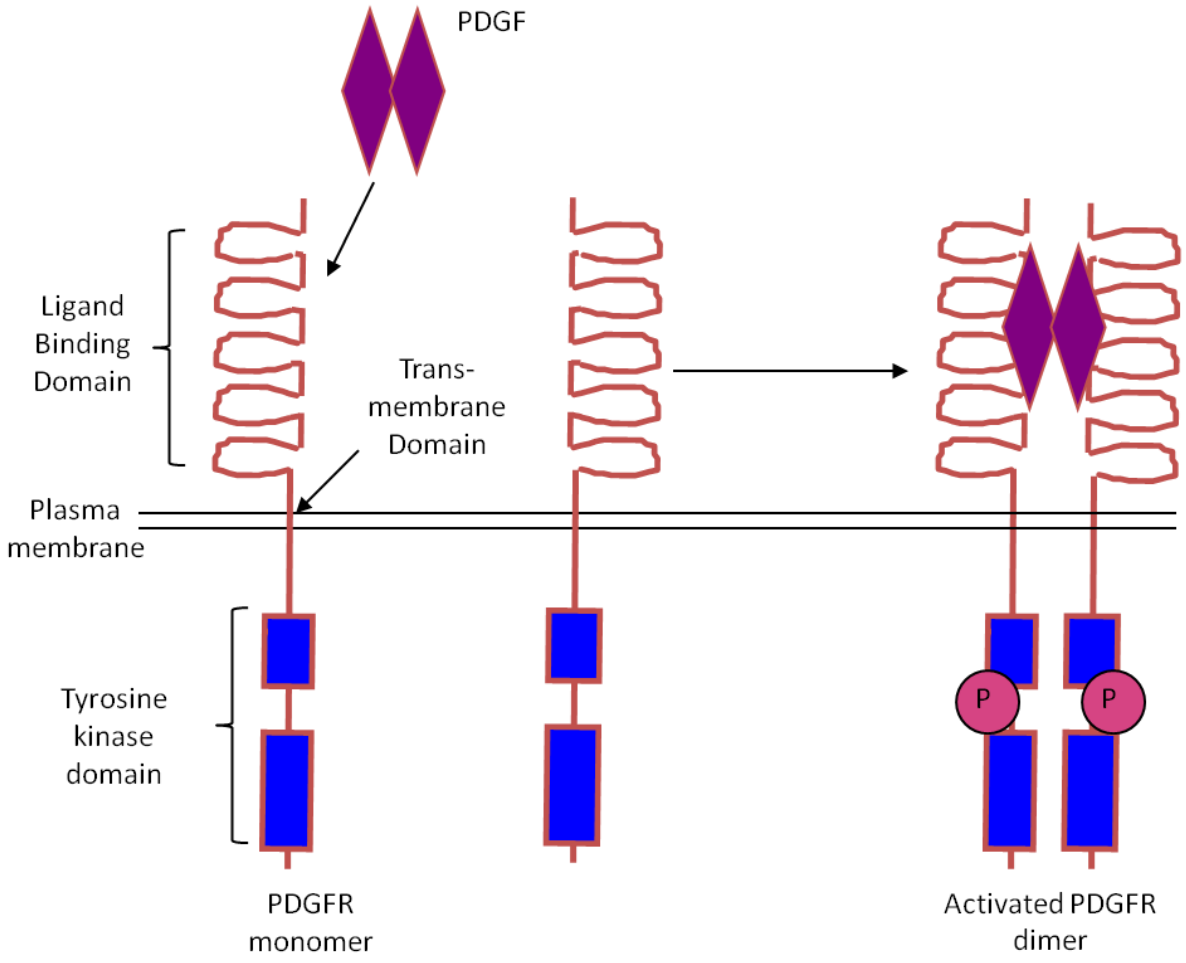

Figure 1.1 – Receptor tyrosine kinase activation. Receptor tyrosine kinases (RTKs) generally consist of an extracellular ligand binding domain, a transmembrane domain, and an intracellular tyrosine kinase domain which contains multiple phosphorylation sites. Upon binding their corresponding ligand to their extracellular binding domain, RTKs such as the platelet-derived growth factor receptor dimerize. This allows for autophosphorylation of the intracellular domain of the receptor.

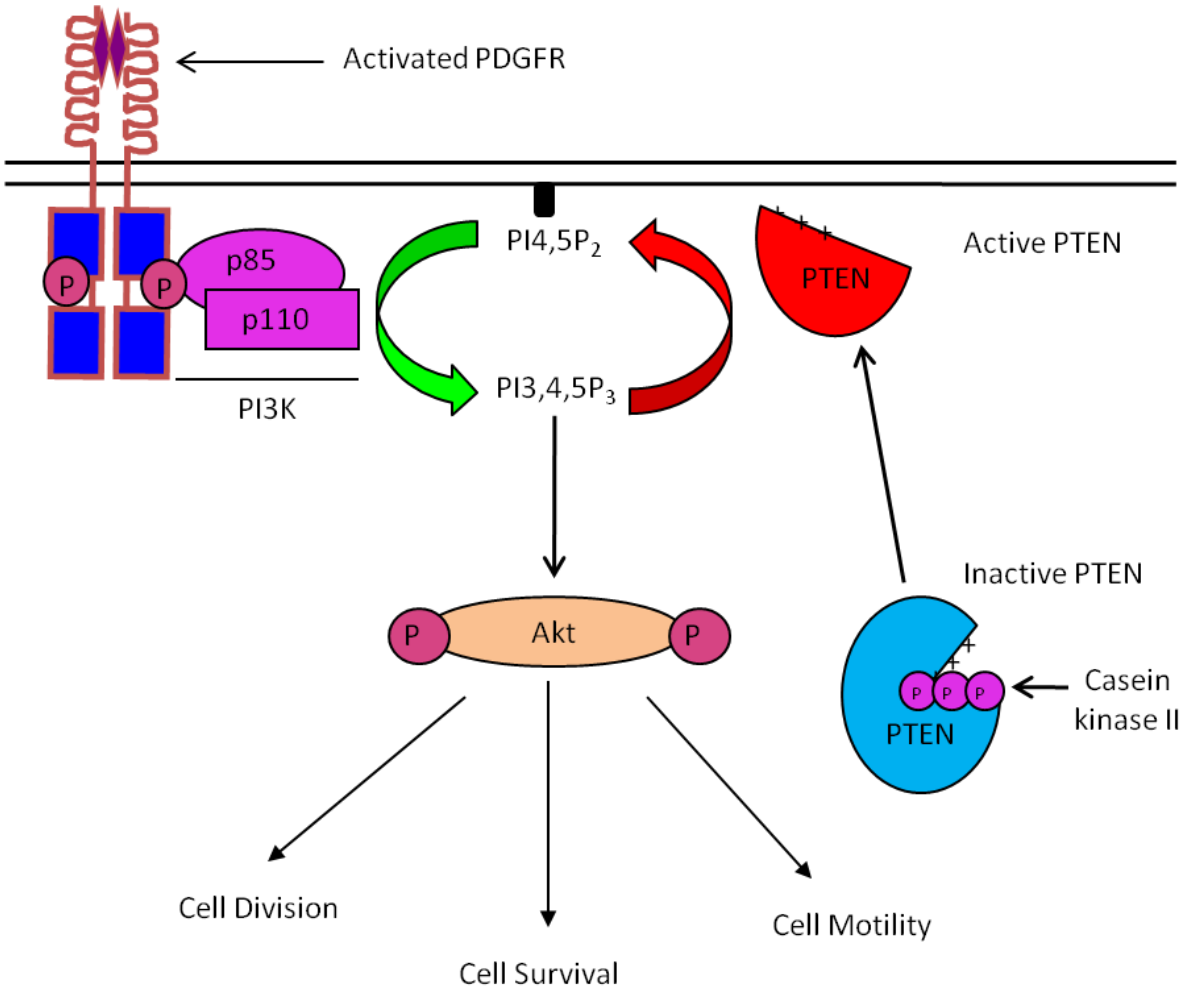

Figure 1.2 – PDGFR activates the PI3K/Akt signalling pathway, promoting cell division, survival, and motility. Upon PDGF stimulation, the PDGFR subunits dimerize which leads to autophosphorylation of tyrosine residues on the intracellular domains of the PDGFR subunits. The PI3K enzyme complex is recruited to the PDGFR via the SH2 domains in the p85 regulatory subunit binding to the phosphorylated tyrosine residues. When localized to the plasma membrane, p110 can phosphorylate $PI4,5P_2$ to produce $PI3,4,5P_3$, recruiting the serine/threonine kinase Akt which is involved in downstream signalling. $PI3,4,5P_3$ can then be deactivated by the phosphatase enzyme PTEN which is itself activated by dephosphorylation by an unknown phosphatase. This exposes positively charged residues on PTEN which allow it to associate with the plasma membrane. PTEN is then deactivated by phosphorylation by casein kinase II (Fruman *et al*., 1998; Ueki *et al*., 2002).

sitol 4,5-bisphosphate ($PI4,5P_2$) to phosphatidylinositol 3,4,5-trisphosphate ($PI3,4,5P_3$) which functions as a second messenger for 3-phosphoinositide dependent protein kinase-1 (PDPK1). This enzyme proceeds to phosphorylates the serine/threonine kinase Akt, which then activates a number of downstream proteins which promote anti-apoptotic signals (Fruman *et al*., 1998; Ueki *et al*., 2002).

1.3 Phosphatidylinositol 3'-kinase (PI3K)

PI3K belongs to an important enzyme superfamily which plays pivotal roles in metabolic and mitogenic signalling pathways. PI3K enzymes are lipid kinases and fall into three distinct classes, labelled Class I to III. Class I PI3Ks are heterodimers consisting of a catalytic subunit (p110) and a regulatory or adaptor subunit (p85). Class I PI3K can be further divided into Class IA and IB by sequence similarity and are the only PI3K enzymes activated in response to RTK activation (Carpenter and Cantley, 1996).

The catalytic subunit of Class IA PI3K enzymes consist of one of three isoforms of p110: p110α, β, and δ (Fig. 1.3A). Of these isoforms, p110α and p110β are expressed in all cells, while p110δ is primarily expressed in leukocytes (Arcaro *et al*., 2000; Fruman *et al*., 1998; Ueki *et al*., 2002). Of these three isoforms p110β and δ exhibit more primary sequence similarity towards each other than to p110α, though all three share a similar domain structure (Vanhaesebroeck and Waterfield, 1999) (Fig. 1.3A). All three isoforms contain an N-terminal adaptor protein binding domain (ABD; i.e., p85 binding domain), followed by a Ras-binding domain (RBD), a protein kinase-C-homology domain 2 (C2 domain) responsible for lipid binding, a helical domain, and a kinase domain (Zhao and Vogt, 2008).

Like p110, the regulatory or adaptor subunit of Class IA PI3K, p85, also has different isoforms (Fig. 1.3B). These consist of p85α as well as the splice variants p55α and p50α, (all encoded by the *Pik3r1* gene), the p85β (encoded by the *Pik3r2* gene), and the p55γ (encoded by the *Pik3r3* gene) (Fruman *et al*., 1998; Ueki *et al*., 2002). The p85 subunit of class IA PI3K acts to localize the catalytic subunit p110 to the plasma membrane in response to growth factor stimulation and activation of growth factor receptors such as the PDGFR (Engelman *et al*., 2006). When not bound to an activated growth factor receptor, p85 assumes a conformation which inhibits the lipid phosphorylation activity of p110, a repression which is relieved following binding to an activated RTK (Gearing, 2007; Yu *et al*., 1998).

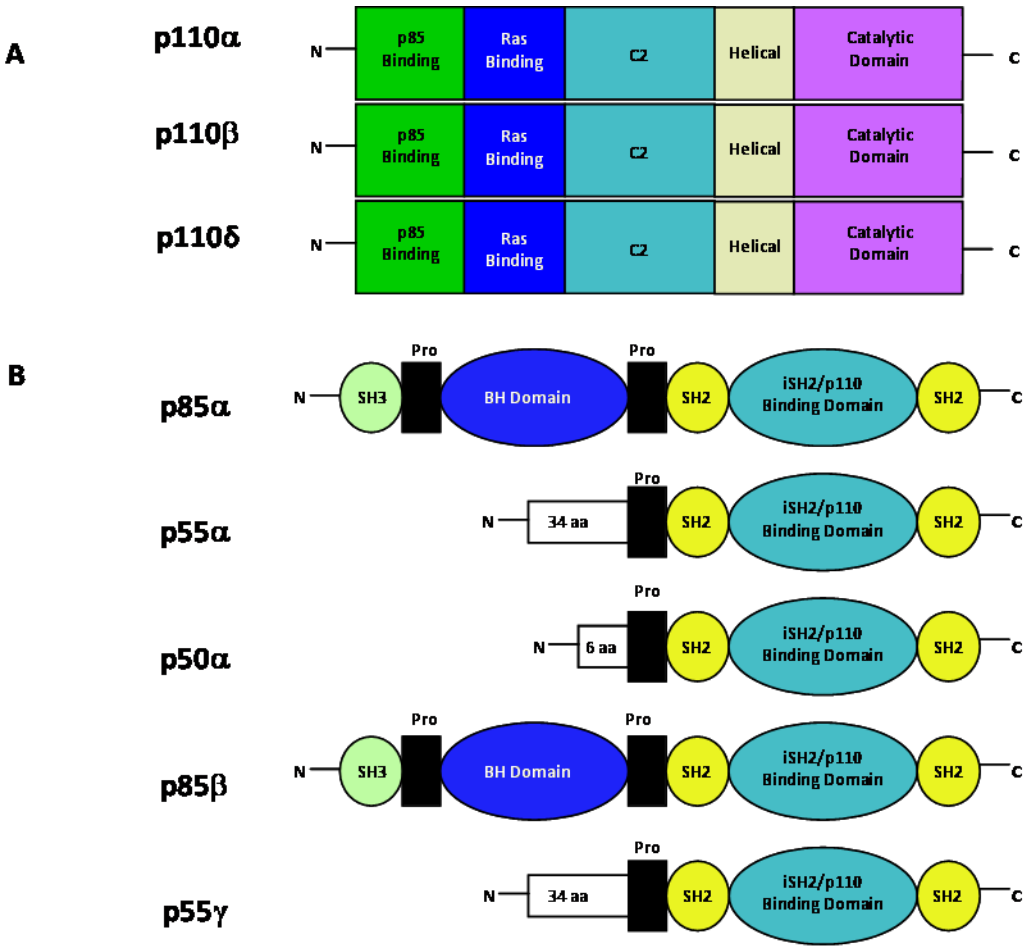

Figure 1.3 – Domain Structure of PI3K protein components. **A)** There are three different isoforms of the p110 catalytic subunit of Class IA PI3K: p110α, p110β, and p110δ. While all three have different primary sequences, all three of these isoforms have similar domain structures containing an adaptor protein binding domain (ABD), a Ras binding domain (RBD), a protein kinase-C-homology 2 (C2) domain, a helical domain, and a catalytic domain. There is 39% similarity between p110α and p110β, and 39% similarity between p110α and p110δ, and 56% similarity between p110β and p110δ. **B)** There are five isoforms of the p85 regulatory domain found in Class IA PI3K. The first three (p85α, p55α, and p50α) are formed from alternative splicing from the *Pik3r1* gene, while the others are obtained from the *Pik3r2* gene (p85β, 57.7% homology to p85α) or the *Pik3r3* gene (p55γ). The p85 protein contains several different domains in various combinations depending on the isoform: the SH3 binding domain, a breakpoint cluster region homology (BH) domain typically flanked by two proline-rich regions, a p110 binding domain (also known as the interSH2 or iSH2) which is flanked by two SH2 domains.

The p85 protein structure includes many protein-protein binding domains allowing it to bind to a variety of different partners. These domains consist of an N-terminal Src homology 3 (SH3) domain, and a breakpoint cluster region homology (BH) domain which is flanked by two proline rich regions. Following the second of the proline-rich regions are two SH2 domains, between which is the p110 binding domain (Fruman *et al*., 1998) (Fig. 1.3B).

SH3 domains bind to a consensus sequence motif of PxxP. The SH3 domain is a very common protein-protein interaction domain, found in a broad range of different protein pathways. It is known to bind with proteins such as focal adhesion kinase and the E3 ubiquitin ligase Cbl (Odai *et al*., 1995). The N-terminal proline rich regions of p85 are known to form dimers between p85 proteins by interacting with SH3 domains on their respective proteins (Booker *et al*., 1993; Guinebault *et al*., 1995; Harpur *et al*., 1999; Hunter *et al*., 1997; Mayer, 2001). It is not presently known if one proline-rich region is selected over another for binding. The BH domain is also known to self dimerize and has sequence similarity to GTPase activating proteins (GAP), discussed later (Chamberlain and Anderson, 2005; Harpur *et al*., 1999). The proline rich regions flanking the BH domain are known to bind to the SH3 domains of Src family kinases and to the Abl tyrosine kinase in addition to the SH3 domain of p85 itself (Harpur *et al*., 1999; Kapeller *et al*., 1994; Pleiman *et al*., 1994). The two SH2 domains bind to phosphorylated tyrosine sequences pY-X-X-M (pY being phosphotyrosine) in proteins such as activated receptor tyrosine kinases and/or adaptor proteins (Piccione *et al*., 1993; Shoelson *et al*., 1993). The final domain, located between the two SH2 domains is the p110-binding domain, or alternatively the interSH2 (iSH2) domain. This domain contains two critical functions: to bind to the ABD and C2 domains of p110, and to stabilize the resulting heterodimer (Fruman, 2010; Miled *et al*., 2007; Huang et al., 2007).

In contrast to Class IA PI3K, Class IB PI3K enzymes consist of the p110γ catalytic subunit and the p101 adaptor subunit and are activated by the βγ subunit of heterotrimeric GTP-binding proteins (Arcaro *et al*., 2000). All Class I PI3K enzymes have been shown to phosphorylate phosphatidylinositol (PI), PI4-phosphate (PI4P), and $PI4,5P_2$ to produce the lipid products PI3P, $PI3,4P_2$, and $PI3,4,5P_3$ respectively *in vitro*. However, *in vivo* studies have only observed that class I PI3K phosphorylates $PI4,5P_2$ to $PI3,4,5P_3$ (Arcaro *et al*., 2000; Carpenter and Cantley, 1996; Ilic and Roberts, 2010). Class II PI3K consists of a single catalytic subunit with no regulatory subunit, and are distinguished by a carboxy-terminal C2 (CalB) domain

(Schu *et al*., 1993). There are three isoforms of class II PI3K, named C2α, C2β, and C2γ (Carpenter and Cantley, 1996; Fruman *et al*., 1998). The Class II PI3K phosphorylates PI or PI4P *in vitro*, though some evidence supports their ability to also phosphorylate PI4,5P_2 (Arcaro *et al*., 2000; Domin *et al*., 1997). Class III PI3Ks are involved in membrane trafficking through production of PI3P (Herman and Emr, 1990; Volinia *et al*., 1995). Class III PI3K enzymes are structurally more similar to class I PI3K than the class II PI3K, since they consist of a catalytic (Vps34) and regulatory (Vps15/p150) subunit. However, like class II PI3K their main lipid product is PI3P (Leevers *et al*., 1999).

1.4 Endocytosis

Endocytosis is the process where extracellular material or cell surface receptors are internalized into the cell through the formation of vesicles (Marsh and McMahon, 1999). There are many different types of endocytosis, ranging from phagocytosis where large extracellular particles, such as apoptotic bodies, are taken into the cell, to pinocytosis where extracellular fluids are taken into the cell along with any dissolved nutrients therein (Mukherjee *et al*., 1997). One form of endocytosis, known as receptor-mediated endocytosis, is specifically activated when cell-surface receptors are activated and require internalization for either deactivation or to transduce their information into the cell. An example of this is the RTK PDGFR, which is internalized into endosomes and trafficked through the endocytic pathway (Rosenfeld *et al*., 1984).

There are two main pathways used to internalize activated cell surface receptor complexes via receptor-mediated endocytosis: the clathrin-mediated endocytosis pathway, and the caveolin-mediated endocytosis pathway (Doherty and McMahon, 2009; Sorkin and von Zastrow, 2009). Clathrin-mediated endocytosis utilizes a protein lattice which coats the inside surface of pits made in the plasma membrane (Edeling *et al*., 2006). Caveolin-mediated endocytosis, on the other hand, utilizes lipid rafts consisting of large concentrations of cholesterol and glycosphingolipids known as caveolae which contain the protein caveolin (Anderson, 1998; Li *et al*., 2005; Miaczynska and Zerial, 2002). Caveolin associates with the membrane creating a spiral-like structure. It is believed that this spiral formation warps the plasma membrane into a concave structure, thereby creating an invagination. These invaginations are often used for the uptake of cell surface receptors as well as lipids

(Anderson, 1998). Regardless of the method of endocytosis, endocytic vesicles are internalized from the plasma membrane through scission events mediated by the large GTPase dynamin, a protein which has its activity upregulated by the p85 adaptor subunit of PI3K (Gout *et al*., 1993).

Once internalized, the vesicles, known as early endosomes, are routed through the endosomal pathway. They are small enclosed membrane structures which act as intracellular taxis for proteins as they move between different endosomal compartments. Early/sorting endosomes are much larger, semi-permanent structures which act as a warehouse in the cell where the vesicle cargos are sorted to other parts of the cell. The most prominent examples of endosome types are early endosomes, early/sorting endosomes, the recycling endosomes, and the late endosomes (Miaczynska and Zerial, 2002). Activated receptor complexes are internalized into vesicles which are then trafficked into the early/sorting endosome formed by the homotypic fusion of these early endosomal vesicles. The endocytosed material is then sorted from the early/sorting endosome for either degradation (via the lysosome by way of the late endosome) or for recycling (via the recycling endosome) back to the plasma membrane (Miaczynska and Zerial, 2002) (Fig. 1.4).

1.5 Rab Proteins

Rab proteins (or *ras* gene from **ra**t **b**rain proteins) are members of a family of monomeric G proteins which regulate the composition of endosomal domains as well as the fusion and fission of endosomes (Touchot *et al*., 1987). There are more than 60 Rab proteins reported in humans with each one regulating a specific trafficking function in the cell in relation to endosomes (Barr and Lambright, 2010; Pereira-Leal and Seabra, 2000; Seabra and Wasmeier, 2004; Stenmark and Olkkonen, 2001). While some Rab proteins are only expressed in certain tissues, others such as Rab5 are more broadly expressed in many different tissues (Stenmark and Olkkonen, 2001). Rab proteins typically contain prenyl groups which are inserted into membranes when the proteins are activated through an as yet unknown method (Stenmark and Olkkonen, 2001).

A Rab protein is considered to be in its active state when it is GTP-bound, and inactive when GDP-bound or lacking an associated guanosine nucleotide. Rab proteins can be ‘turned on’ through the displacement of their associated GDP molecules by guanine nucleotide excha-

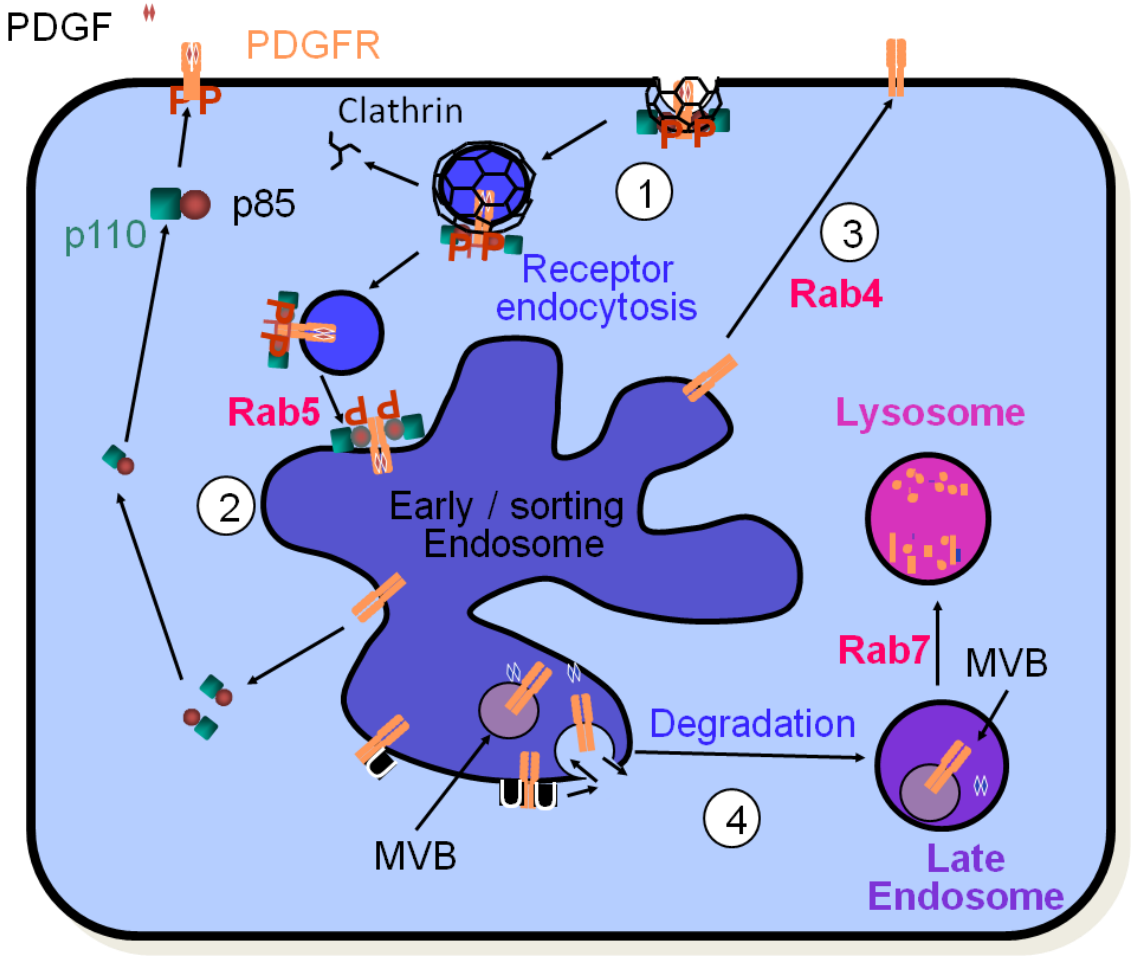

Figure 1.4 – PDGF-mediated endocytosis and trafficking of the PDGFR is regulated by Rab GTPases. **1**) Uptake of activated PDGFR complexes from the plasma membrane to intracellular vesicles is mediated by endocytosis. **2**) Rab5 regulates vesicle fusion events to move activated PDGFR complexes to the early/sorting endosome. **3**) From the early/sorting endosome, PDGFRs can be either recycled to the plasma membrane following deactivation or **4**) targeted into multivesicular bodies (MVBs) for lysosomal degradation.

nge factors (GEFs) which facilitate the exchange of a GDP molecule for a GTP molecule. The GTP-bound state moves two distinct regions known as Switch I and Switch II into position which allows for effector proteins such as the early endosomal autoantigen 1 (EEA1) to bind to the Rab protein (Pereira-Leal and Seabra, 2000; Seabra and Wasmeier, 2004; Stenmark and Olkkonen, 2001; Terzyan *et al*., 2004) (Fig. 1.5). Rab proteins, like all small monomeric G proteins, contain a weak intrinsic GTPase activity which can be enhanced by a GTPase activating protein (GAP), to hydrolyze bound GTP to GDP. There have been many putative Rab GAPs identified over the years, with many such proteins containing a Tre-2/Bub2/Cdc16 (TBC) domain. However, most GAPs tend to be protein-specific and only a few putative GAPs have been matched to their corresponding Rab proteins (Albert *et al*., 1999; Bernards, 2003; Strom *et al*., 1993).

When in the inactive, GDP-bound state, Rab proteins are located in the cytoplasm bound to a guanosine nucleotide dissociation inhibitor (GDI) protein (Kinchen and Ravichandran, 2010; Stenmark and Olkkonen, 2001). GDI proteins mask the prenylation of the Rab protein, preventing its insertion into membranes and segregating it to the cytoplasm. This GDI protein can be removed through the actions of a GDI-displacement factor (GDF). Human GDFs are not well characterized, though in yeast Yip proteins are known to fill this role (Pfeffer and Aivazian, 2004). When the GDI is removed, the Rab proteins associate with vacuoles and endocytic vesicle membranes. Once the Rab proteins are membrane-associated, GEF proteins can displace the bound GDP to allow GTP binding, activating the Rab.

Presently there are only two known GDI proteins in humans that act on all known Rab proteins in the cytosol (Stenmark and Olkkonen, 2001). In addition to these two known GDI proteins, there is another protein known as the Rab escort protein (REP) that has high levels of sequence similarity to the known GDI proteins. The REP has the same function as the known GDI proteins, but only acts upon newly synthesized Rab proteins, allowing them to be prenylated by geranylgeranyl transferase at a C-terminal cysteine motif (CXXX, CC, CXC, CCXX or CCXXX where X is any other amino acid) via a covalent bond to the sulfur atom on the target cysteine (Itzen and Goody, 2011; Stenmark and Olkkonen, 2001).

Once the GDI or REP has been removed, the Rab protein is then inserted into the specific target membranes. The precise method of insertion is unknown, primarily due to the

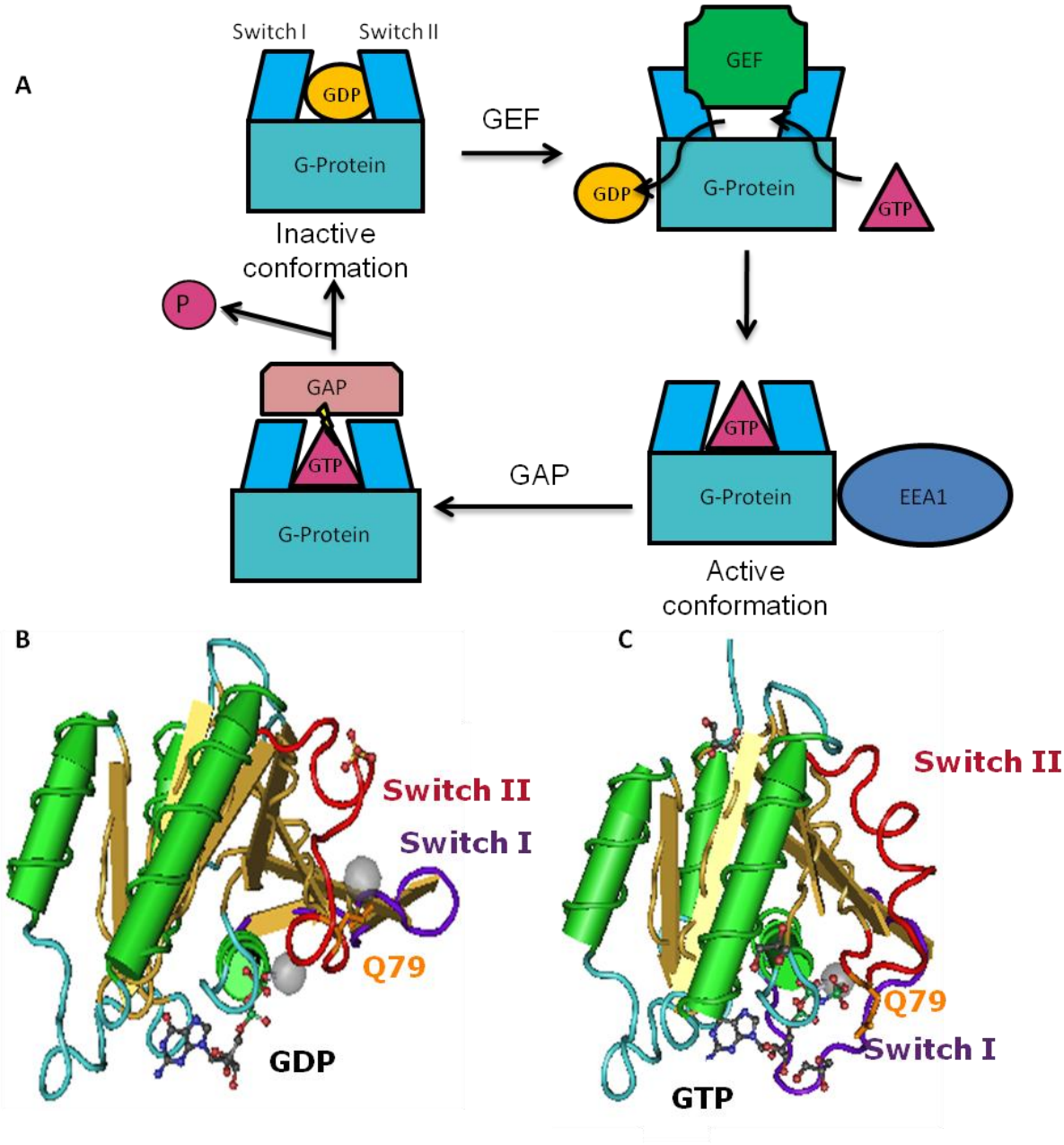

Figure 1.5 - Rab5 conformations. **A)** When Rab5 is GDP-bound it is in an inactive conformation. Through the action of a GEF, the GDP is displaced in favour of a GTP molecule. This then changes the Switch regions of Rab5 to an active conformation that can bind downstream effectors such as EEA1. Rab5 contains intrinsic GTP hydrolysis activity, which is enhanced by the presence of a GAP protein. **B)** Crystal structure of inactive state Rab5A-GDP complex. Switch I (purple), switch II (red) and the catalytic glutamine (Q79, orange) are highlighted. The nucleotide structures, Mg^{2+} (grey spheres) and small water molecules are also shown. **C)** Crystal structure of active state Rab5A-GTP complex. Drawn using PDB entries 1N6H (GTP) and 1TU4 (GDP) and coloured using Cn3Dv4.1 (Zhu *et al.*, 2003).

lack of identified GDFs. It is known that the C-terminal hypervariable region of the Rab contains an essential conserved short sequence motif consisting of two hydrophobic aliphatic side chains (φ-x-φ motif, where φ is an aliphatic residue) that are involved in the hydrophobic interaction with the GDI and REP (Itzen and Goody, 2011). It is possible that this same region is involved in the association of the GDF on the membranes of specific Rab targets (Pfeffer and Aivazian, 2004).

Following Rab-GDP insertion into the membrane via the prenyl group, the Rab protein interacts with a GEF and becomes active following the exchange of GDP for GTP (Barr and Lambright, 2010; Seabra and Wasmeier, 2004; Stenmark and Olkkonen, 2001). GEF proteins act by displacing the switch I region and allowing for the opening of the glycine brace region (Neuwald, 2009) . They also aid in the displacement of bound Mg^{2+} molecules by displacing a threonine residue responsible for co-ordinating Mg^{2+} (Nuoffer and Balch, 1994; Rossman et al., 2005; Vetter and Wittinghofer, 2001). This Mg^{2+} is essential for stable binding of GNPs to the Rab protein, which also facilitates the removal of GDP. Once GDP is removed, GTP can be recruited by the Rab protein (Barr and Lambright, 2010). An example of a GEF protein is Rin1, a known GEF for Rab5 (Barbieri *et al*., 2004; Barbieri *et al*., 2003; Kong *et al*., 2007; Tall *et al*., 2001). Once GTP-bound, the activated Rab protein can recruit effector proteins such as EEA1 to the endosome or vesicle, thereby promoting membrane fusion.

Rab proteins are deactivated through their own intrinsic GTPase activity. However, this activity is quite weak and is typically regulated through the addition of a GAP. GAP proteins increase GTP hydrolysis by providing a catalytic 'arginine finger' residue which helps catalyze the hydrolysis reaction. It does this by effectively making the bound GTP a better substrate for nucleophilic attack by water, lowering the transition state energy for the hydrolysis reaction (Dumas *et al*., 1999; Scheffzek *et al*., 1997) (Fig. 1.6). GAP proteins also stabilize the switch regions of Rab proteins, which further increase GTP hydrolysis (Scheffzek *et al*., 1998; Terzyan *et al*., 2004). Following GTP hydrolysis, the Rab protein assumes its inactive conformation, and GDI is once again recruited, removing Rab5-GDP from the membrane.

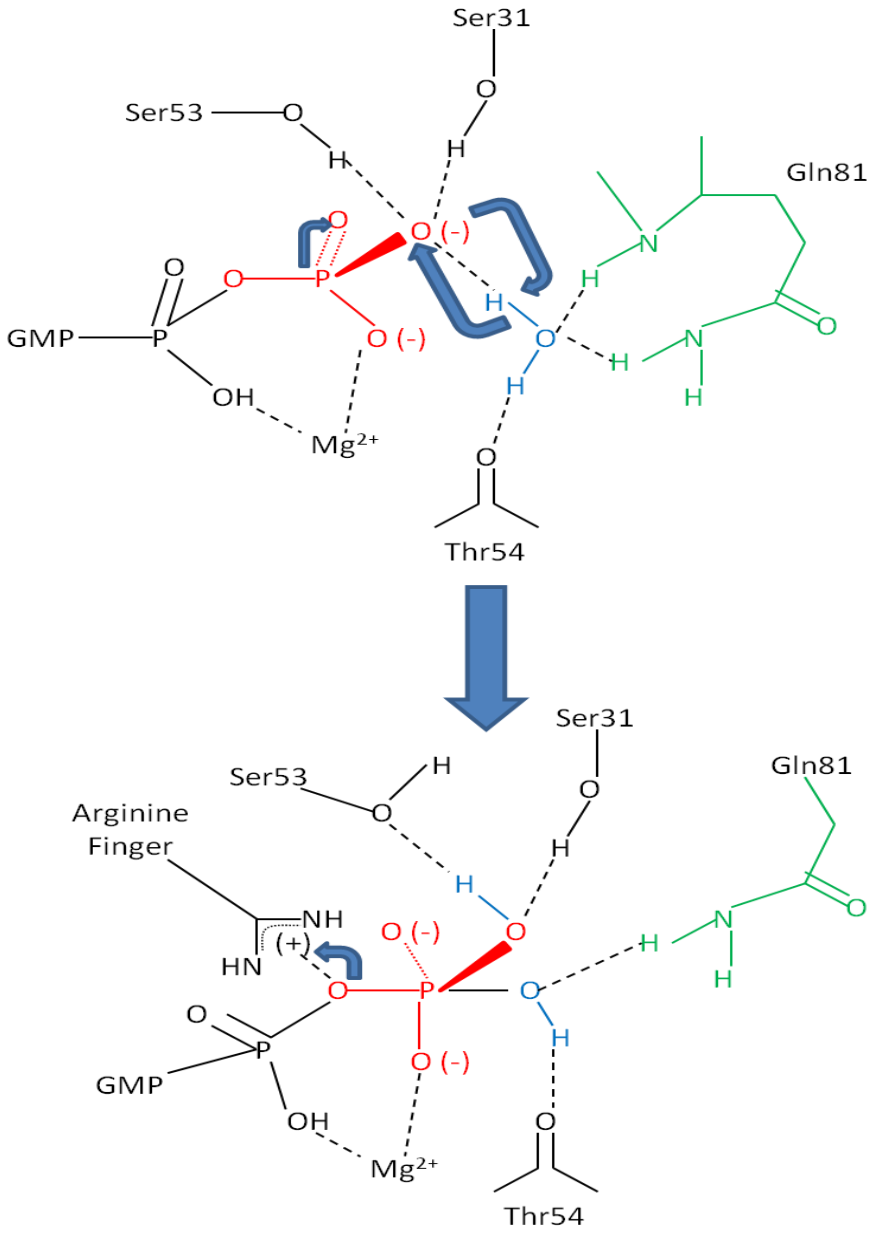

Figure 1.6 – GTP hydrolysis in the Rab3A active site. In this proposed mechanism for Rab3A GTPase activity, several residues from the switch regions (I and II) of Rab3a (black and green) stabilize the γ phosphate (red) of GTP and a water molecule (blue). During GTP hydrolysis, the phosphate group is subject to a nucleophilic attack by the water molecule, creating a pentavalent intermediate. In the presence of an arginine finger provided by a GAP, the β and γ phosphates are stabilized, making the bound GTP a better substrate for nucleophilic attack (Dumas *et al.*, 1999).

1.5.1 p85 is a Rab5GAP

Rab5 is one of the best described human Rab proteins. The active form of Rab5 is involved in the fusion of vesicles from the plasma membrane with the early/sorting endosome (Armstrong, 2000; Mills *et al*., 1999; Mohrmann and van der Sluijs, 1999; Somsel Rodman and Wandinger-Ness, 2000; Ullrich *et al*., 1994) (Fig. 1.10). Active Rab5-GTP interacts with EEA1 which, in addition to binding Rab5, also binds to PI3P. PI3P can be formed as either the lipid product of class III PI3K or via the dephosphorylation of the class 1A PI3K lipid product $PI3,4,5P_3$ through the function of PI4- and 5-phosphatases (PI4- and 5-Pase) (Shin *et al*., 2005). EEA1:Rab5 forms a tether between the endocytic vesicle and the early/sorting endosome. This tether allows for a soluble N-ethylmaleimide sensitive factor (NSF) attachment receptor (SNARE) complex to form, fusing the membranes together (Christoforidis *et al*., 1999; McBride *et al*., 1999; Mills *et al*., 1998; Rubino *et al*., 2000; Simonsen *et al*., 1998). It is through SNARE-mediated fusion that many receptors are transported through the endosomal system.

Recent evidence has shown that the p85 adaptor subunit of class IA PI3K acts as a Rab5GAP protein (Chamberlain *et al*., 2004). This Rab5GAP activity was first discovered by analyzing the sequence similarity of p85 to known GAPs for the Rac/Rho/Cdc42 family of G-proteins which are similar to Rab5 (Heasman and Ridley, 2008). This analysis found that the BH domain of p85 contained putative GAP activity, and *in vitro* studies have confirmed it to have GAP activity towards both Rac1 and Cdc42 (Bokoch *et al*., 1996; Chamberlain *et al*., 2004; Zheng *et al*., 1994). A sequence alignment of a GAP protein for Cdc42 (Cdc42GAP) and p85 proteins revealed that p85 contains an arginine (R151) in its BH domain which corresponds to the arginine finger of the Cdc42GAP (Fidyk and Cerione, 2002). However, it was revealed that p85 had a much lower GAP activity towards Cdc42 in comparison to the known Cdc42GAP protein. Further analysis of the seqences of p85 and Cdc42GAP showed that the p85 BH domain lacked the residues used to stabilize the switch regions of Cdc42, requiring high concentrations of p85 to elicit significant GAP activity (Fidyk and Cerione, 2002).

When the RabGAP activity of p85 was measured towards Rab5 and Rab4, it was found that p85 also displayed GAP activity towards those proteins (Chamberlain *et al*., 2004; Chamberlain *et al*., 2010). Rab5 and Rab4 are both involved in the trafficking of RTKs

through their degradation pathway (Hutagalung and Novick, 2011; Mitra *et al*., 2011; Stenmark, 2009). Mutation of the R151 residue of p85, speculated by sequence similarity to be involved in GAP activity, showed only minor changes to the Rab5GAP activity of p85 (Chamberlain *et al*., 2004; Chamberlain *et al*., 2010). The mutation of another arginine residue in the BH domain (R274) showed that this residue was the arginine finger necessary for RabGAP activity (Chamberlain *et al*., 2004; Chamberlain *et al*., 2010).

Using this information, a model describing Rab5 regulation was proposed by our laboratory (Fig. 1.7). Following RTK activation the PI3K complex (i.e., p85-p110) is recruited to the receptor through the interaction of the SH2 domains of p85. The receptor is then internalized via either clathrin- or caveolin-mediated endocytosis. Following the decoating of the vesicles, the GDI which masks the prenylation of Rab5 when in its inactive GDP-bound state is displaced, allowing Rab5 to embed itself in the membrane of the vesicle. Rab5-GDP then interacts with the p85 subunit of PI3K, forming a complex upon the surface of the vesicle. At this point a Rab5GEF, most likely RTK-associated Rin1, displaces the Rab5-associated GDP with a GTP, thereby 'activating' Rab5 allowing it to bind to EEA1 to form the tether required for membrane fusion. Following the SNARE-mediated fusion event, the PI3K:Rab5 complex dissociates from the RTK. Aided by the Rab5GAP activity of p85, Rab5 hydrolyses the gamma-phosphate of its bound GTP, producing GDP. Now in its inactive state, Rab5-GDP dissociates from the endosomal membrane, once again becoming GDI-bound.

1.5.2 Tau Proteins Have Rab5GAP Activity

It has also been shown that the 383 amino acid Tau protein—a class of microtubule-associated proteins (MAP)—known as Tau4 was observed to associate with Rab5 and appears to act as a Rab5GAP (personal correspondence, with Grégoire Morisse and Dr. Nicole Leclerc, Université de Montréal). Microtubules are components of the cytoskeleton which play critical roles in a number of cellular processes including cell division, motility, intracellular trafficking, and maintaining cellular shape (Bhat and Setaluri, 2007; Lewis *et al*., 1988). Microtubules are composed of αβ-tubulin heterodimers and are intrinsically dynamic polymers which form hollow, helical, cylindrical filaments containing thirteen tubulin dimers per turn (Desai and Mitchison, 1997; Li *et al*., 2002). There are a number of proteins which associate with micro-

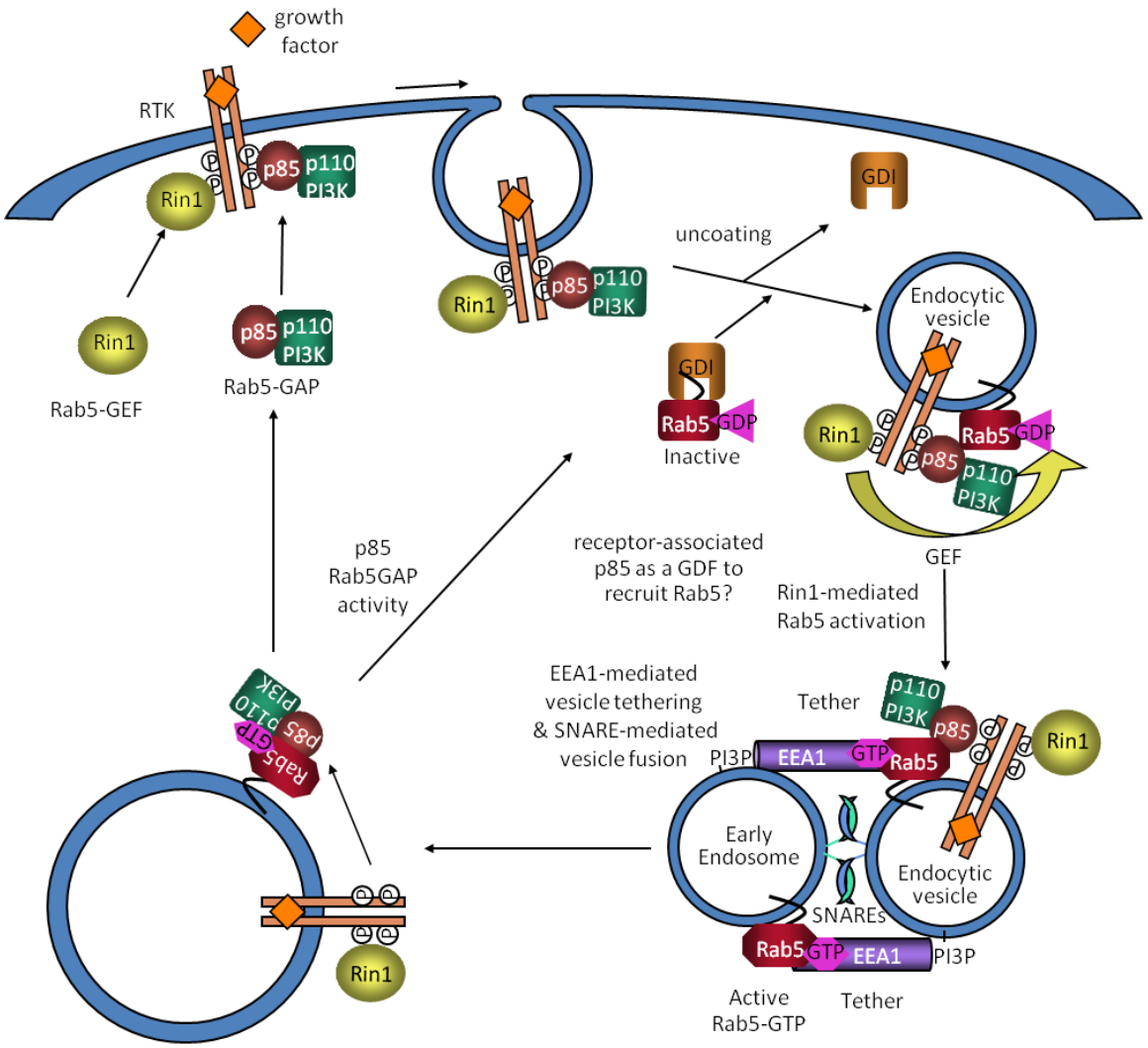

Figure 1.7 - Mechanism of Rab5 regulation. Following RTK activation, PI3K (p85/p110) and Rin1 are recruited and the receptor complex is internalized by either clathrin- or caveolin-mediated endocytosis. GDI is displaced from Rab5, allowing Rab5 to embed itself in the membrane of the endocytic vesicle via its prenylation and to associate with the p85 subunit of PI3K. Rin1, a RTK-associated Rab5GEF, displaces the GDP of inactive Rab5 and replaces it with a GTP, activating the Rab5 protein. Rab5 then binds to EEA1, a PI3P-associating protein to form a tether between the endocytic vesicle and the early/sorting endosome which allows for SNARE proteins to fuse the vesicle to the endosome. Following vesicle fusion, PI3K dissociates from the activated RTK. Rab5 hydrolyzes its bound GTP with the help of the Rab5GAP p85, which causes it to be removed from the endosomal membrane and once again becomes GDI-bound.

tubules which bear the name MAP which are known to aid in assembly and disassembly *in vivo* (Goedert *et al*., 1991; Lewis *et al*., 1988).

Tau proteins are found primarily in the nervous system (Alonso *et al*., 2001; Goedert *et al*., 1989; Lewis *et al*., 1988). In adult brain tissue six Tau proteins, all isoforms of the same Tau gene generated by alternative splicing, have been identified (Alonso *et al*., 2001; Goedert *et al*., 1989) (Fig.1.8). Tau proteins are often differentiated into two primary domains, known as the projection domain and the assembly domain. The projection domain is a 255-amino acid N-terminal segment which lacks the structures associated with microtubule binding. This domain does not appear to be involved in pathological aggregation in diseases such as Alzheimer's disease and is known to bind to the membrane (Arikan *et al*., 2002). The projection domain consists of zero to two of 'insert' regions of 29 amino acids as well as several conserved domains common in all forms of Tau known as A1, A2, B, and C (Alonso *et al*., 2001; Friedhoff *et al*., 2000). Conversely, the assembly domain is the C-terminal segment of the protein and contains three to four tubulin binding motifs consisting of 31 to 32 amino acids with a characteristic P-G-G-G motif (Alonso *et al*., 2001; Goedert *et al*., 1989). It is this section of the protein which has been observed to aggregate in diseases such as Alzheimer's disease (Bertrand *et al*., 2010; Goedert *et al*., 1989). There are also two conserved proline-rich regions located between the N-terminal projection domain and the C-terminal assembly domain. Additionally, Tau proteins which are produced in peripheral neurons have been shown to also include an additional "Big Tau" insert, though this form is not present in the central nervous system (Goedert *et al*., 1992).

Tau proteins may contain as many as 85 phosphorylation sites, nine of which have been shown to be phosphorylated in human adult brain (Bertrand *et al*., 2010). These sites appear to be involved in a number of disease states of tau, specifically in Alzheimer's disease where hyperphosphorylated tau proteins detach from microtubules and accumulate in neurons. Examples of this hyperphosphorylation can be found at disease-associated phosphorylation sites such as S262 or the sites forming the AT8 epitope seen in early-stage Alzheimer's disease (Augustinack *et al*., 2002; Bertrand *et al*., 2010; Kimura *et al*., 1996). Tau proteins could also be involved in endocytic pathways, possibly in the retrograde transport of neurotrophins from the pre-synaptic terminal to the cell body (personal correspondence with Grégoire Morisse and Dr. Nicole Leclerc).

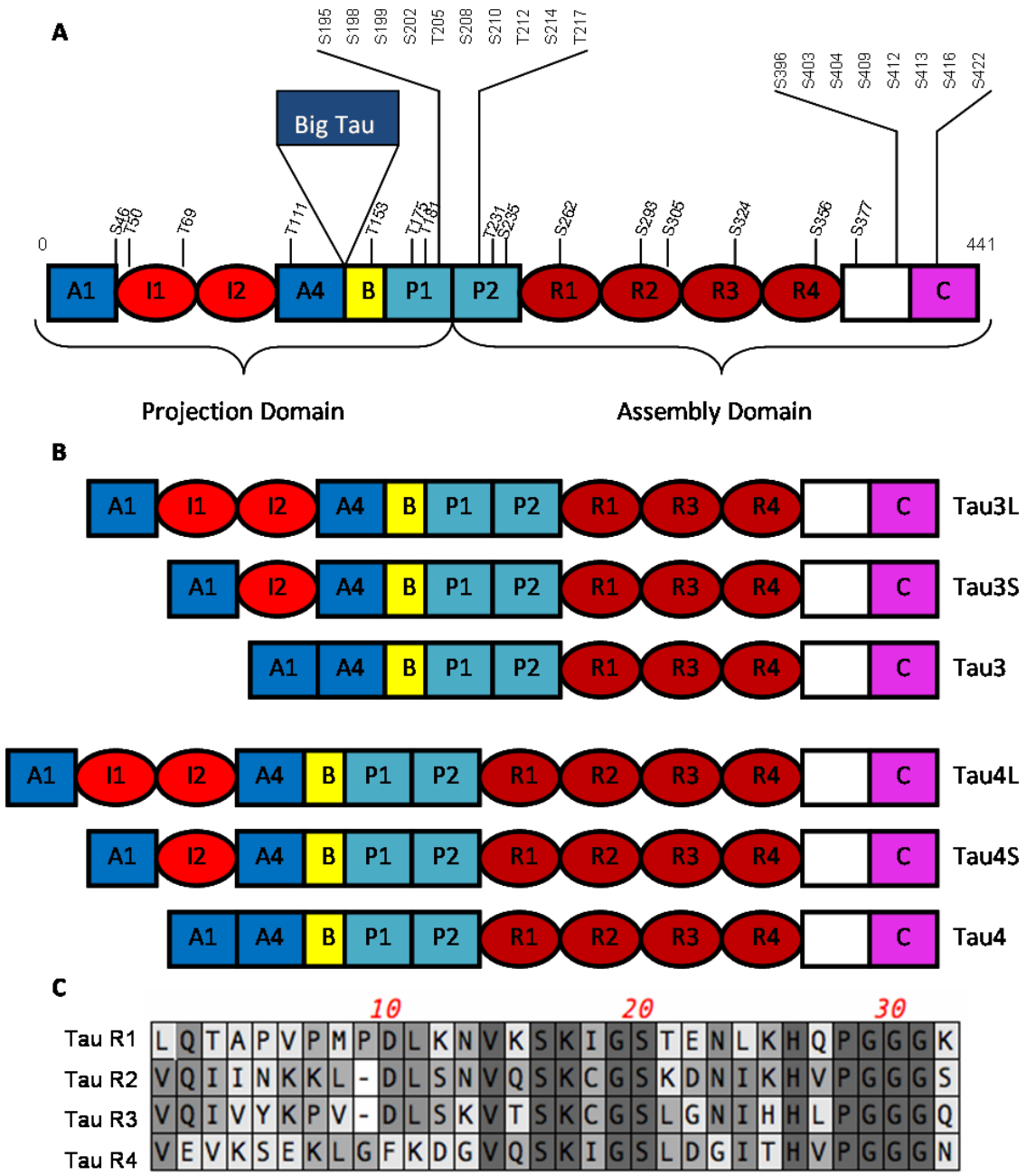

Fig 1.8 – Domain Structure of the Tau protein. A) Tau protein is made of several different domains, each coded for by a different exon. Exons 2 and 3 (I1 and I2) code for 29-residue domains, while exons 9, 10, 11, and 12 (R1, R2, R3, and R4) code for homologous 31- to 32-residue tubulin binding domains. P1 and P2 are proline rich regions while A1, A2, B, and C are conserved domains. In peripheral nerves there can also be a "Big Tau" (exon 4A) insert added as well. Included is a number of categorized possible phosphorylation sites. **B)** There are six primary isoforms of Tau which are obtained through alternate splicing. **C)** Alignment of tubulin binding domains.

1.6 Protein-Protein Interactions

All of the above pathways previously mentioned are dependent on protein-protein interactions, of which there are many different types present in any cellular system. At their most basic, protein-protein interactions consist of intermolecular forces acting between the components of the protein complex whether it is transient or stable. The most prominent of these interactions are ionic interactions as well as the hydrophobic effect (Gorham *et al*., 2011). The residues responsible for these interactions are often grouped in small secondary structures called binding domains. Examples of these binding domains are the SH2 domain which binds to motifs consisting of a phosphorylated tyrosine plus several surrounding amino acids (Felder *et al*., 1993; Waksman *et al*., 1992). These binding domains often have highly variable dissociation constants in the nanomolar to micromolar range.

The affinity of two proteins for one another is a function of the free energy of association and their equilibrium binding constants. The standard factors that are involved in these measurements in biochemistry are the equilibrium association and dissociation constants (K_A and K_D) (Roos *et al*., 1998; Zhou *et al*., 2008) as well as the free energy (ΔG) of the complex formation. Under specific conditions, kinetic rate constants (k) are used to approximate the values of the equilibrium constants (K). The association and dissociation constants relate to one another using the following formula:

$$K_A = 1/K_D$$

When it comes to reporting affinity constants, K_D is often used to measure affinity because it is measured in molar units (Roos *et al*., 1998). This is especially so when dealing with simple binding interactions with only two proteins. K_D specifically refers to the propensity of a binary complex to dissociate reversibly into its constituent components, and is described by the equation:

$$K_D = [B][L]/[BL]$$

In this equation, B and L refer to the unbound 'bait' protein and the 'ligand' protein, respectively, while BL refers to the binary complex (Phizicky and Fields, 1995).

Over the past 30 years a number of techniques have been developed to measure the binding affinity of two interacting biological molecules. Genetic analysis and library-based techniques can be used to discover which proteins bind to one another, but actual quantification of the binding interactions generally requires physical binding analysis methods (Phizicky and Fields, 1995). Binding affinities are analyzed by altering the concentration of one of the two proteins while keeping the other protein at a constant, but low, concentration. From this, binding information can be gathered through different methods, from the change of fluorescence to change in optical density to simply measuring the concentration of the elutant (Phizicky and Fields, 1995). It is also possible using kinetic analyses to approximate the K_D of two proteins by measuring the on- and off-rate of the binding, thereby calculating the dissociation constant K_D.

1.7 Surface Plasmon Resonance

One of the techniques commonly used for measuring binding affinity between two molecules is surface plasmon resonance (SPR). Surface plasmons are plasma waves which propagate across a metal-dielectric interface, typically a thin plane of gold or silver nanoparticles on a glass slide in the presence of a liquid under conditions of total internal reflection (Aslan *et al*., 2005; Jonsson *et al*., 1991; Rich and Myszka, 2000) (Fig.1.9A). When a mass associates with the interface, it shifts the resonance energy of the surface plasmon in a detectable fashion. This results in a change in the resonance angle, the angle light is reflected from the gold surface, which is detected and used to quantify the association between the interface and the analyte (Jonsson *et al*., 1991; Phizicky and Fields, 1995).

Gold is not a suitable surface for immobilizing proteins. As such, many SPR sensor chips utilize a matrix of dextran, a flexible unbranched carbohydrate polymer. Typically this dextran surface will contain some sort of reactive group or affinity resin which allows for the binding of a 'bait' protein to the interface such as carboxymethyl groups (Fig.1.9B). An example of this is the presence of a carboxymethylated dextran surface. This surface will form N-hydroxysuccinimide esters from the carboxyl groups of the carboxymethylated dextran matrix via reaction with N-hydroxysuccinimide and N-ethyl-N'-(dimethylaminopropyl) carbodiimide hydrochloride in water. These esters then react with proteins which are passed

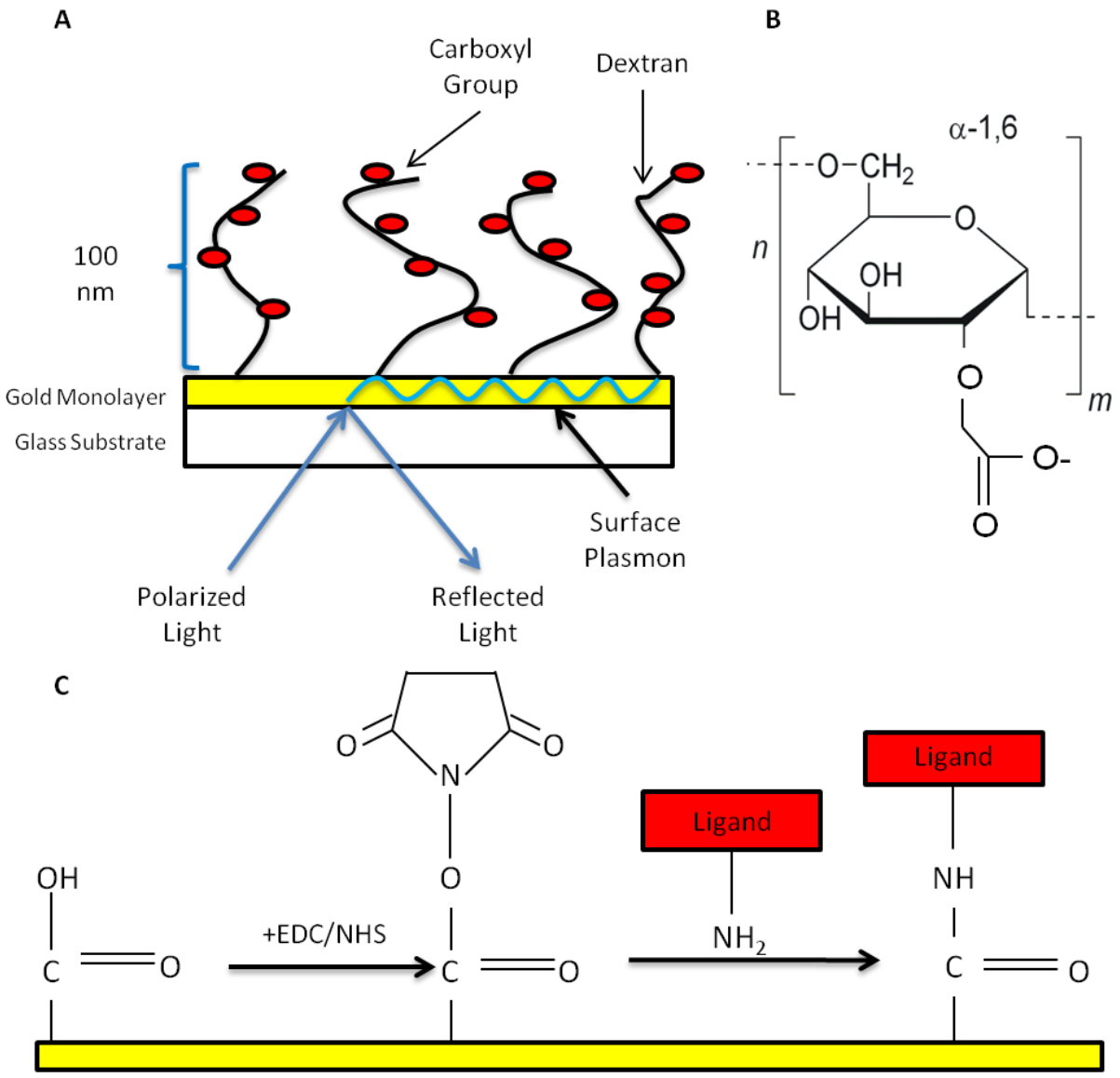

Figure 1.9 – The CM5 Surface plasmon resonance chip. A) The CM5 chip is used with surface plasmon resonance. Surface plasmons are generated by reflecting a beam of polarized light at a metal-dielectric interface. While most of the light is reflected, some of the light propagates parallel to the interface under conditions of total internal reflection. Bound to the gold monolayer of the metal-dielectric interface of a CM5 sensor chip are 100 nm dextran molecules which have been carboxylated in order to bind proteins via amine coupling. **B)** Structure of carboxymethylated dextran. **C)** The carboxyl-groups of the CM5 dextran surface are activated by a 1:1 solution of N-hydroxysuccinimide (NHS) and N-ethyl-N'-(dimethylaminopropyl) carbodiimide hydrochloride (EDC) to give reactive succinimide esters. The desired ligand (i.e., Rab5) (in a buffer of appropriate pH to grant it a positive charge) is then passed over the surface and the esters react spontaneously with amino groups. Any free amine group can react with this surface.

over the activated surface of the matrix, forming amides which covalently link the 'bait' protein to the matrix (Johnsson *et al*., 1991) (Fig.1.9C).

As proteins all share a similar refractive index, there is a linear correlation between the shift in the resonance angle and the amount of protein bound at the surface (Jonsson *et al*., 1991; Malmqvist, 1993). This means that you can directly measure the binding of ligand proteins to the bait proteins in real time, allowing for the measurement of both the association and dissociation rates of the two molecules (Phizicky and Fields, 1995). It has been noted that the data could be skewed by mass transfer effects caused by the movement of buffer containing solute over the sensor chip (Schuck and Minton, 1996; Shen *et al*., 1996), though these effects can be predicted by computer simulation found in many current model analysis software as well as experimentally (Schuck, 1996).

It is possible to calculate the total mass and even molar concentration of protein bound to a sensor chip. SPR detectors measure signal in response units (RU) with 1000 RU corresponding to approximately 1 ng/mm^2 of proteins on the SPR surface (Backmann *et al*., 2005). If the surface area is known, it is possible to calculate the mass of bound protein. Furthermore, if the relative masses and stoichiometry have been determined for the bait and ligand in the experiment, it is possible to determine the maximum binding (Rmax) of the ligand to the bait using the following equation from the BIAcore Sensor Surface Handbook:

$$\text{Rmax} = \frac{\text{Mass ligand}}{\text{Mass bait}} \times \text{RU of immobilized Bait (RB)} \times \text{Stoichiometry}$$

For example, Rab5 has a mass of approximately 24 kDa and p85 has a mass of approximately 83 kDa. Assuming 1:1 stoichiometry, 1000 RU of Rab5 should bind approximately 3460 RU of p85 at maximum saturation. Through this method it should be possible to analyze the interactions between the various protein components observed in the model previously described (1.5.1).

2.0 Hypothesis and Objectives

Upon nucleotide exchange by a guanine nucleotide exchange factor (GEF) such as Rin1, Rab5 becomes GTP-bound (Barbieri *et al*., 2004; Barbieri *et al*., 2003; Kong *et al*., 2007; Tall *et al*., 2001). Previous studies have shown that p85 functions as a Rab5GAP (Chamberlain *et al*., 2004). Following binding of p85 to the PDGFR, p85 is known to undergo a conformational change in its SH2 domain regions which is known to derepress the catalytic activity of p110 (Miled *et al*., 2007; Piccione *et al*., 1993; Shoelson *et al*., 1993; Yu *et al*., 1998). Previous studies have not shown if this conformational change affects the Rab5GAP activity of p85. It is possible that once p85 has dissociated from the PDGFR, it provides its catalytic arginine finger to the Rab5 protein, increasing its rate of GTP hydrolysis, deactivating Rab5.

Previous studies by our lab have shown that p85 can associate with Rab5-NF (nucleotide-free), -GDP, and –GTP nucleotide binding states (Chamberlain *et al*., 2004). While the binding of p85 to Rab5-GTP is expected as it is a Rab5GAP, its binding to Rab5-NF and Rab5-GDP indicates that p85 may have additional functions towards Rab5 beyond serving as a Rab5GAP. The ability of p85 to bind Rab5-GDP suggests that p85 could fulfill the function of a Rab5GDF, removing the GDI protein from inactive, cytosolic Rab5-GDP, as it may recruit Rab5-GDP to membranes containing activated PDGFR:p85 complexes.

2.1 Hypothesis

Activated PDGFR decreases the Rab5GAP activity of p85 in order to allow sufficient time for endosomal fusion events between the early/sorting endosome and the receptor-containing endocytic vesicle. In addition, p85 has different affinities towards Rab5 in its different nucleotide-associated states: Rab5-NF, Rab5-GDP, and Rab5-GTP.

2.2 Objectives

The goals of this study were two-fold:

1) To test if the binding of PDGFR to p85 affects the observed Rab5GAP activity of p85. To test this, peptides corresponding to the p85 binding site on the PDGFR in both its active (phosphorylated) and inactive (non-phosphorylated) states of PDGFR were purchased.

GAP assays (Anderson and Chamberlain, 2005) were performed to compare the GAP activity of p85 in the different states in the presence and absence of PDGFR peptide binding.

2) To test if the presence or absence of GTP and GDP affects the affinity of p85 for Rab5, both in the presence and absence of PDGFR peptide. Surface plasmon resonance studies were performed to analyze the binding affinities of p85 to Rab5 in its three nucleotide bound states.

3.0 Materials and Methods

3.1 Reagents and Supplies

All chemicals and reagents were of analytical grade or higher. They were purchased from VWR or Sigma-Aldrich unless otherwise stated. The glutathione Sepharose resin (GE Healthcare) were prepared according to the manufacturer's instructions and stored for up to several months at 4 °C with no loss of stability. The [α-^{32}P]GTP (Cat # BLU506H) was purchased from PerkinElmer and likewise stored at 4 °C. All experiments using these isotopes met with all regulations mandated by the University of Saskatchewan. The materials for use with the BIAcore-X surface plasmon resonance detector, including the CM5 sensor chips (Cat # BR-1000-12) and immobilization reagents (Cat # BR-1005-57), were purchased from GE Healthcare. PDGFR peptide (sequence: DGGYMDMSKDESVDYVPML) and ppPDGFR peptide (sequence: DGGpYMDMSKDESVDpYVPML, with pY representing a phosphorylated tyrosine) were purchased from GeneScript of Piscataway, New Jersey, USA at >98% purity.

The following primary antibodies were used: anti-p85 (B-9, Cat # sc-1637), anti-p110 (I-19, Cat # sc-1637), anti-His_6 (H-15, Cat # sc-803), anti-PDGFR (958, Cat # sc-432), anti-pTyr (PY20) and all were purchased from Santa Cruz Biotechnology, Inc. Secondary antibodies used were goat anti-rabbit (IRDye®800CW, Cat# LIC-926-32211), goat anti-mouse (IRDye®800CW, Cat# LIC-926-32210), goat anti-mouse (IRDye®680CW, Cat# LIC-926-32220) and goat anti-rabbit (IRDye®680CW, Cat# LIC-926-32221), all purchased from LI-COR Biotechnology.

3.2 Methods

3.2.1 Bacterial Strains and Growth Media

The pGEX6P1 (GE Healthcare) and pQE9 (Qiagen) vectors are designed for inducible protein expression in bacteria. Transformation of bacteria with these vectors produces high levels of proteins fused to glutathione S-transferase (GST; pGEX) or His_6 (pQE9) after induction with isopropyl β-D-thiogalactopyranoside (IPTG). Both vectors contain ampicillin resistance genes. The pGEX6P1 vector contains a PreScission cleavage site (LEVLFQ*GP). The pGEX6P1 vector was used with all proteins produced except for the p110 clones generated

by Dielle Detillieux. All plasmids were made previously by our laboratory. All pGEX6P1 plasmids containing inserts were expressed in *Escherichia coli* (*E. coli*) BL21 cells [F^- *ompT* $hsdS_B$ ($r_B^- m_B^-$) *gal dcm*] (Novagen) while all pQE9 plasmids containing inserts were expressed in *E. coli* M15pREP cells [Nal^S, Str^S, Rif^S, Thi^-, Lac^S, Ara^+, Gal^+, Mtl^-, F^-, $RecA^+$, Uvr^+, Lon^+] (Qiagen). The production of the plasmid DNA was performed using *E. coli* TOP10 cells [F^- *mcrA* (*mrr*$^-$*hsdRMS*$^-$*mcrBC*) *80lacZM15 lacX74 recA1 ara139 (ara-leu)7697 galU galK rpsL (strR) endA1 nupG*] (Invitrogen).

All cells were grown in Luria-Bertani Broth (LB, EMD Chemicals USA, Cat # 1.10285.5007) containing 1% (w/v) bacto-tryptone, 0.5% (w/v) bacto-yeast extract, and 1% (w/v) sodium chloride (NaCl) pH 7.0, per litre. All plasmids contained an ampicillin resistance gene, therefore the *E. coli* BL21 and M15pREP cells were grown in LB containing 100 µg/mL ampicillin (LBA, Sigma-Aldrich).

3.2.2 Eukaryotic Cell Lines and Growth Media

Mouse fibroblast cells, NIH 3T3, were obtained from American Type Culture Collection (CRL-1658) and grown in Dulbecco's Modified Eagle Medium (DMEM) supplemented with 10% fetal bovine serum (FBS), 100 units/mL penicillin G and 100 µg/mL streptomycin (P/S) (all purchased from Gibco) at 37 °C in a 5% CO_2 incubator.

Growth factor stimulations of NIH 3T3 cells were performed with PDGF-BB (Cedarlane, Cat# 220-BB-050) since these cells endogenously express the PDGFR. PDGF-BB was resuspended in PDGF dilution buffer [10 mM acetic acid and 2 mg/mL bovine serum albumin (BSA)] and further diluted in spent starving media (DMEM + 1% P/S + 0.5% FBS) to a final concentration of 50 ng/mL. PDGF stimulations were performed for 5 minutes at 37 °C in a 5% CO_2 incubator prior to cell lysis.

To prepare lysates, 10 cm plates of cells (of approximately 85% confluence) were placed on ice and washed once with cold PBS. Each 10 cm plate of cells was scraped into 1 mL lysis buffer [50 mM N-(d-hydroxyethyl) piperazine-N'-(2-ethanesulfonic acid), pH 7.5, 150 mM NaCl, 10%(v/v) glycerol, 1%(v/v) Triton X-100, 1.5 mM $MgCl_2$, 1 mM ethylenediaminetetraacetic acid, 10 mM sodium pyrophosphate, 100 mM sodium fluoride, and also containing 10 µg/mL aprotinin, 10 µg/mL leupeptin, 1 mM 4-(2-Aminoethyl) benzenesulfonyl fluoride hydrochloride (AEBSF), and 1 mM sodium orthovanadate]. Cells

were incubated on ice for at least 10 minutes and centrifuged at 21,920 x g for 10 minutes in order to remove insoluble cellular debris. Lysates were stored at -80 °C.

3.2.3 Purification of GST-Fusion Proteins

LBA volumes of 100 mL were inoculated with *E. coli* BL21 cells transformed with the appropriate plasmid encoding for the desired protein, which had been fused to GST. Cells were allowed to grow overnight at 37 °C with vigorous shaking. The next day, four flasks each containing 1 L of LBA were inoculated with 25 mL of the overnight culture each. The resultant culture was allowed to grow at 37 °C until an OD_{600} of 0.6-0.8 was reached (~1.5 hours). IPTG was added to a concentration of 0.3 mM to induce protein expression. After the addition of the IPTG the temperature was reduced to room temperature (~23 °C) and the cells were allowed to grow overnight to promote slower protein induction and improve protein solubility. Cells were harvested by centrifugation at 420 x g for 15 minutes at 4 °C. The cell pellet was then frozen at -20 °C or lysed immediately.

For lysis, the cell pellet was resuspended in 10 mL of PreScission buffer (50 mM tris(hydroxymethyl)aminomethane hydrochloride (Tris-HCl), pH 7.0, 150 mM NaCl, 1 mM EDTA, 1 mM DTT) containing 10 µg/mL aprotinin, 10 µg/mL leupeptin, and 1 mM AEBSF, all of which were added fresh. The cells were lysed by the addition of 20 mg/mL lysozyme to a final concentration of 1 mg/mL and incubated on ice for one hour. The lysates were sonicated six times for 10 seconds each on a setting of 2.5 using a Model 250/450 Sonifier (Branson Ultrasonics) with 60 seconds chilling on ice between bursts. Triton X-100 was then added to a concentration of 1% in order to minimize protein-protein interactions and reduce impurities in the sample. Samples were centrifuged at 12000 x g for 30 minutes at 4 °C. The supernatant was filtered through a 0.8 µm cellulose acetate membrane (Nalgene, Cat # 8-1020-05) and mixed with 2 mL of a 50% slurry of glutathione Sepharose resin (Amersham Biosciences, Cat# 17-0756-01).

The lysate and beads were incubated together for 45 to 60 minutes at 4 °C while mixing. The beads were recovered by centrifugation at 500 x g for 5 minutes and washed 5 times with 50 mL of ice-cold PreScission buffer. To cleave the protein of interest from the GST-tag, the bead-immobilized GST-fusion protein was resuspended in PreScission buffer and treated with 35 units of PreScission Protease (GST-3C, GE Healthcare Life Sciences, Cat# 27-

0843-01) and allowed to cleave over a period of 48 hours at 4 °C while mixing. The bead solution was added to a gravity column and the desired protein was collected in the supernatant. The beads were washed with 16 mL of ice-cold PreScission Buffer, with the washes collected in aliquots equal to the bead volume (i.e. 1 mL).

3.2.3.1 Ion Exchange Chromatography

p85 proteins were further purified using ion exchange chromatography. As wild type p85 has a pI of 5.74 it was determined that a buffer with a pH above 7.5 would be ideal for anion exchange chromatography purification. The proteins were buffer exchanged into Anion A buffer (50 mM Tris-HCl, pH 8.0, 50 mM NaCl) using either an Amicon® Ultra-4 Centrifugal filter unit (Millipore) or by dialysis. They were then concentrated using the Centrifugal filter unit to a volume of 2 mL. Protein concentration was determined by measuring the A_{280} and calculating protein concentration to ensure that the protein concentration was no higher than 25 mg/mL. This was done using the Beer-Lambert Law in combination with the amino acid sequence and the known absorptions of Tyr and Trp at 280 nm.

Using an ÄKTA$_{FPLC}$™ (GE Healthcare) for the anion exchange, a Resource Q anion exchange column with a bed volume of 1 mL (GE Healthcare) was washed with 20 column volumes of distilled water, followed by 20 column volumes of Anion A buffer to equilibrate the column. The protein sample was injected into the fast protein liquid chromatography (FPLC) machine, allowed to bind to the anion resin, and washed with 20 column volumes of Anion A buffer. The proteins were eluted from the column with a salt gradient using increasing concentrations of Anion B buffer (50 mM Tris-HCl, pH 8.0, 1 M NaCl) and collected in 0.5 or 1 mL fractions. Aliquots of these fractions were resolved using SDS-PAGE and visualized by Coomassie Blue stain to locate the purified p85.

3.2.3.2 Dynamic Light Scattering

Aggregation and homogeneity of the purified protein solutions were analyzed using dynamic light scattering with a DynaPro-MS800 instrument (DynaPro, USA, Saskatchewan Structural Sciences Centre, U of S Campus). Samples were diluted to concentrations between 0.1 and 1 mg/mL and filtered to remove dust or other particulates. Samples (40 to 100 µL)

were then placed in a DLS cuvette, removing as much air as possible. The cuvette was placed into the Micro Sampler of the machine. The proteins were analyzed with a beam of monochromatic light that is directed through the sample with the fluctuations of intensity of the light scattered by the particles of the solution analyzed. With this data it is possible to characterize the size of the particles in question, and from that aggregation state and molecular mass.

3.2.4 Purification of His_6-Tagged Proteins

Growth and induction of bacterial cells were performed as per the same procedure as the GST-fusion proteins (3.2.3), with the addition of 10 µg/mL kanamycin when initially growing cells. For lysis, the cells were resuspended in TALON Equilibrium/Wash Buffer (50 mM sodium phosphate, pH 8.0, 300 mM NaCl, 20 mM imidazole) containing 10 µg/mL aprotinin, 10 µg/mL leupeptin, and 1 mM AEBSF, all of which were added fresh. Cell lysis procedure was performed using the lysozyme procedure described for the GST-fusion proteins (Section 3.2.3) until lysates were ready to bind to beads.

The lysates were then incubated with 2 mL of a 50% slurry of TALON resin (Clontech, Cat# 635504). The lysate and resin were incubated together for 45 to 60 minutes at 4 °C while mixing. The resin was washed by adding 40 mL of Equilibrium/Wash buffer, allowed to mix for 5-10 minutes, and centrifuging at 700 x g for 5 minutes. This was performed five times. The resin was transferred to a gravity column and excess liquid was allowed to drain to just above the top of the resin. The His_6-tagged proteins were eluted from the resin using ten 1 mL aliquots of TALON Elution Buffer (50 mM sodium phosphate, pH 8.0, 300 mM NaCl, 250 mM imidazole) and collected in fractions equal to the volume of the resin (i.e., 1 mL).

3.2.5 SDS-PAGE gels, Coomassie Blue Staining, and Western Blot Analysis

3.2.5.1 SDS-Polyacrylamide Gel Electrophoresis (SDS-PAGE)

Proteins were resolved by SDS-PAGE for protein staining with Coomassie Blue or for Western blot analysis (Laemmli, 1970). SDS-PAGE was performed using the Mini-Protean II apparatus (Bio-Rad). Gels were cast between two glass plates with 1 mm spacers. The resolving gels contained 7.5-15% acrylamide solution (29.2:0.8 acrylamide:bisacrylamide), 37

mM Tris-HCl, pH 8.8 and 0.1% (w/v) SDS. Polymerization was initiated by the addition of 0.06% (w/v) ammonium persulfate and 0.1%(v/v) N,N,N',N'-Tetra-methylethylenediamine (TEMED). After the resolving gel was polymerized, a 2 mL stacking gel containing 4.5% acrylamide solution, 125 mM Tris-HCl, pH 6.8, and 0.1% (w/v) SDS was poured on top of the resolving gel and a 10- or 15-well comb was inserted to form wells. The stacking gel was polymerized with the same procedure as the resolving gel. After the stacking gel was polymerized, the gel was assembled into the electrophoresis apparatus. The protein samples were prepared in SDS sample buffer (62.5 mM Tris-HCl, pH 6.8, 5%(v/v) β-mercaptoethanol, 2.3% (w/v) SDS, 0.1% (w/v) bromophenol blue, 10%(v/v) glycerol) and heated to 100 °C for 5 minutes. The samples and molecular weight markers (Fermentas SM0671 or SM0661) were loaded on the gel. Electrophoresis was performed at a constant voltage of 180 V in running buffer (25 mM Tris, 192 mM glycine, and 0.1% (w/v) SDS) until the bromophenol blue dye had run off the bottom of the gel as described by Laemmli (Laemmli, 1970).

3.2.5.2 Coomassie Blue Stain Analysis

To stain proteins, the gel was incubated in Coomassie Blue stain [0.14% (w/v) Coomassie Blue R-250 (Bio-Rad), 41.4%(v/v) methanol, and 5.4%(v/v) acetic acid] at room temperature for 20 minutes and destained in destaining solution [41.4%(v/v) methanol and 5.4%(v/v) acetic acid] until bands were visible. The gel was imaged using the Gel-Doc 2000 system using Quality One software (Bio-Rad).

3.2.5.3 Western Blot Analysis

For Western blot analysis, the gels resolved by SDS-PAGE were soaked in transfer buffer (48 mM Tris-HCl, pH 9.2, 39 mM glycine, 0.038% (w/v) SDS, 20%(v/v) methanol) for 15 to 20 minutes. Meanwhile, 6 pieces of 3 MM filter paper (Whatman, Cat # 3030 700) were soaked into the transfer buffer and a nitrocellulose membrane (Whatman, Cat # 09301108) was hydrated in distilled water. All 3 MM and nitrocellulose was cut to fit the gel (8.2 x 5.4 cm). The proteins were transferred using an Owl Panter^{TM} Semi-Dry Electroblotter (VWR, Cat # 27372-374). The apparatus was set up with three layers of soaked 3 MM paper on the base of the apparatus, followed by the SDS-PAGE gel, then the nitrocellulose membrane, and finally three more layers of the soaked 3 MM paper. Air bubbles were removed by rolling a tube over

the layers. The proteins were transferred to the nitrocellulose membrane at a constant current of 400 A for 15 minutes per gel.

The membrane was blocked in PBS Blocking Solution [10 mM sodium phosphate, pH 7.3, 2.7 mM KCl, 137 mM NaCl supplemented with either 5% (w/v) Carnation skim milk powder (Canada Safeway) or 1% (w/v) BSA fraction V (EMD, Cat # 126593-25GM)] for 1 hour at room temperature or overnight at 4 °C. Primary antibodies were diluted in the PBS blocking solution to 1 μg/mL for anti-PDGFRβ, anti-p85, anti-p110, and anti-His_6; and 2 μg/mL for anti-pTyr. It should be noted that only the pTyr blots used a BSA-containing blocking solution with all others using milk blocking solution. Each blot was incubated with primary antibodies for 1 hour at room temperature or overnight at 4 °C. The membrane was washed three times for 5 minutes in PBST (PBS + 0.05% (v/v) Tween-20). Secondary antibodies, conjugated to IRDye®800 or IRDye®680 were diluted to a concentration of between 20 and 100 ng/mL into PBST with either milk or BSA fraction V as appropriate. The membrane was incubated in the absence of light for 1-3 hours at room temperature and washed three times in PBST for 5 minutes each, again in the absence of light. The membrane was scanned using the LI-COR Odyssey Infrared Imager (LI-COR) and analyzed with the Odyssey V3.0 software provided by the manufacturer.

3.2.6 ppPDGFR Peptide Competition Assays to Disrupt PDGFR:GST-p85 Binding

Competition assays were performed to analyze the effectiveness of the ppPDGFR peptide and PDGFR peptide in binding competitively with wild type phosphorylated PDGFR to p85. Wild type phosphorylated PDGFR was obtained by treating NIH 3T3 cells with PDGF for 5 minutes prior to lysis. To avoid non-specific interaction with the glutathione Sepharose beads, the lysates were pre-cleared by incubating them with the 100 μL of the beads for 30 minutes. The beads were then removed by centrifugation. These cleared lysates were stored at -80 °C until required.

GST (serving as a negative control) and GST-p85 were isolated and separately immobilized on glutathione Sepharose beads. Both were quantified using a Lowry protein assay (Sigma-Aldrich, Cat # TP0300). Immobilized GST and GST-p85 proteins were diluted to a concentration of 0.1 μg/μL in PBS in a final volume of 100 μL. To these samples were added either the ppPDGFR peptide or PDGFR peptide to concentrations of 1 μM, 10 μM, or

100 µM. These samples were incubated at 4 °C while mixing to allow interaction between the peptides and the GST-p85.

Pre-cleared PDGF-activated NIH 3T3 lysate (200 µL) was then added to the bead slurry. The samples were again allowed to incubate at 4 °C while mixing to allow interaction between the phosphorylated PDGFR from the cell lysate and the immobilized GST-p85 or GST control. Protein complexes were collected by centrifugation at 500 x g for 1 minute and washed four times with 500 µL of $HNTG^{++++}$ washing buffer [20 mM 4-(2-hydroxyethyl)-1-piperazineethanesulfonic acid, pH 7.5, 10%(v/v) glycerol, 0.1%(v/v) Triton X-100, 150 mM NaCl, and also containing 10 µg/mL aprotinin, 10 µg/mL leupeptin, 1 mM AEBSF, and 1 mM sodium orthovanadate]. Samples were resuspended in 20 µL of SDS sample buffer, heated to 100 °C for 5 minutes and resolved by SDS-PAGE in duplicate. One gel was transferred to a nitrocellulose membrane and analyzed by Western blot analysis for the presence of tyrosine-phosphorylated PDGFRβ (pTyr) and the other probed for total PDGFRβ.

3.2.7 GTPase Activating Protein Assays (GAP Assay)

A modification of an existing procedure used in the lab (Anderson and Chamberlain, 2005), the GAP assay is used to measure the hydrolysis of GTP by the Rab5 protein by measuring the amount of GDP produced. The Rab5 protein was loaded with [α-^{32}P]GTP which was hydrolyzed to [α-^{32}P]GDP by the intrinsic GTPase activity of Rab5. The [α-^{32}P]GTP and [α-^{32}P]GDP were separated by thin-layer chromatography (TLC). The technique chosen for these analyses was a steady-state GAP assay where the amount of GDP generated via hydrolysis by Rab5 during a specific time in the presence of increasing concentrations of the p85 GAP protein was measured.

3.2.7.1 Pre-Preparation for GAP Assays

Prior to the assay, the TLC chamber was pre-equilibrated with the developing solvent (0.75 M KH_2PO_4; 180 mL) for 1-24 hours. The PEI Cellulose F plates (VWR, Cat# EMD-5579-7) were stored in a sealed, plastic bag to prevent hydration and stored at 4 °C. Plates were labelled using a pencil with 1.2 cm lanes denoted with 1.5 cm intervals between lanes starting 1.5 cm from each outside edge of the plate and 2 cm from the bottom of the plate. To

reduce wicking up the sides of the plate from the stand holding it, the sorbent material on either side of the plate was removed at 1 cm to create a barrier for the resolving liquid.

3.2.7.2 Preparation of Reaction Mixture

A hydrolysis mixture consisted of the various concentrations of GAP protein (Tau or p85) in loading buffer (20 mM Tris-HCl, pH 8.0, 2 mM EDTA, 1 mM DTT) containing 10 mM $MgCl_2$ was prepared. The total reaction volume was 15 µL, though the above hydrolysis mixture was made in a volume of 10 µL which would then be brought to the final volume with the addition of a master mix containing Rab5 diluted in loading buffer to a final concentration in 15 µL of 100 to 400 nM depending on the experiment, and 50 nM [α-^{32}P]GTP (3000 Ci/mmol). In order to minimize GTP hydrolysis prior to the addition of the p85 to solution, the [α-^{32}P]GTP was added to the Rab5 master mix solution and mixed by pipetting immediately prior to activation of the reaction. Upon addition of the p85/Mg^{2+} (or Tau/Mg^{2+}) samples were incubated at 24 °C for 10 to 20 minutes, depending on the experiment, before being stopped by the addition of 3 µL of elution buffer [1% (w/v) SDS, 25 mM EDTA, 25 mM GDP, 25 mM GTP] and were heated for 2 minutes at 65 °C.

3.2.7.3 Separation and Analysis of Radiolabelled Nucleotides

Onto the thin layer chromatography (TLC) plate was applied 9 µL of the resulting stopped solution. The sample was spotted in a 1.2 cm line over the course of 60 seconds and allowed to dry between applications. A control sample containing only the nucleotide stock was spotted to assess the fraction of the pre-existing [α-^{32}P]GDP already present in the radiolabelled nucleotide product, which varied considerably from batch to batch. After the plate was loaded with all samples, it was allowed to dry for 15 minutes at room temperature. The plate was inserted into the TLC chamber where the developing solvent was several millimetres below the line marking the lanes so that the solvent did not smear the samples. Samples were allowed to migrate until the solvent front was 2 cm from the top of the plate (~1.5 hours). After the plate was removed, it was dried at room temperature for 30 to 45 minutes. The plate containing the separated [α-^{32}P]GTP and [α-^{32}P]GDP was analyzed using a phosphorimager (Molecular Imager FX Pro Plus, Bio-Rad) and quantified using Quality One software (Bio-Rad). The sum total of the signal of the GTP and GDP bands were taken (from

non-saturated images) and the percentage of total signal for each band was calculated. The values from the nucleotide-alone wells were subtracted from this percentage since it was the background of [α-^{32}P]GDP present in the absence of Rab5.

3.2.8 Surface Plasmon Resonance (SPR) Analysis

Analysis of Rab5:p85 binding was performed using the BIAcore-X instrument (GE Healthcare) and analyzed using the BIAevaluation software (GE Healthcare, Structural Sciences Centre, U of S Campus). This machine is a label-free system for detailed studies of biomolecular interactions that utilizes SPR. SPR is an optical phenomenon arising in thin metal films under conditions of total internal reflection. This can be used to measure the change in the concentration of molecules on the surface layer of solution in contact with the sensor surface.

3.2.8.1 Preparation of CM5 sensor chip and binding of Rab5

Rab5 samples were buffer exchanged into a Rab5 loading solution (50 mM sodium acetate, pH 5.5, 50 mM NaCl) to a concentration of 0.1 mg/mL. A CM5 sensor chip was pre-equilibrated with BIAcore Running buffer (50 mM HEPES, pH 8.0, 150 mM NaCl). The chip was then activated as per manufacturer's instructions with a 1:1 solution of N-ethyl-N'-(dimethylaminopropyl) carbodiimide hydrochloride (EDC) and N-hydroxysuccinimide (NHS) for 7 minutes at a flow rate of 5 µL/min across both flow cells (Fc1 and Fc2). The Rab5 solution was then bound to Fc2 only to a concentration of approximately 3000 response units (RU), or 3 ng/mm^2 (Backmann *et al*., 2005) by directly binding to the carboxymethylated dextran surface of the CM5 sensor chip by amine coupling. Fc1 did not receive any Rab5, and as such serves as a control for the experiments where the ligand protein will be flowed over both flowcells. Both flowcells were washed three times with ethanolamine (provided with the EDC and NHS) for 7 minutes each at a flow rate of 5 µL/min to deactivate the surface. Both flowcells were washed thoroughly with running buffer to remove any unbound protein, ethanolamine, or activating reagents. In some experiments, Rab5 protein was bound with both Mg^{2+} and nucleotide (either GDP (Sigma-Aldrich, Cat # G7127) or the non-hydrolysable GTP-analogs GTPγS (Sigma-Aldrich, Cat # G8634) or GppCp (Jena Biosciences, Cat # NU-405)).

In these cases $MgCl_2$ and the appropriate nucleotide were added to the running buffer prior to the addition of p85.

3.2.8.2 Preparation of p85 Ligand protein

p85 proteins were obtained via GST-fusion protein purification procedure (3.2.3) as well as all the other listed purification steps. The p85 was buffer exchanged into p85 loading buffer which consisted of BIAcore running buffer with 0.05% Tween-20 added to keep the proteins from aggregating. Concentrations of p85 used were chosen based on data gathered in the GAP assays and other binding experiments. The concentrations chosen ranged from 0 µM to 30 µM, doubling each concentration (i.e., 1 µM, 2 µM, 4 µM, etc.)

3.2.8.3 BIAcore Binding Assay

p85 ligand protein solutions were passed over both flowcells of the Rab5-immobilized CM5 sensor chips at a flow rate of 20 µL/min, with the flowcell without Rab5 serving as a control. The order of different concentrations of p85 injected was determined randomly with each injection lasting for 120 seconds, followed by 120 seconds to measure dissociation prior to the resumption of constant flow of the BIAcore running buffer over the chip. The signals for Fc1 (control) were subtracted from the signal from Fc2 (Rab5-bound) (Fc2-Fc1) in order to determine the relative change in RU (ΔRU). The peak values (around 100 to 110 seconds into injection) were then recorded and then converted into percent theoretical saturation of the chip. Maximum binding was plotted versus p85 concentration using the Prism software (GraphPad Software, Inc.). Non-linear regression curve fitting allowed binding affinities to be determined. The flowcells were then washed after every run for 2 minutes with running buffer and after every second run with Regeneration buffer (50 mM glycine, pH 9.0, 500 mM NaCl 1% Tween-20) to remove any accumulated p85, followed by another wash with running buffer.

4.0 Results

4.1 Rab5 and p85 Protein Purification

Rab5 and p85 proteins were prepared in order to analyze the effect of PDGFR (through the use of the PDGFR peptide and ppPDGFR peptide) on p85:Rab5 interactions. These interactions were analyzed using GAP assays to measure the effect of the peptides on the p85 Rab5GAP activity, as well as for measuring the binding affinity of the two proteins to one another using SPR. All experiments were performed using proteins that were purified by making GST-fusion proteins of the desired proteins using pGEX6P1 vectors expressed in protease deficient BL21 cells. Protein expression was induced with IPTG and the bacteria were lysed to harvest the resultant GST-fusion proteins. These proteins were isolated using glutathione Sepharose resin and GST-tags were removed by PreScission cleavage to yield purified proteins. Samples were resolved by SDS-PAGE and visualized using Coomassie Blue stain and were also quantified using a Lowry protein assay (Fig.4.1). An additional clone of p85 containing both an N-terminal GST-tag and a C-terminal His_6 was also assayed but was shown to have no GAP activity towards Rab5 (data not shown).

These proteins were then analyzed using a GAP assay to measure the Rab5GAP activity of p85 that had previously been shown by our lab (Chamberlain *et al*., 2004) (Fig. 4.2). These early positive data prompted the continuation of further projects using these GAP assays (Fig. 4.3). Unfortunately the data gathered in subsequent GAP assays was not consistent to one another. While nearly all of them showed p85 Rab5GAP activity, the exact activity varied greatly between protein batches. Furthermore it was found that the p85 preparations displayed an ability to independently hydrolyze GTP in the absence of the known GTPase, Rab5 (Fig. 4.4). These preparations were also less effective at hydrolyzing GTP reaching 15-20% GTP hydrolysis at 32 μM p85 as compared to almost 60% GTP hydrolysis for the initial preparations (Fig. 4.3). As p85 has not been shown to have any endogenous ability to hydrolyze GTP previously, it was believed that the purity of the proteins was the issue. As such, additional purification steps were considered.

Additionally, subsequent GAP assays displayed lower GTP hydrolysis than earlier studies which seemed to go beyond simple batch-to-batch variation. Spectrophotometric analysis of purified Rab5 samples suggested that this may have been caused by the presence

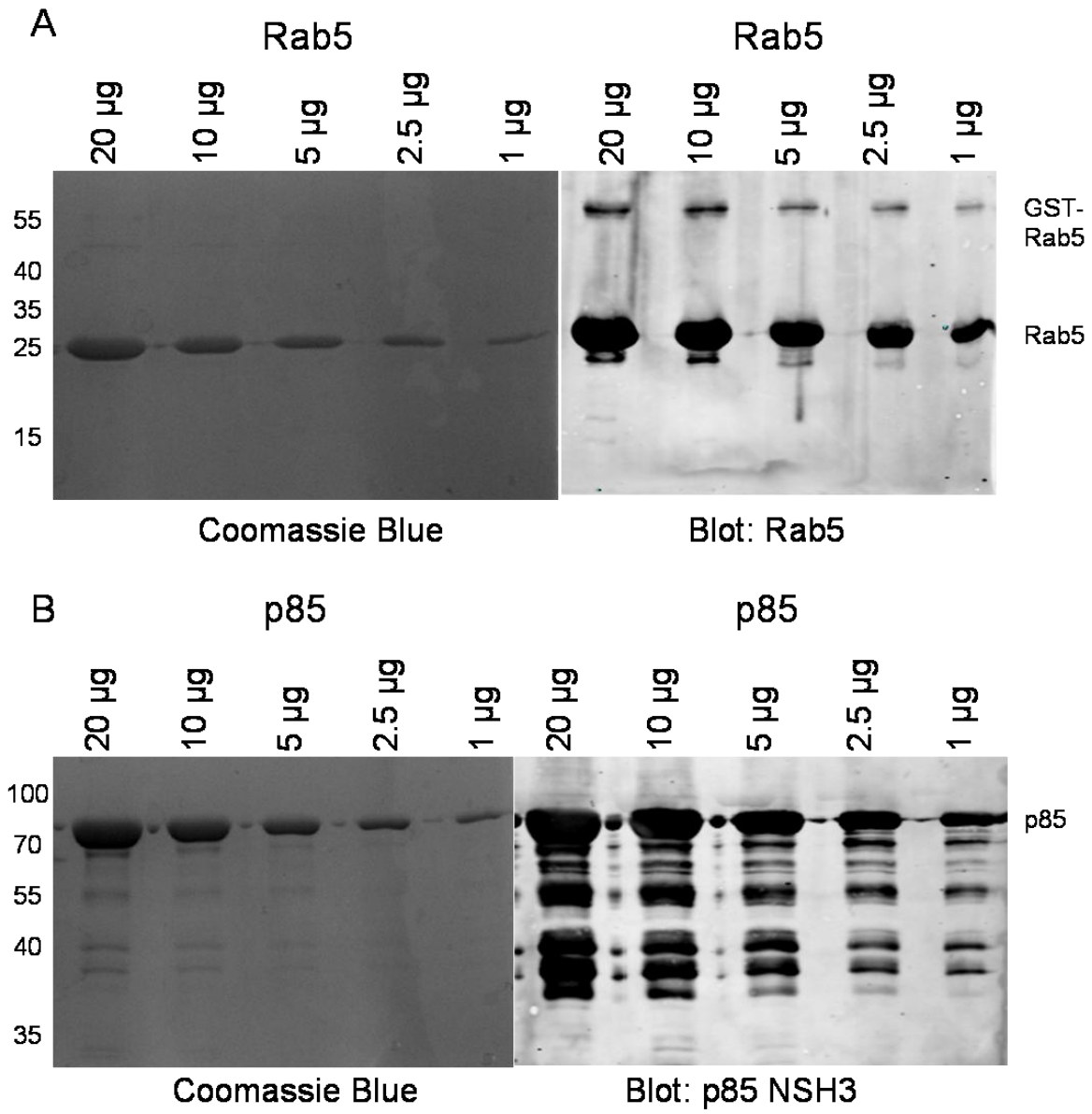

Figure 4.1 – Purification of Rab5 and p85 proteins. Rab5 and p85 proteins were generated as GST-fusion proteins in BL21 cells. The BL21 cells were lysed and the proteins were recovered using glutathione Sepharose resin. The beads were washed and the GST-tag was removed using PreScission protease. The cleaved proteins were recovered and concentrated to a final concentration of 3-5 µM for Rab5 and 70-80 µM for p85 using a concentrator and quantified using a Lowry assay. The indicated amounts were then resolved on either a 10% (p85) or 15% (Rab5) SDS-PAGE gel and visualized with Coomassie Blue stain for Rab5 (**A**, left) and p85 (**B**, left). A duplicate gel was also prepared and the proteins were transferred to a nitrocellulose membrane and blocked in milk. Following blocking, the membranes were incubated with a primary antibody against Rab5 (**A**, right) or p85 (**B**, right), then with a secondary antibody containing a fluorescent tag. The results of the Western Blot were visualized using the LI-COR Odyssey Infrared Imager.

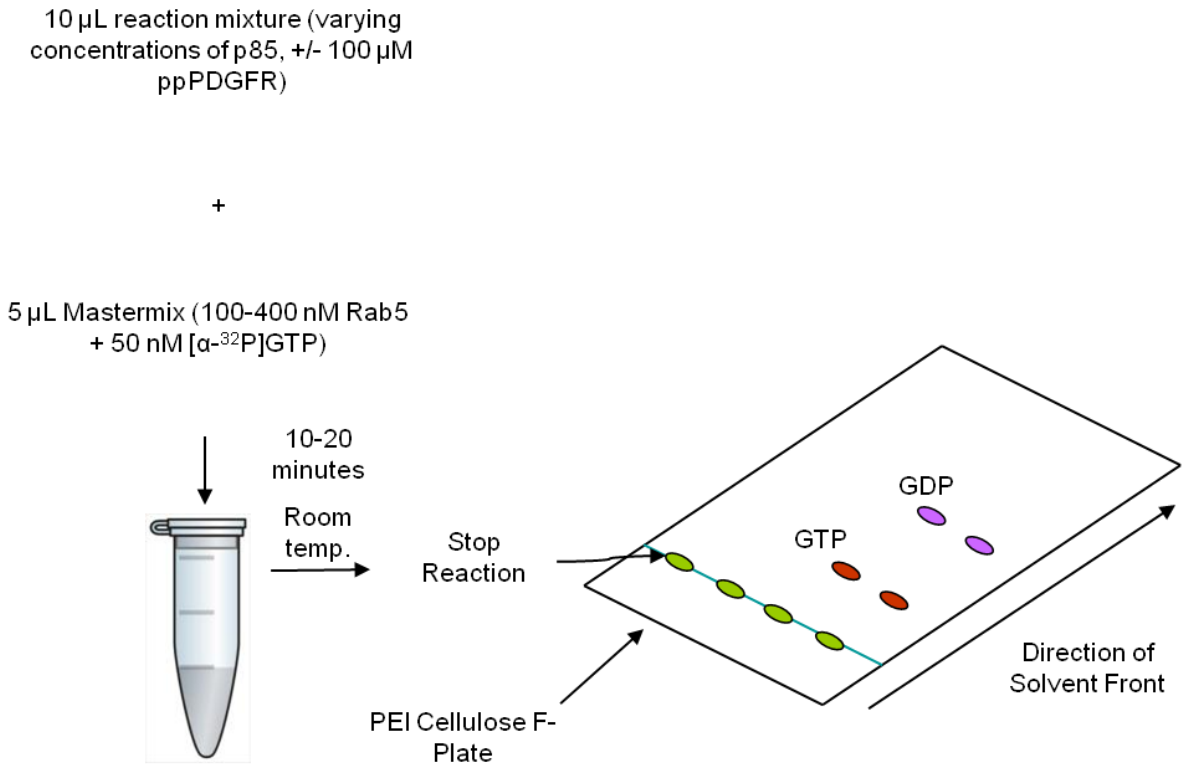

Figure 4.2 – Experimental Model of GAP assay. Rab5 samples were loaded with [α^{32}P]GTP and incubated +/- p85 +/- ppPDGFR peptide or PDGFR peptide as per the directions above and allowed to react for 10-20 minutes. Reactions were then stopped with 3 µL of a buffer containing 1% SDS, 25 mM EDTA, and 25 mM each of unlabelled GDP and GTP. These were heated to 65 °C for 5 minutes to elute the nucleotides from Rab5, spotted onto a PEI Cellulose F-Plate, and resolved using a buffer containing 0.75 M KH_2PO_4, pH 4.0. Plates were allowed to dry and data was captured using a Storage Phosphor Screen and a phosphorimager.

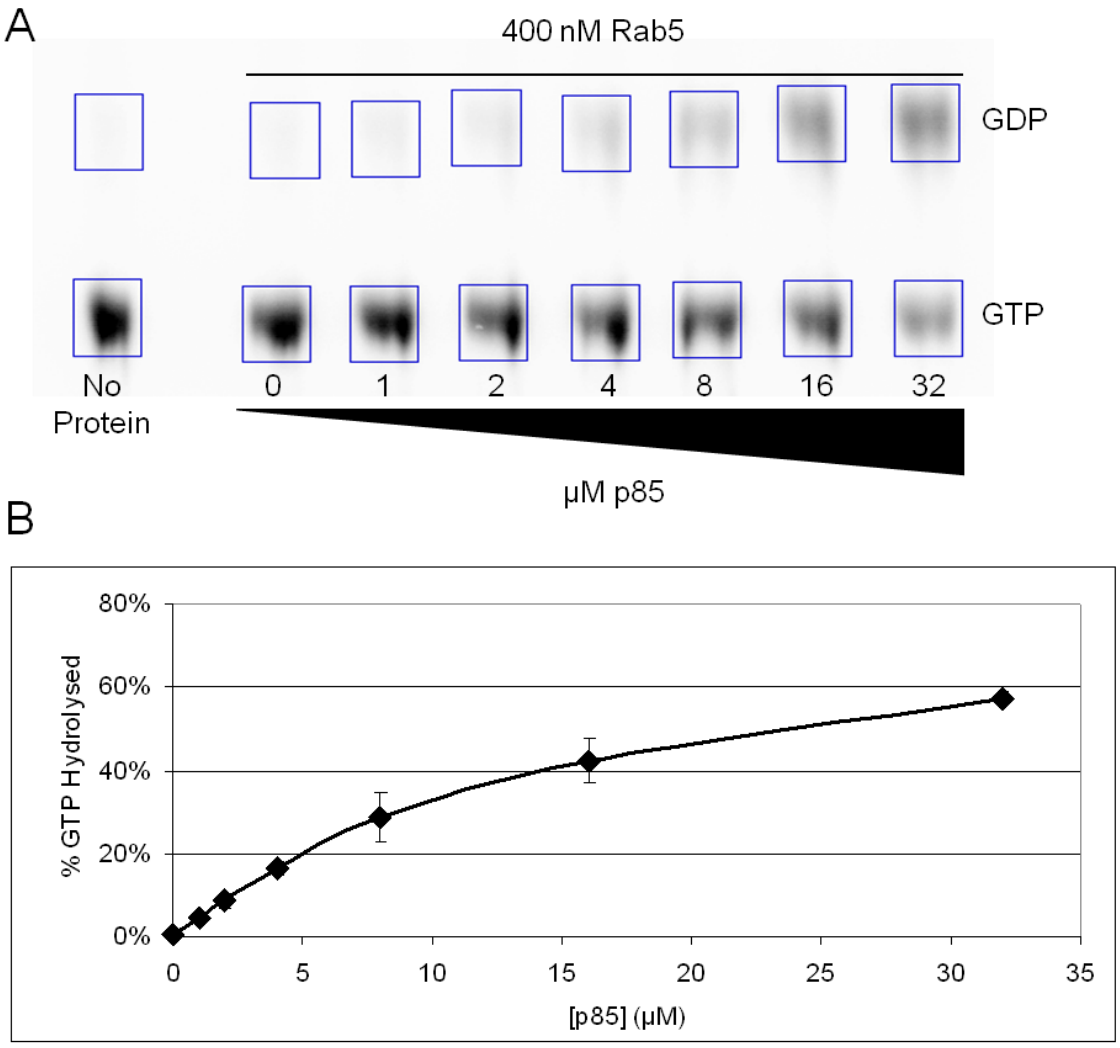

Figure 4.3 – Analysis of p85 Rab5GAP activity using GAP assay. Increasing concentrations of p85 were incubated with or without 400 nM Rab5 in the presence of Mg^{2+} and [α-^{32}P]GTP for 15 minutes in order to measure the GTP hydrolysis of the purified p85 sample compared to the GTP hydrolysis in the p85+Rab5 samples. **A)** Nucleotides were resolved using PEI cellulose-F TLC plates with a 0.75 mM KH_2PO_4 developing solvent. The plates were then exposed to a storage phosphor screen and imaged using a Phosphorimager. The results shown are typical for three independent experiments. **B)** Pixel densities were quantified using the Gel-Doc 2000 system using Quality One software and plotted using Microsoft Excel. Mean +/- standard deviation for three independent experiments.

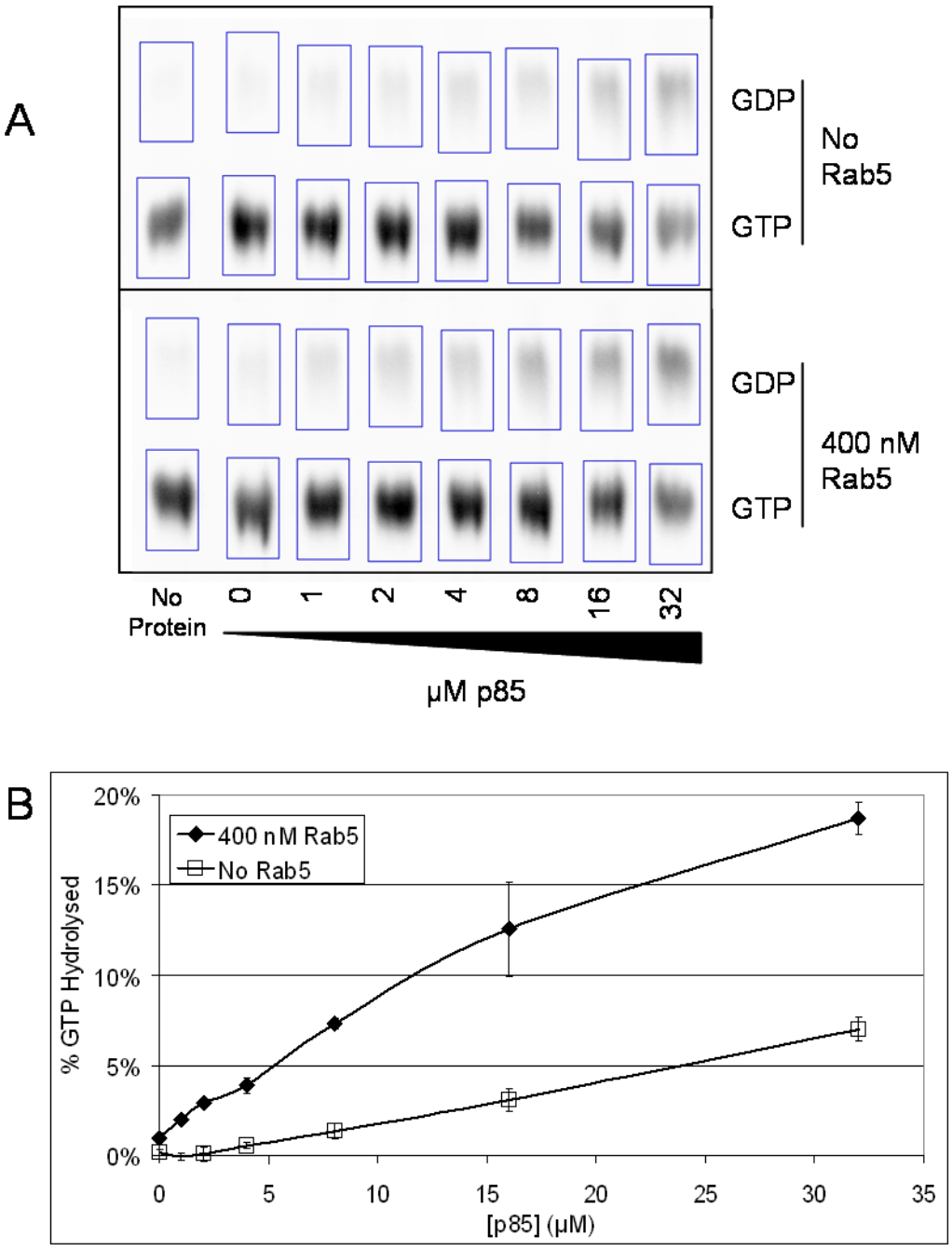

Figure 4.4 – p85 samples appear contaminated with an unknown GTPase protein. 400 nM Rab5 was incubated in the presence of Mg^{2+}, [α-^{32}P]GTP, and increasing concentrations of p85 for 15 minutes. Similar control assays were also carried out in the absence of Rab5. **A)** Nucleotides were resolved on PEI Cellulose F TLC plates as per standard GAP assay procedure. **B)** Pixel densities were quantified using the Gel-Doc 2000 system using Quality One software and plotted using Microsoft Excel. Mean +/- standard deviation for three independent experiments.

of a Rab5-GDP that was likely not efficiently exchanged for [α-^{32}P]GTP by EDTA and Mg^{2+} treatments. Typically, ultraviolet spectra of protein samples had a 'shoulder' at 260 nm caused by the presence of phenylalanine residues (with some contribution from tyrosine and tryptophan), but this should be proportional to the much larger signal absorbed at 280 nm from phenylalanine, tyrosine, tryptophan, and—to a much lesser extent—cysteine residues (Pace *et al*., 1995) (Fig. 4.5). The result is an A_{280}/A_{260} ratio that may be calculated from the amino acid composition. The most common contaminant in protein samples which absorbs at 260 nm are nucleotides and nucleic acids (Glasel, 1995). As Rab5 is known to be a small monomeric G-protein that binds nucleotides (specifically GDP and GTP) *in vivo*, and that it shows intrinsic GTP hydrolysis activity, it was likely that GDP was remaining bound to Rab5 following its purification.

In order to analyze what fraction of the A_{260} signal was provided by the protein and how much was provided by the nucleotide the concentration of Rab5 (#Tryp = 2, #Tyr = 5, #Cys = 4, #Phe = 10) was determined. Using the formula of (#Trp x 5,500) + (#Tyr x 1,490) + (#Cys x 125) the ε_{280} of Rab5 is 18950 $M^{-1}\cdot cm^{-1}$ (Pace *et al*., 1995). Using data provided by Dr. Stanley Moore, based on the works of multiple studies (Edelhoch, 1967; Pace *et al*., 1995; Wetlaufer *et al*., 1958), the ε_{260} of Rab5 was calculated using the formula ε_{260} ($M^{-1}\cdot cm^{-1}$) = (#Phe x 144) + (#Tyr x 600) + (#Trp x 3,300). From this, an ε_{260} of Rab5 was determined to be 11,040 $M^{-1}\cdot cm^{-1}$. The ε_{260} of guanosine has been reported as 11,500 $M^{-1}\cdot cm^{-1}$(Cantor *et al*., 1970). An A_{260} measurement was used to calculate Rab5 protein concentration using the Beer-Lambert Law ($A=\varepsilon cl$ where A = absorbance, c = concentration, l = path length). The theoretical absorbance of Rab5 at 260 nm based on the concentration determined at 280 nm was then calculated, and subtracted from the observed A_{260} (Fig. 4.5B). The difference was presumed to be due to a nucleoside and, using the ε_{260} of guanosine (same ε_{260} for guanine) the relative percent saturation was calculated. It was determined that the purified Rab5 samples were contaminated with nucleotide, with saturations ranging from 45% to 100%.

4.2 Optimization of Protein Purification

Both the p85 and Rab5 samples required additional purification steps to remove contaminants. For the p85 samples, GTP-hydrolyzing activity contaminants needed to be removed (4.2.1). Rab5 required purification in order to minimize bound nucleoside (4.2.2).

A

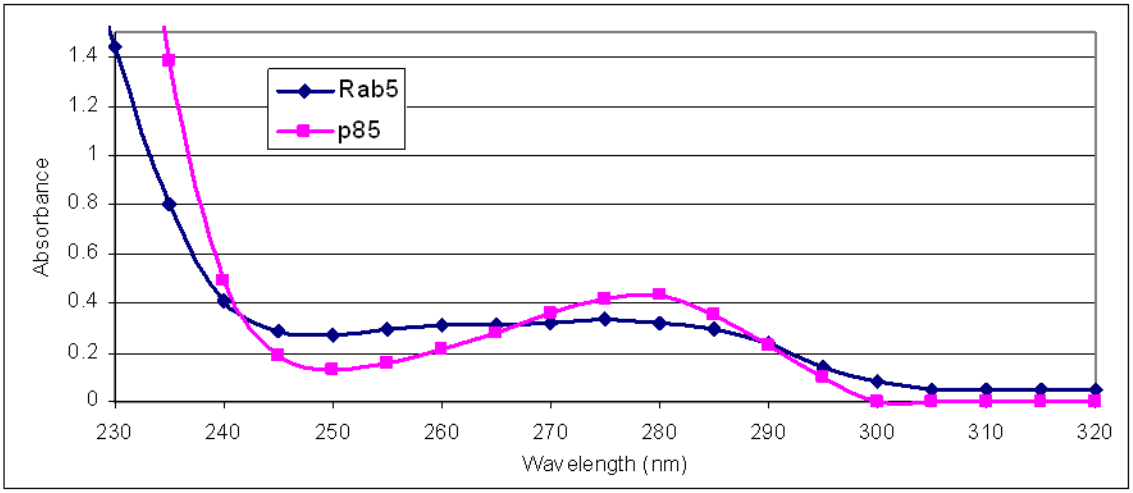

B

Protein Concentration derived from absorbance at 280 nm

$A_{280} = \varepsilon cl$

$0.991 = (18{,}950\ M^{-1}\cdot cm^{-1})c(1\ cm)$

$c = 16.73\ \mu M$ Rab5

Theoretical absorbance at 260 nm of 16.73 µM protein

$A_{260} = \varepsilon cl$

$A_{260} = (11{,}040\ M^{-1}\cdot cm^{-1})(16.73\ \mu M)(1\ cm)$

$A_{260} = 0.185$

Observed A_{260} – Theoretical A_{260}

$A_{260\ Observed} - A_{260\ Theoretical} = A_{260\ Net}$

$0.310 - 0.185 = A_{260\ Net}$

$A_{260\ Net} = 0.125$

Guanosine nucleside concentration derived from $A_{260\ Net}$

$A_{260} = \varepsilon cl$

$0.125 = (11{,}500\ M^{-1}\cdot cm^{-1})c(1\ cm)$

$c = 10.87\ \mu M$ guanosine

Therefore, approximately 65% of the Rab5 molecules are contaminated with guanosine, assuming 1:1 binding.

Figure 4.5 – Rab5 contains bound nucleosides. A) Purified Rab5 and p85 were subjected to spectrophotometric analysis measuring the absorptions between 230 and 320 nm in increments of 5 nm. Absorptions were entered into Microsoft Excel and graphed. The absorbance spectrum of purified p85 is typical for proteins not contaminated with nucleotide, with a distinct trough at 255 nm. Rab5 shows a markedly higher signal than is typical at 260 nm, which is indicative of nucleic acid contamination. **B)** Sample calculation used to determine % nucleotide saturation of Rab5.

4.2.1 Alteration of GST-p85 Protein Purification Procedure

The first series of trials involved the addition or substitution of reagents to the standard PreScission protease buffer that was used during the purification of the GST-p85 proteins. The standard lysis buffer used contains 1% Triton X-100, a non-ionic surfactant capable of breaking down the plasma and nuclear membrane of a cell. This detergent was substituted for the less stringent detergent NP-40 at a concentration of 0.5%. In some trials, the concentration of NaCl was raised to 0.5 M instead of the standard 0.15 M in order to disrupt ionic bonds which may be forming between p85 and other proteins. In order to try to break any non-covalent bonds present between p85 and an unknown protein, 0.5 M urea was also added to on treatment. BL21 cells that were induced to produce GST-p85 were lysed in all of these different buffers. Soluble GST-p85 proteins were recovered using glutathione Sepharose resin and cleaved from the GST tag using PreScission protease. The resultant proteins were analyzed using a GAP assay with and without Rab5 proteins.

The percent GTP hydrolyzed was very similar across all of the different conditions (Fig. 4.6A). The only exception to this appeared to be the condition where the standard PreScission buffer used during p85 purification contained 0.5 M NaCl which resulted in increased GTP hydrolysis in the absence of Rab5. Due to the fact that all of the other conditions yielded very similar results, it was decided that this experiment was an outlier and represented human error. All of the p85 samples were pooled together except for the one isolated in the standard PreScission buffer with 0.5 M NaCl. This pooled p85 sample was further analyzed for GTP hydrolysis and Rab5GAP activities over a concentration range of p85 (Fig. 4.6B). It was found that the purified p85 continued to show the ability to hydrolyze GTP (~5%) independent of Rab5 in all of the conditions regardless of these changes to the PreScission buffer during purification. As such, it was decided to utilize the original purification procedure, but more thoroughly wash the GST-p85 proteins while bound to glutathione Sepharose resin prior to the addition of PreScission protease to remove any contaminants which may have bound to p85 or the resin itself.

4.2.2 Removal of Contaminating Nucleotide from Rab5

In order to efficiently load new nucleotide (i.e., [α-^{32}P] GTP, GTP, GTPγS, and GppCp) onto Rab5, bound nucleotides associated with Rab5 during purification must first be removed.

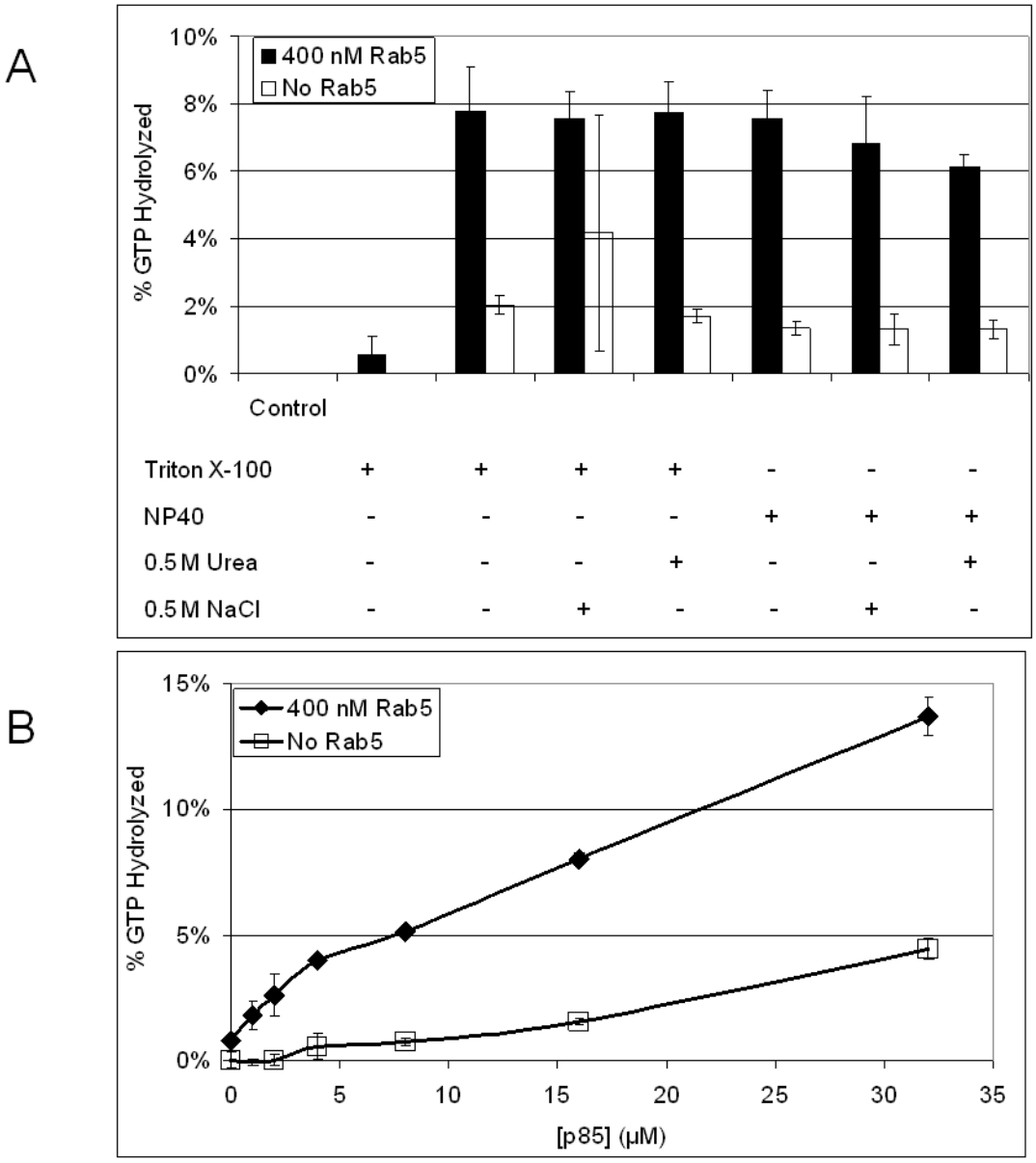

Figure 4.6 – Comparison of Rab5-dependent and Rab5-independent GTP hydrolysis in the presence of p85 purified using different purification conditions. A) p85 proteins were purified using standard PreScission buffer (50 mM Tris-HCl, pH 7.0, 150 mM NaCl, 1 mM EDTA, 1 mM DTT) under six different modifications. These include increasing the concentration of NaCl to 0.5 M and adding 0.5 M urea. In the standard protein purification procedure 1% Triton X-100 is added to cell lysates prior to centrifugation, though three of six samples substitute this for 0.5% NP-40. Following purification, p85 samples were assayed at a single concentration (15 µM) for GTP hydrolysis in the presence or absence of 400 nM Rab5. **B)** GTP hydrolysis of a titration of p85 pooled in all above conditions except normal PreScission + Triton X-100+ 0.5 M NaCl in the presence and absence of Rab5. Experiment was done twice with the mean +/- standard deviation shown.

As Rab5 requires Mg^{2+} to bind nucleotide effectively (Pan *et al*., 1996), EDTA was added to ten times the 1 mM EDTA normally found in PreScission buffer during Rab5 purification. It was hoped that the higher concentration of EDTA would chelate the Mg^{2+}, thereby removing it and any bound nucleotide from Rab5. However, spectrophotometric analysis of the purified Rab5 samples continued to suggest the presence of nucleotide at roughly the same concentrations as in Rab5 proteins purified in PreScission buffer containing normal concentrations of EDTA.

Two published methods (John *et al*., 1990; Simon *et al*., 1996) were modified to be used with what materials were available in our laboratory in an effort to produce nucleotide-free Rab5. GST-Rab5 was immobilized on glutathione Sepharose resin and treated with the high-EDTA PreScission buffer to remove any free Mg^{2+} from the solution. The beads and their bound GST-Rab5 proteins were treated with alkaline phosphatase and/or snake venom phosphodiesterase overnight. The alkaline phosphatase hydrolyzes phosphate bonds, while phosphodiesterase removes diester bonds. These two enzymes should degrade any GDP or GTP that was Rab5-associated into guanosine monophosphate (GMP). The hydrolyzed GMP would be expected to have a lower affinity for Rab5 and be released. The original procedure called for the addition of GppCp, a non-hydrolyzable form of GTP, to be added during the alkaline phosphatase treatment, presumably to replace degraded GDP which was the original reason for the phosphodiesterase. This step was omitted as it was not seen to be necessary. However, spectrophotometic analysis showed similar spectra to the Rab5 not treated with these enzymes (data not shown, refer to Fig. 4.5). Furthermore, Rab5 proteins treated with snake venom phosphodiesterase showed marked degradation compared to those not treated, as seen in the bead washes following PreScission cleavage (Fig. 4.7).

4.2.3 Ion Exchange Chromatography of p85

It was observed that in many cases purified p85 samples contained multiple small molecular weight bands aside from the expected 84 kDa band representing p85 on a Coomassie stain gel. The most prominent of these was a band of approximately 75 kDa (Fig. 4.8A). In an effort to further purify p85, PreScission-cleaved p85 samples were subjected to ion exchange chromatography. Because p85 has a pI of 5.74 it was determined that anion exchange

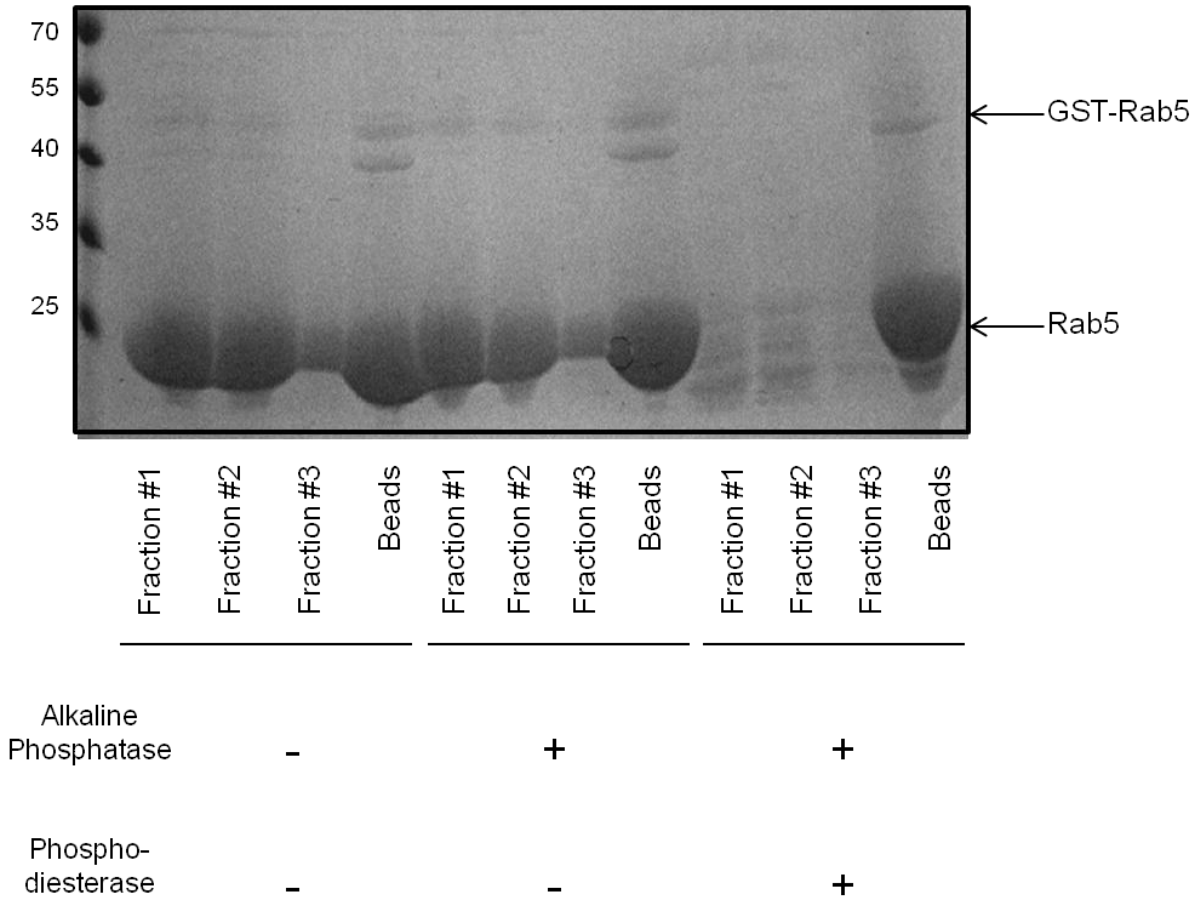

Figure 4.7 – Removal of GTP/GDP from Rab5 leads to degradation of Rab5. GST-Rab5 proteins were immobilized on glutathione Sepharose resin and separated into three batches. The first batch was cleaved with PreScission protease. After 48 hours the beads are washed with cold buffer and the fractions are collected. The second batch was treated with 5 units/mL alkaline phosphatase overnight at 18 °C, washed to remove enzyme, and treated with PreScission protease and collected. The third batch was treated with alkaline phosphatase as above, washed, and treated with 5 units/mL snake venom phosphodiesterase overnight at 15 °C, washed, and treated with PreScission protease and collected. Aliquots from all samples were resolved using 15% SDS-PAGE and visualized with Coomassie Blue stain.

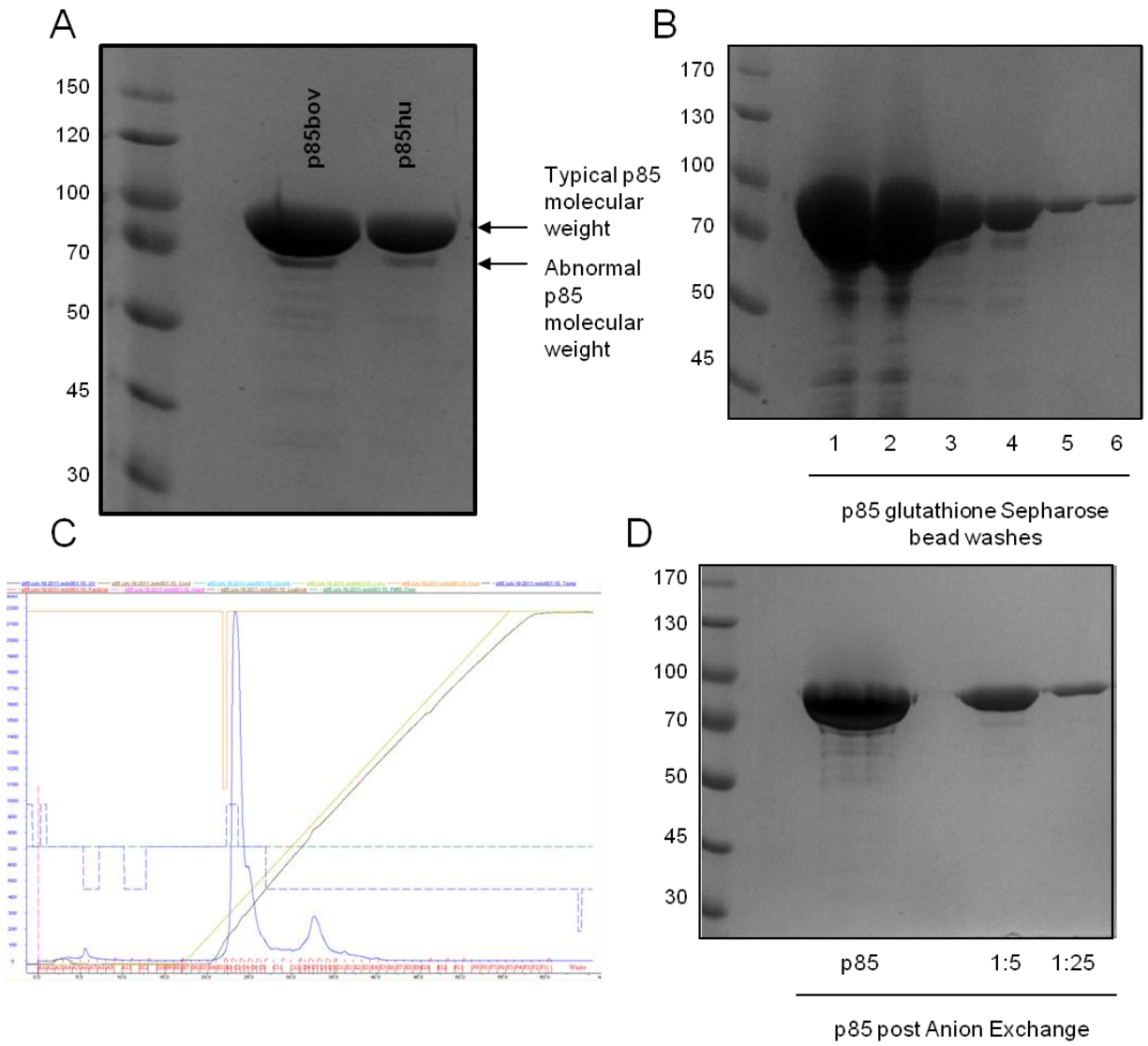

Figure 4.8 – Ion exchange chromatography improves p85 purity. p85 proteins were purified using the standard protein purification procedure and resolved using 12% SDS-PAGE and visualized with Coomassie Blue stain. **A)** Purified p85 bovine (bov) and human (hu) were resolved using a 10% SDS-PAGE gel. **B)** p85 proteins washed from glutathione Sepharose resin after cleavage from their GST-tags by PreScission protease. Shown are aliquots (10 µL) of the first six washes of the beads which were collected in 2 mL volumes. **C)** Elution profile of p85 purification using ÄKTA$_{FPLC}$™. Blue line represents the A_{280} reading, denoting protein in a particular fraction. Light green denotes the progress of the programmed procedure, brown denotes the salt gradient from 0.05 M to 1 M NaCl. **D)** Pooled p85 after being purified using anion exchange chromatography. Included is an undiluted sample as well as a 1:5 dilution and a 1:25 dilution, each with 10 µL loaded onto the gel, resolved and stained with Coomassie Blue.

chromatography at pH 8.0 using a Resource Q column would be the most effective means of purifying p85. This technique resulted in a significant improvement in the purity of p85 (Fig. 4.8B and C). However, these purified p85 samples did not appear to provide different GAP assay results compared to the p85 proteins which were not purified with anion exchange chromatography (data not shown).

4.2.4 Ion Exchange Chromatography of Rab5

It was decided to also attempt to further purify Rab5 by ion exchange chromatography to attain the most pure proteins possible for future assays. In addition, it was hoped that the technique's ability to separate proteins based on charge would allow for the separation of contaminating nucleotides, or even the separation of Rab5 in different nucleotide-bound states. As Rab5 has a pI of 8.22, it was decided that cation exchange chromatography in the range of 5.5 to 6.5 using a Resource S column would be optimal. Unfortunately, all attempts to have Rab5 bind to the cation exchange media failed, as did attempts to bind Rab5 to anion exchange media under the same conditions used to purify p85.

4.2.5 Dynamic Light Scattering (DLS) Analysis of p85 and Rab5 Samples

DLS analysis was carried out on all proteins intended for SPR studies. DLS allows for the measurement of the diameter of particles in solution, and can be used to analyze if there are higher or lower molecular weight particles in solution aside from the target protein. Using this technique it is possible to identify the presence, and even the percent total mass, of particles which do not match the desired size of the protein, providing a measure of heterogeneity/homogeneity of the samples. Using standard data on the relative hydrodynamic radius of globular proteins of specific molecular weights, it is possible with a fair degree of certainty to estimate the molecular mass of the detected particles. When originally used to analyze p85 in its original BIAcore buffer (50 mM HEPES, pH 8.0, 150 mM NaCl), a large number of particles of high hydrodynamic radius were detected which was suggestive of aggregation (Fig. 4.9A). In an effort to reduce or prevent this aggregation, 0.05% Tween-20 was added to the above buffer. This greatly decreased the amount of high hydrodynamic radius particles and produced a solution which was monomodal with a polydispersity between 6-12%. Polydispersity measures the fraction of particles in the sample which are of non-uniform size.

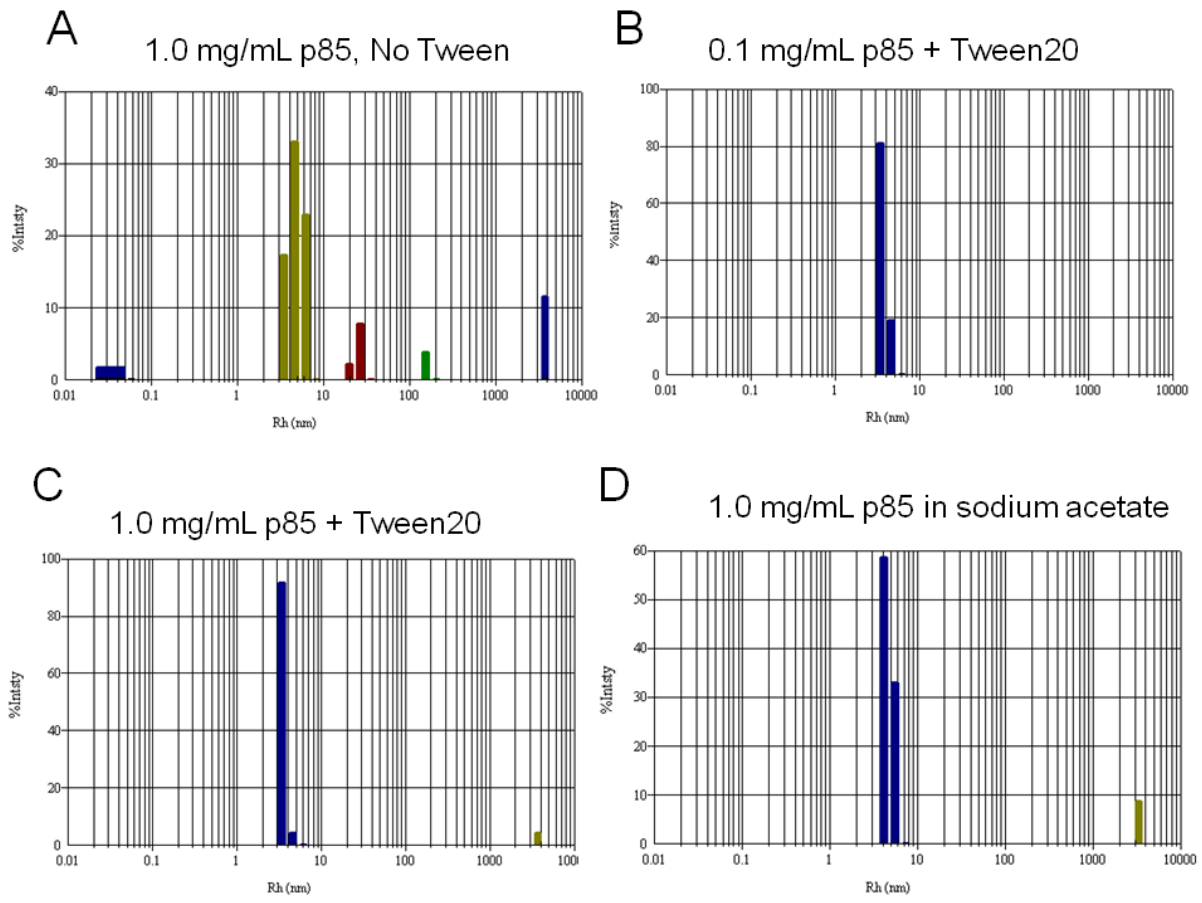

Figure 4.9 – Dynamic light scattering spectra of p85. p85 proteins were analyzed by DLS to analyze the hydrodynamic radius (Rh) of the particles in solution and what percentage of the total solute concentration was made up of particles of that radius (%Intsty = Percent Intensity). Each individual Bar represents the intensity of a given Rh, while each colour defines a different population highlighted by the analysis software. **A)** 1.0 mg/mL p85 in standard BIAcore Running buffer with no Tween-20. **B)** 0.1 mg/mL p85 in BIAcore Running buffer (50 mM HEPES, pH 8.0, 150 mM NaCl) in the presence of 0.05% Tween-20 to prevent aggregation. **C)** 1.0 mg/mL p85 BIAcore Running buffer (50 mM HEPES, pH 8.0, 150 mM NaCl) in the presence of 0.05% Tween-20 to prevent aggregation. **D)** 1.0 mg/mL p85 in 50 mM sodium acetate, pH 7.0, 50 mM NaCl.

These results indicate that between 88% and 94% of the solution contained particles of the same hydrodynamic radius as p85 as a monomer or dimer at concentrations of 0.1 and 1.0 mg/mL (Fig. 4.9B and C). As detergent may interfere with GAP activity, only p85 samples used in SPR studies contained the added 0.05% Tween-20. It was also observed that if p85 is stored in a solution of 50 mM sodium acetate, 50 mM NaCl, pH 7.0, it also appeared to have equally low polydispersities (Fig. 4.9D). However, it was observed in binding studies that storage in this buffer appears to ablate the ability of p85 to bind to Rab5 effectively and as such this buffer was not used for SPR studies.

Rab5 samples were observed to have similar polydispersities as the p85 samples in the presence of Tween-20 in the absence of any added detergents, and it was determined they were not needed to ensure monomodal distribution (data not shown).

4.3 ppPDGFR Peptide Competes with Activated Wild Type PDGFR

The p85 protein is known to bind to phosphorylated PDGFR through both of its SH2 domains which causes a conformational change in p85 (Piccione *et al*., 1993; Shoelson *et al*., 1993). In order to ascertain if this conformational change impacts the GAP activity previously shown for p85 towards Rab5 *in vitro*, GAP assays would have to be performed in the presence of activated PDGFR. However, due to the difficulties associated with using large eukaryotic integral membrane receptor protein complexes in such an assay, a small phosphopeptide called ppPDGFR peptide (sequence: DGGpYMDMSKDESVDpYVPML) was used. In addition to the ppPDGFR peptide the corresponding nonphosphorylated peptide, called PDGFR peptide (sequence: DGGYMDMSKDESVDYVPML), was also used as a negative control. Previous studies using the same peptides showed that only the phosphorylated peptides bound to p85 and induced the appropriate conformational change (Panayotou *et al*., 1992; Shoelson *et al*., 1993).

Experiments were performed to assess the functionality of these custom synthesized peptides prior to using them in the GAP assays. A GST-p85 pull-down assay had been used previously to bind activated and phosphorylated PDGFR from mammalian cell lysates. Each peptide was tested for its ability to compete with full-length PDGFR binding to GST-p85 immobilized on glutathione Sepharose resin (Fig. 4.10A). NIH 3T3 cells were activated for five minutes with PDGF and lysed in the presence of sodium orthovanadate and protease inhibitors to preserve the phosphorylated state and integrity of the activated PDGFR.

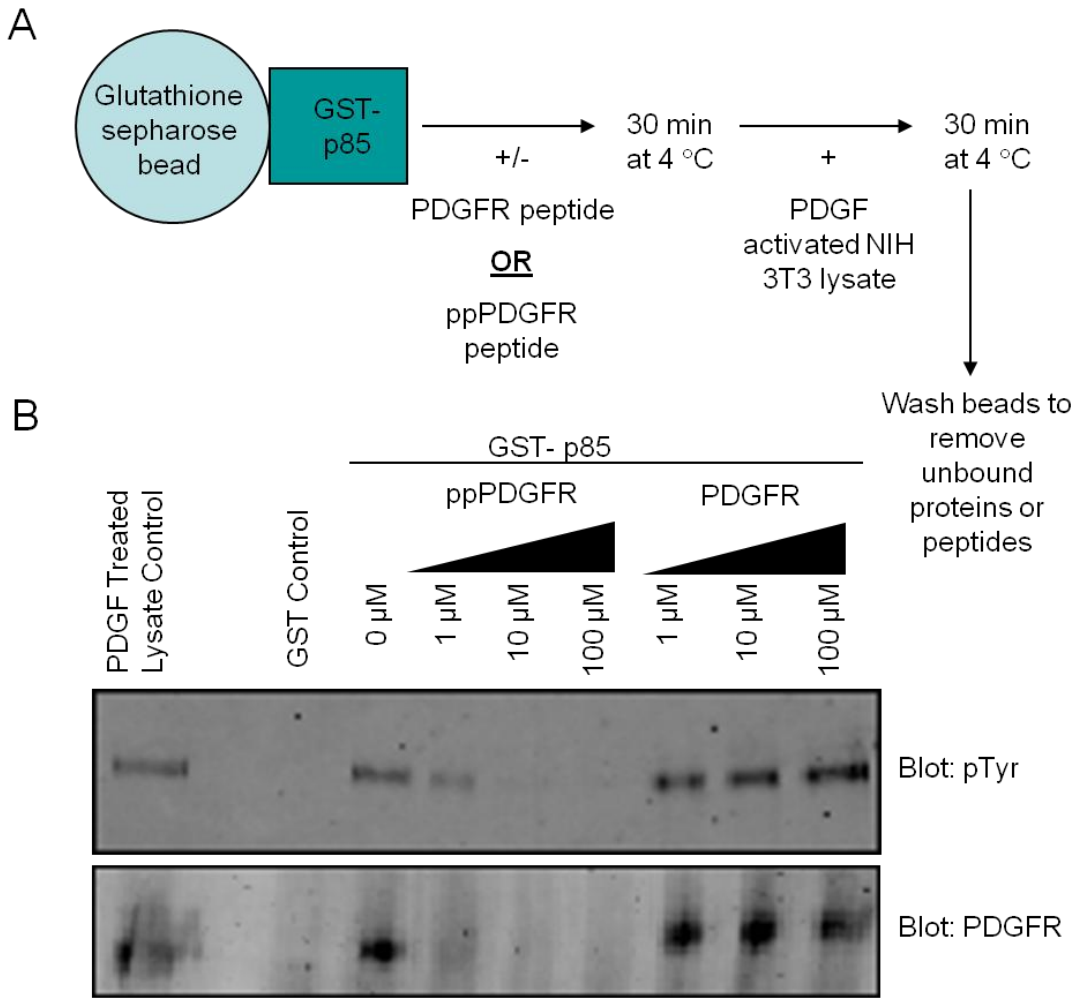

Figure 4.10 – ppPDGFR peptide competes with activated PDGFR for p85 binding while the corresponding unphosphorylated peptide does not. A) Experimental strategy. GST-p85 fusion proteins were immobilized on glutathione Sepharose resin and incubated in the presence or absence of either ppPDGFR peptide or PDGFR peptide. Lysates from NIH 3T3 cells which had been activated for 5 minutes with PDGF were added and activated PDGFR were allowed to bind. Non-bound proteins and/or peptides were washed off. **B)** The beads were recovered and resolved on a 7.5% SDS-PAGE gel and transferred to a nitrocellulose membrane. The membrane was analyzed by Western blot analysis. The membranes were blocked in either milk (PDGFR) or BSA fraction V (pTyr). The results of the Western Blot were visualized using the LI-COR Odyssey Infrared Imager. The results shown are typical for at least three independent experiments.

GST-p85 was diluted to a concentration of 0.1 µg/µL bound to glutathione Sepharose in a total volume of 100 µL. The samples were pre-incubated with increasing concentrations of either the ppPDGFR peptide or the PDGFR peptide. PDGF-activated NIH 3T3 cell lysate (200 µL; 20% of a 10 cm plate) was added and allowed to bind with immobilized GST-p85. The beads were washed thoroughly and analyzed by Western blotting to detect both PDGFR and tyrosine phosphorylated PDGFR proteins (pTyr) (Fig. 4.10B). In the absence of peptide, tyrosine phosphorylated PDGFR bound to the immobilized GST-p85 as expected but not to the control protein, GST. The ppPDGFR peptide competed with the wild type activated PDGFR at concentrations as low as 1 µM and showed complete competition at 10 µM. In contrast, the unphosphorylated PDGFR peptides did not compete with the activated PDGFR from the NIH 3T3 lysate. This shows that the ppPDGFR peptide is a suitable alternative to wild type activated PDGFR when studying the effects of the PDGFR on p85:Rab5 interactions.

4.4 GTPase Activating Protein (GAP) Assays

In order to determine the effectiveness of a protein to serve as a GAP (i.e. p85) for other proteins (i.e., Rab5) the GAP assay was used. This assay consists of loading the Rab5 GTPase protein with the [α-^{32}P]GTP and incubating it with increasing concentrations of the p85 Rab5GAP protein for a set amount of time prior to stopping the reaction. The samples are then loaded onto a PEI cellulose-F plate and resolved. The PEI (polyethylenimine) acts as a cationic polymer that will separate purine and pyrimidine nucleotides based on their respective nucleosides and free bases (Gupta *et al.*, 1976; Reyes, 1972). The [α-^{32}P]GTP and [α-^{32}P]GDP were resolved using a buffer of 0.75 M KH_2PO_4 as established previously (Anderson and Chamberlain, 2005). Data from the TLC plates were captured using a storage phosphor screen and quantified using a phosphorimager (Fig. 4.2).

A series of GAP assays were performed with different combinations of proteins, though the primary focus was on the analysis of p85 GAP activity towards Rab5. In addition, due to observations made during the course of this study, the GAP activity of p85 towards other Rab proteins (Rab4, Rab7, and Rab11) were also studied. Lastly, the Rab5GAP activity of the Tau protein was studied in collaboration with Grégoire Morisse of the laboratory of Dr. Nicole Leclerc at the Université de Montréal in Montreal, Quebec, Canada.

4.4.1 GAP Assay Analysis of p85:Rab5 Interactions

Previous work in our lab had shown that p85 interacts with Rab5, functioning as a Rab5GAP (Chamberlain *et al*., 2004). A titration of p85 was chosen for analysis ranging from 0 µM p85 to 32 µM p85, diluted serially. These p85 samples were incubated with 200 to 600 nM of Rab5 loaded with [α-^{32}P]GTP and assayed for 10 to 20 minutes depending on the experiment and the observed of activity of the protein preparations in question. Previous data had shown that there was 570- to 1700-fold increase in the rate of Rab5-mediated GTP hydrolysis upon addition of high concentrations of p85. This was calculated by taking the average percentage of GTP hydrolyzed by Rab5 in the presence of p85 at higher concentrations and dividing it by the average percent GTP hydrolyzed of Rab5 in the absence of p85 (Fig. 4.3). In order to reduce batch variation between radiolabelled GTP, a nucleotide-alone sample was also run with the % GDP subtracted as a background control. This value depended on the batch of the p85 and Rab5 preparations used, and was consistent with previously recorded data that supported p85 being a Rab5GAP (Chamberlain *et al*., 2004). However, further assays of this type showed a marked drop in the degree of GTP hydrolysis, likely tied to issues surrounding protein purity (Fig. 4.4).

4.4.2 Impact of PDGFR Binding on p85 GAP Activity Towards Rab5

Further GAP assays were performed using the synthesized PDGFR-analog peptides to analyze the effects of the PDGFR protein binding on Rab5GAP activity of p85. These assays were performed using the same procedure as the standard p85:Rab5 GAP assays, but with the addition of 100 µM of the peptides to the p85 reaction mixture. These peptides were allowed to bind to p85 for 30 minutes at 4 °C prior to initiation of the reaction. GTP hydrolysis (%) results from each of the three conditions (p85:Rab5, ppPDGFR:p85:Rab5, and PDGFR:p85:Rab5) were normalized to that for Rab5 alone and plotted on a graph (Fig. 4.11). It was determined that the PDGFR peptide and ppPDGFR peptide did not affect the ability of p85 to function as a Rab5GAP.

4.4.3 Testing the Tau Protein as a Possible Rab5GAP

Tau proteins are proteins which are found primarily in neurons of the central nervous system (Drubin and Kirschner, 1986). Their primary function is to stabilize microtubules,

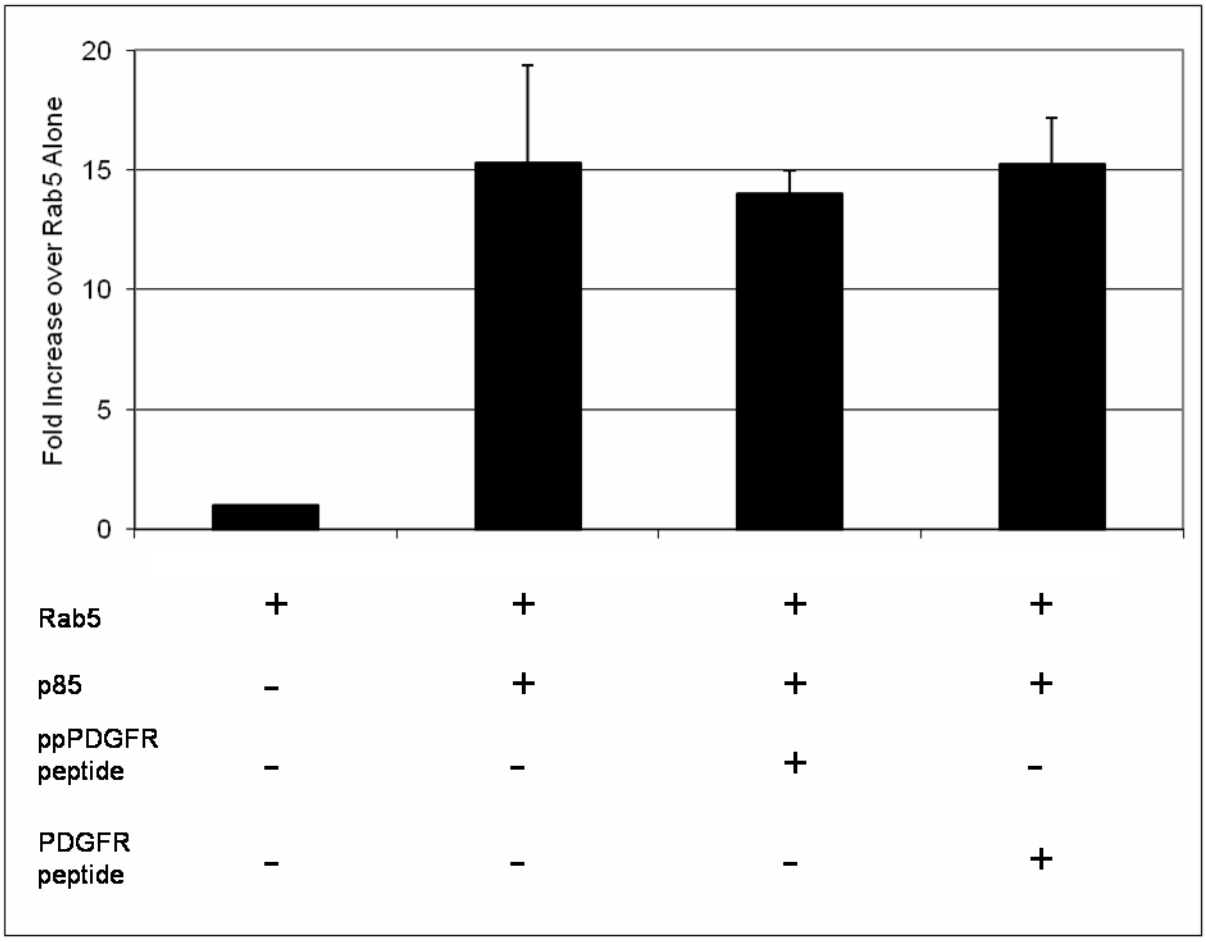

Figure 4.11 – Comparison of GAP activity of p85 towards Rab5 in the presence and absence of ppPDGFR peptide and PDGFR peptide. Purified p85 proteins (15 μM) were incubated with 100 μM of peptide (ppPDGFR peptide or PDGFR peptide) for 30 minutes at 4 °C prior to performing the standard GAP assay. The % GTP hydrolysis was then measured, and normalized to the % GTP hydrolysis of Rab5 in the absence of p85 and/or peptide (2%). The results shown are the average of three separate experiments +/- standard deviation.

though Tau has also been shown to be involved in other processes such as signal transduction, actin cytoskeletal regulation, and vesicle transport (Cunningham *et al*., 1997; Drubin and Kirschner, 1986; Flanagan *et al*., 1997; Jenkins and Johnson, 1998; Mandelkow and Mandelkow, 1998). Unpublished work from Grégoire Morisse in the laboratory of Dr. Nicole Leclerc (Université de Montréal) has recently shown that Tau proteins interact with Rab5a, suggesting that they could be Rab5GAP proteins. In order to test this possibility, our lab was sent samples of purified Tau proteins. There were three proteins that were tested: wild type Tau, TauR379A, and TauR349A. The two R/A mutants of Tau were chosen in hopes of discovering which, if either, of the two mutated arginine residues were the catalytic 'arginine finger' typical of GAP proteins.

Though the proteins provided by Grégoire Morisse contained impurities (Fig. 4.12A), they were sufficiently pure to perform basic GAP assays as per our standard procedure in order to determine if they functioned as Rab5GAPs. Due to the limited quantities and relatively low concentrations of the Tau proteins, a titration of 0 µM to 10 µM was chosen for these studies. When assayed, all of the Tau proteins showed Rab5GAP activity, and the two mutants showed similar or higher Rab5GAP activities as compared to the wild type Tau protein (Fig. 4.12B and C). This suggested that the two arginines chosen for mutation were not the catalytic 'arginine finger' residue.

4.4.4 p85 GAP Activity Towards Other Rab Proteins

Previous data generated from our lab has shown that p85 has GAP activity towards other Rab proteins (Chamberlain *et al*., 2004). Additional unpublished data indicated that p85 has the greater GAP activity towards Rab7 compared to Rab5, with equivalent GAP activity towards Rab4 as Rab5 (Chamberlain, 2007). Also observed was that p85 appeared to have little or no GAP activity towards Rab11. As such, Rab4 and Rab11 were chosen to serve as positive and negative controls for p85 GAP assays.

When these control assays were performed, however, it was observed that p85 showed strong GAP activity towards Rab11. Because of this, GAP assays analyzing the effects of p85 on the GTP hydrolysis activity of Rab5 were repeated. These assays showed that p85 had

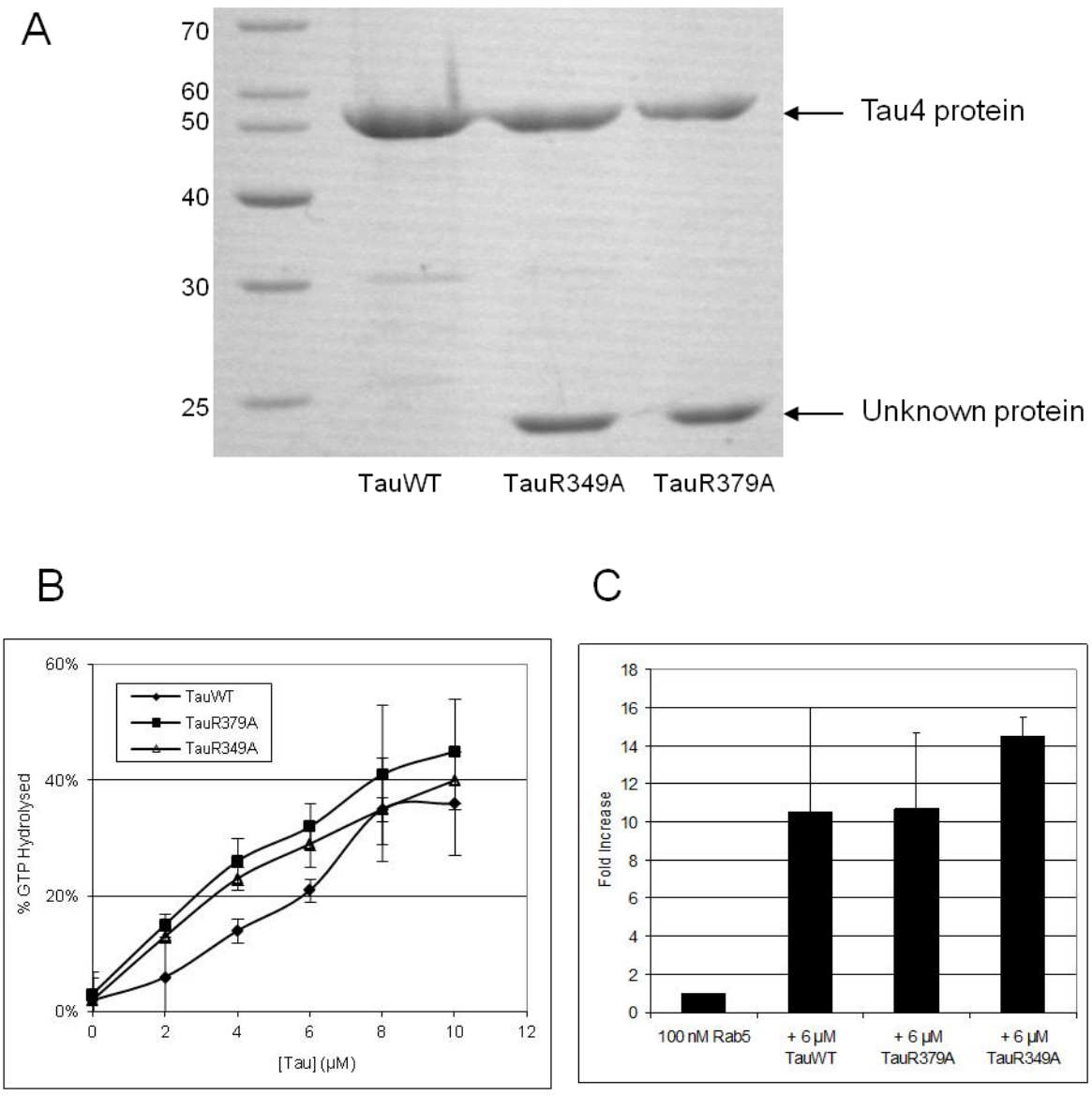

Figure 4.12 – Comparison of Rab5GAP activity of wild type Tau, TauR379A, and TauR349A. Tau proteins were analyzed using the standard GAP assay procedure except that 100 nM Rab5 was used and the titration was 0 to 10 μM Tau instead of 0 to 32 μM used for p85 proteins. **A)** Tau proteins were resolved by 12% SDS-PAGE and stained with Coomassie Blue. **B)** Tau proteins were analyzed by GAP assay and visualized as per the standard procedure. Values shown represent the mean +/- standard deviation from three independent experiments. **C)** The GTP hydrolysis at 6 μM Tau for all three Tau proteins was normalized to the % GTP hydrolysed by 100 nM Rab5 alone, with that value being 1. Values shown represent the mean +/- standard deviation for three independent experiments.

relatively equivalent GAP activity towards Rab4, 7, and 11 which was somewhat lower than its Rab5GAP activity (Fig. 4.13). It should be noted, however, that these assays were done during the period where p85 preparations were displaying Rab5-independent GTP hydrolysis. The GAP activity of p85 towards Rab11 was higher than this background activity, indicating that the observed differences from previous data were not simply due to contaminants in the p85 samples.

4.5 p85:Rab5 Binding Affinity Measurements Using Surface Plasmon Resonance (SPR)

Surface plasmon resonance (SPR) was used to measure the binding affinity of p85 to Rab5 *in vitro*. Surface plasmons are an optical phenomenon arising in thin metal films under conditions of total internal reflection. When light hits the metal surface, much of it reflects and is detected, but some of it is absorbed to form surface plasmons. By increasing the mass on the chip, it alters the amount of light that is absorbed, altering the resonance angle. This produces a sharp dip in the intensity of the reflected light at the resonant angle. The resonant angle itself is determined by many factors, including the refractive index of the medium, which itself is directly linked to the concentration of dissolved material in that medium. Using this information, it is possible to measure binding to the sensor chip surface. SPR analysis functions by having one protein, the bait protein, immobilized on a sensor chip. Over this is flowed another protein solution, known as the ligand protein. The binding affinity can be directly measured by a small change in the resonance angle due to the change in mass caused by the binding of the ligand protein to the bait protein (Fig. 1.8).

Rab5 was immobilized covalently by amine coupling onto a CM5 sensor chip to a density of approximately 3,000 RU (representing either resonance units or response units, and corresponding to a concentration of approximately 3 ng/mm^2). The Rab5 was pre-treated with 10 mM EDTA in an effort to remove any free or weakly associated Mg^{2+} in the Rab5 sample prior to immobilization and to remove bound nucleotide. Depending on the conditions of the experiment, nucleotide (GDP or a non-hydrolysable GTP analog) and Mg^{2+} were added to the running buffer. Mg^{2+} was added since Rab5 requires Mg^{2+} in order to bind to a nucleotide, while the nucleotides were added to analyze their effect on the Rab5:p85 binding. Initial experiments were done with an Mg^{2+} concentration of 20 mM and nucleotide concentrations of

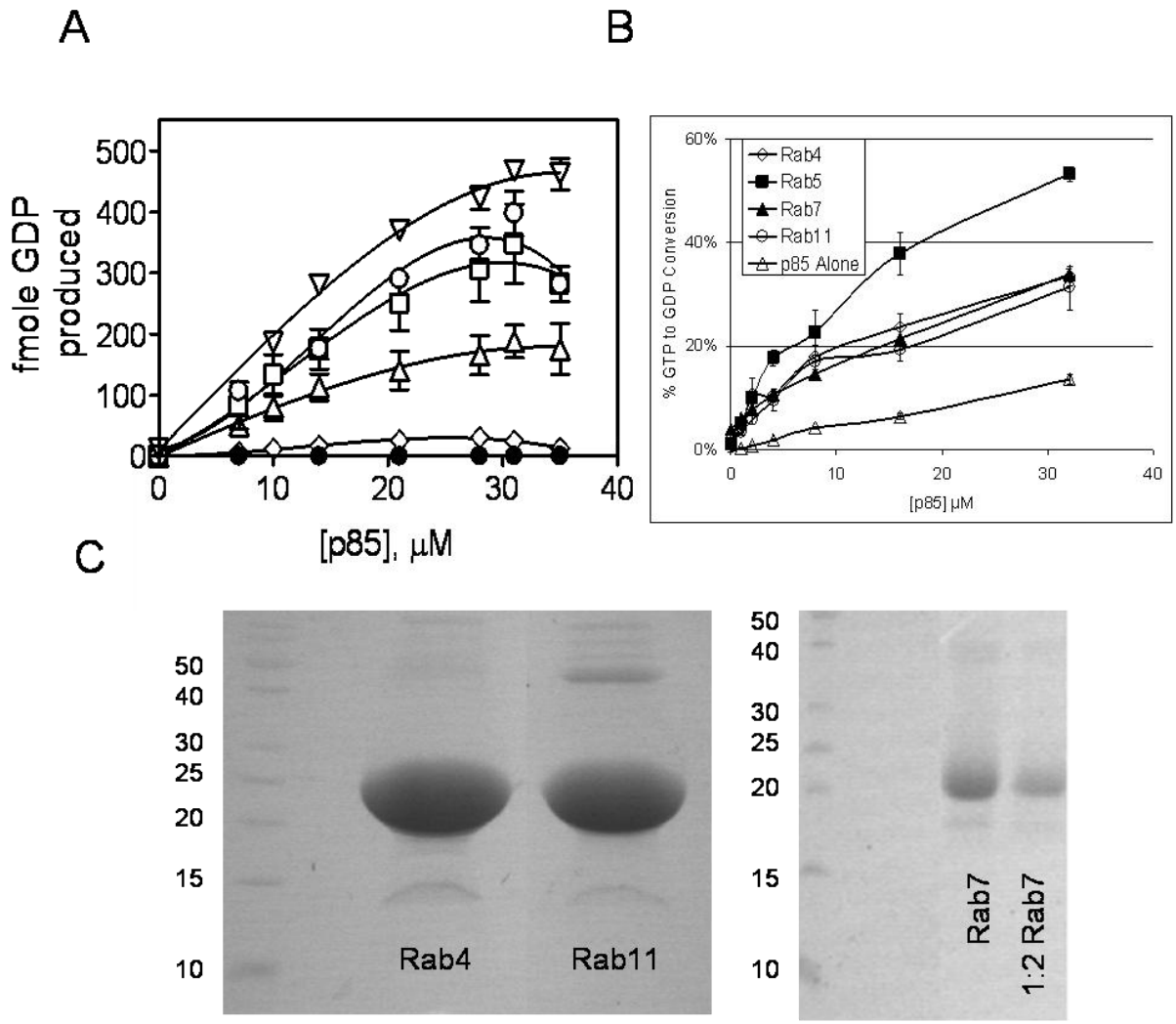

Figure 4.13 – Comparison of p85 RabGAP activity towards Rab4, Rab5, Rab7, and Rab11. Using the standard GAP assay procedure different Rab proteins were assayed for GTP hydrolysis at concentrations of 400 nM in the presence of increasing concentrations of p85. **A**) Shown is the p85 RabGAP assay data generated previously in our lab for the following proteins: Rab5 (circles), Rab4 (squares), Rab6 (triangles), Rab7 (inverted triangles), Rab11 (diamonds), no Rab (closed circles) (Chamberlain *et al*., 2004). **B**) GAP assay results for p85 was reanalyzed for the following proteins: Rab5 (filled squares), Rab4 (open diamonds), Rab7 (triangles), Rab11 (open circles), and no Rab (open triangles). Both graphs (A) and (B) show the mean +/- standard deviation for three independent experiments. **C**) Purified Rab4, 11, and 7 proteins from (B) were resolved using 15% SDS-PAGE and stained with Coomassie Blue stain to analyze purity. For reference on average p85 and Rab5 protein purity, refer to Fig. 4.1.

200 μM based on previous p85:Rab5 interaction assays such as the GAP assay (Anderson and Chamberlain, 2005).

Once Rab5 was immobilized and loaded with the desired cofactor, varying concentrations of p85 protein were flowed over the chip at a flow rate of 20 μL/min. The signal (ΔRU = Rab5 flowcell 2 – control flowcell 1) for each concentration of p85 was determined and graphed. Sample binding data for Rab5-GDP + p85 is shown (Fig. 4.14). When the ligand (p85) binds to the bait (Rab5) there is a sharp increase in the RU. The steeper the initial change in RU corresponds to the faster the on-rate of binding between the two binding partners. Following initial binding, the signal will begin to plateau, representing that the chip is reaching saturating conditions. At lower concentrations, the initial ΔRU is not as steep as there is less ligand to bind, while at higher ligand concentrations the peak plateau much earlier. The concentrations used in this experiment were chosen based on previously observed p85 titrations with respect to Rab5 (Chamberlain *et al*., 2004), and confirmed prior to binding studies.

Experiments were carried out with Rab5 in its three nucleotide-bound states: Rab5-NF, Rab5-GDP, and Rab5-GTP. Using these initial conditions, the binding affinities of the three nucleotide-binding states were determined, with p85:Rab5-NF had a K_D of 1.9 μM, while the K_D of the p85:Rab5-GDP and p85:Rab5-GTPγS (a non-hydrolysable GTP analog) were both 1.5 μM. While these affinity constants appear quite similar, it should be noted that the maximum binding for p85 to Rab5-NF was only approximately 25% compared with p85 binding to Rab5 in one of its nucleotide-bound states, which appeared to be much the same (Fig. 4.15A). This is likely due to the presence of nucleotides (likely GDP) on the ostensibly nucleotide-free Rab5-NF. If there is nucleotide still on some of the Rab5 immobilized to the chip, similar binding affinities will be observed, but lower total binding.

It was observed that following each of the binding study injections, there was a steady increase of the baseline signal. This signal proved very difficult to remove with any treatment that would not denature the Rab5 immobilized onto the sensor chip. As p85 is known to associate tightly with many of its ligands, it was determined that this accumulation of signal represented non-specific interaction between the p85 protein and the sensor chip. In an effort to minimize this non-specific interaction, some changes were made in the composition of the buffer to optimize results. The resultant running buffer contained 0.5 mM Mg^{2+} (originally

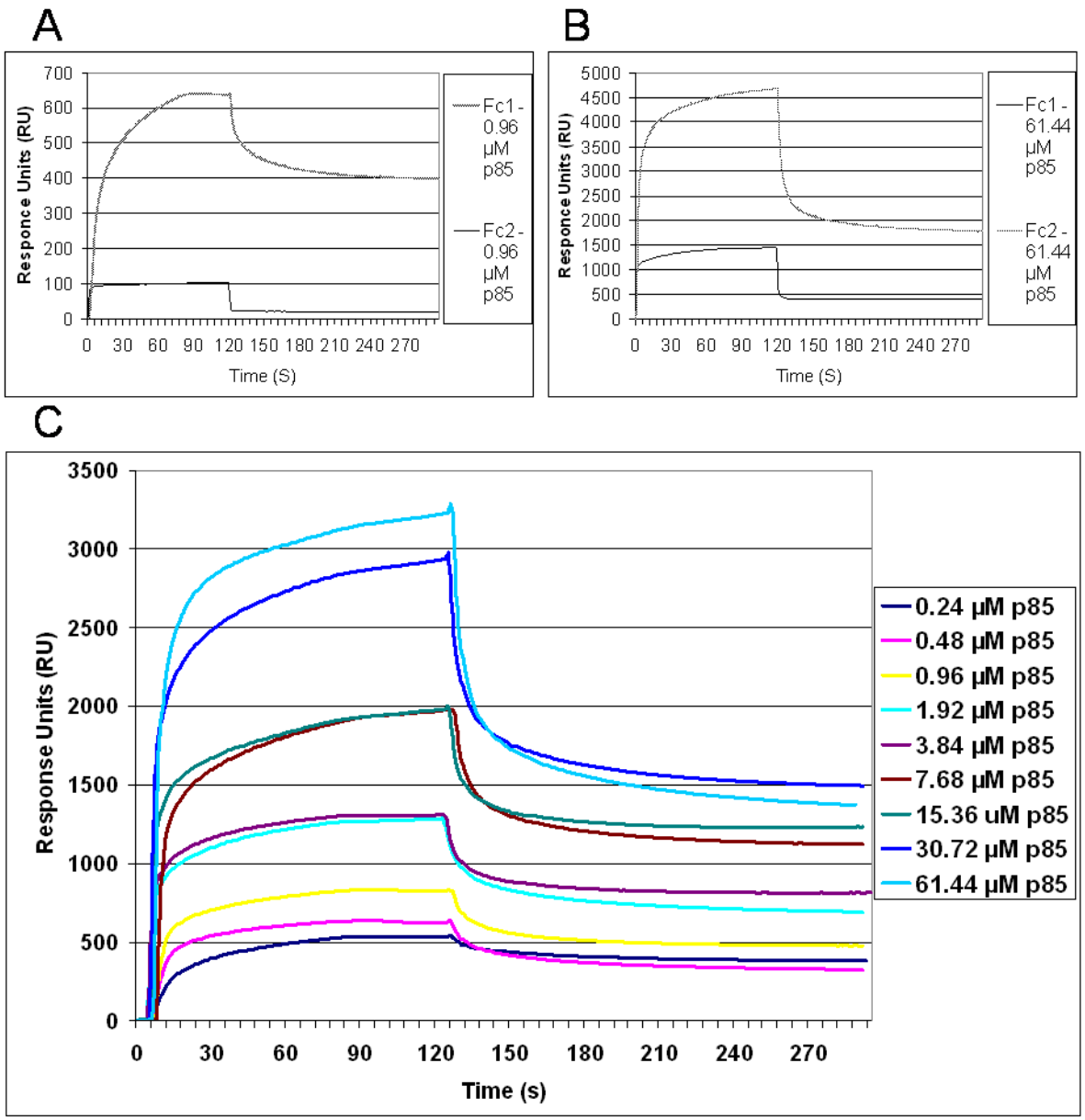

Figure 4.14 – Sensorgrams of p85 binding to immobilized Rab5. EDTA-treated Rab5 protein was immobilized onto a CM5 sensor chip to approximately 3000 RU of signal on Flowcell 2 (Fc2). Flowcell 1 (Fc1) was left clear of immobilized protein to act as a control. Nucleotide, if desired, was then added. Varying concentrations of p85 were then flowed over the chip at a flowrate of 20 µL/min for 120 seconds. **A)** The change in Fc1 and Fc2 signals for the injection 0.96 µM p85. **B)** The change in Fc1 and Fc2 signals for the injection of 61.44 µM p85. **C)** The change in Fc1 signal was subtracted from the change in Fc2 signal, producing the net (Fc2-Fc1) signal for a typical binding experiment for Rab5-GDP and p85.

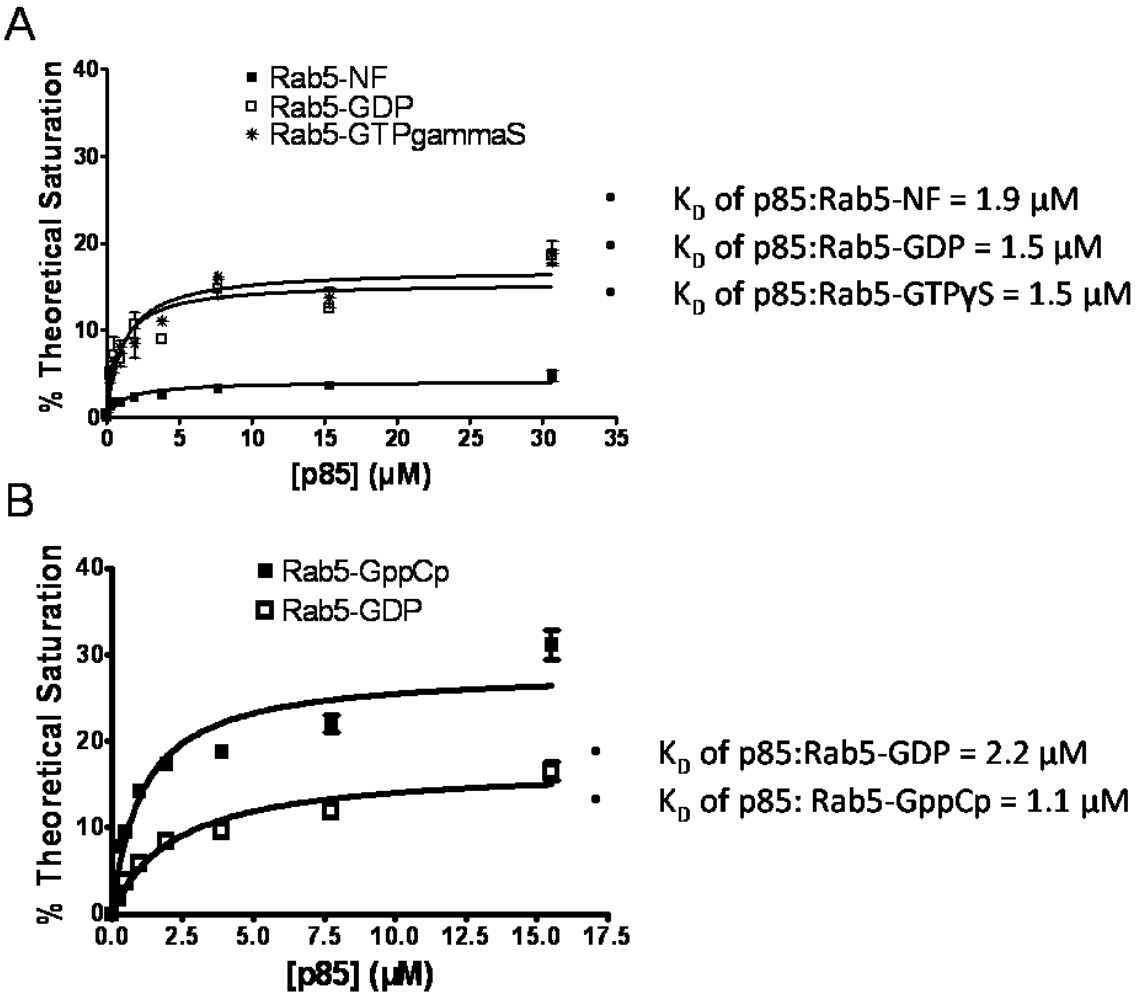

Figure 4.15 – Binding affinity of p85:Rab5 in different nucleotide binding states. The binding peaks at 110 seconds into the 120 second injection were measured and plotted vs. concentration of p85 using the same CM5 chip for each replication. **A)** The binding peaks from three separate binding series on the same sensor chip were converted into % theoretical saturation of the Rab5 immobilized chip and plotted against p85 concentration for binding of p85 to Rab5-NF (nucleotide free), Rab5-GDP, and Rab5-GTPγS. Values shown are the mean +/- standard deviation for three separate binding experiments. **B)** Additional experiments were performed following optimization of the BIAcore Running Buffer (50 mM HEPES, pH 8.0, 150 mM NaCl) to include 0.5 mM Mg2+ and 150 μM nucleotide, as well as the substitution of GTPγS for GppCp. Binding experiments were otherwise performed as per earlier binding studies. Values shown are the mean +/- standard deviation for three separate binding experiments.

10 mM) and 150 μM nucleotide (from 100 μM). Using this buffer, the K_D of p85 to Rab5-GDP was 2.2 μM while the K_D of p85 to Rab5-GppCp (another non-hydrolysable GTP-analog) was 1.1 μM (Fig. 4.15B). Unlike the previous conditions with the non-optimized buffer, the maximum binding in the presence of GDP was only 60% of that observed in the presence of GppCp.

4.6 p110 Expression Studies

p110, the catalytic subunit of PI3K, forms the heterodimeric complex with p85 and may have a role in the binding of p85 and Rab5 and help stabilize the switch regions of Rab5. In order to analyze the role that p110 plays in p85:Rab5 binding as well as assay for possible p110-encoded Rab5GAP activity, p110 must be produced independently from p85. Many attempts have been made over the years to produce soluble p110 independent of p85, but they have not been successful. It appears that p85 is absolutely required for the stability of p110 (Yu *et al*., 1998), and even the coexpression of p85 with p110 generally yields only low levels of functional, soluble p110 protein (unpublished data).

Attempts to express p110 as a GST-fusion protein in BL21 cells yielded little to no detectable p110 in solution or bound to glutathione Sepharose beads. However, analysis of the insoluble pellet following BL21 cell lysis did detect p110, likely in inclusion bodies. Attempts were made to resolublize stable, functional GST-p110 from the insoluble pellets after resolublization using a urea cracking buffer, as well as Sarkosyl sulfate using the method devised by Tao *et al*. (Tao *et al*., 2010). Unfortunately, none of the proteins resolubilized through these methods appeared to renature properly as shown by their inability to bind to glutathione Sepharose beads.

It was theorized that the proteins simply were adopting an improper conformation when resolublized using these methods. To analyze this, a comparison of ‘fast’ and ‘slow’ renaturation was performed. The ‘fast’ renaturation consisted of having the resuspended proteins immediately diluted 1:5 into PreScission buffer and then buffer-exchanged to remove all the denaturant. The ‘slow’ technique, conversely, involved a more gradual dilution over 20 minutes to the same 1:5, followed by buffer-exchanging to remove the denaturants. Unfortunately, neither of these techniques yielded recoverable protein (Fig. 4.16).

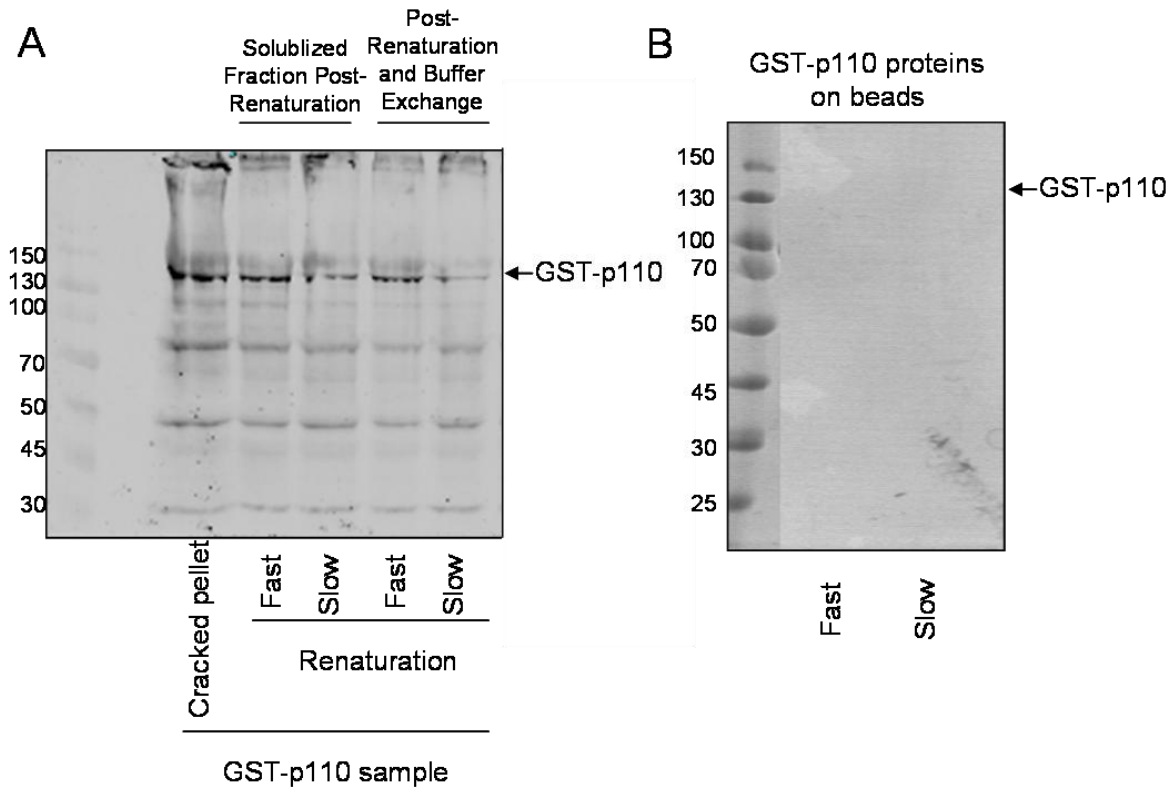

Figure 4.16 - Renaturation of GST-p110. **A)** The insoluble pellets from the GST-p110 purification were solublized using Urea-SDS cracking buffer (0.1 M Sodium phosphate monobasic, 1%(v/v) β-mercaptoethanol, 1% (w/v) SDS, 6 M urea). These samples were immediately diluted 1:5 with PreScission buffer (fast renaturation) and buffer exchanged. Alternatively, samples were diluted 1:5 over the course of 20 minutes (slow renaturation) prior to being buffer exchanged. The resultant supernatant was incubated for 60 minutes at 4 °C with glutathione Sepharose beads. Samples of the glutathione Sepharose resin were resolved using a 10% SDS-PAGE gel and visualized with Coomassie Blue stain. **B)** Glutathione Sepharose resin from (A) were then washed three times with standard PreScission buffer and again loaded on a 10% SDS-PAGE gel and visualized with Coomassie stain to determine of any of the resolubilized could be recovered.

In an effort to obtain soluble portions of p110 capable of binding to p85 and/or Rab5, fragments of both the α and β isoforms of p110 containing a His_6 tag were produced by Dielle Detillieux. Four such clones were generated: p110α and p110β containing the ABD and RBD (p110α 1-293 and p110β 1-291) as well as p110α- and p110β-containing only the ABD and RBD as well as the C2 domain, also known to contact p85 (p110α 1-503 and p110β 1-509). Of these fragments, only the p110β 1-291 fragment showed any detectable expression (Fig. 4.17). However, attempts to further purify this protein were difficult due to an unforeseen issue in removing the protein from the TALON affinity resin despite increasing imidazole levels and altering the pH (Fig. 4.18). Thus, experiments to determine the impact of p110 binding on p85:Rab5 GAP activity or binding affinities were not possible.

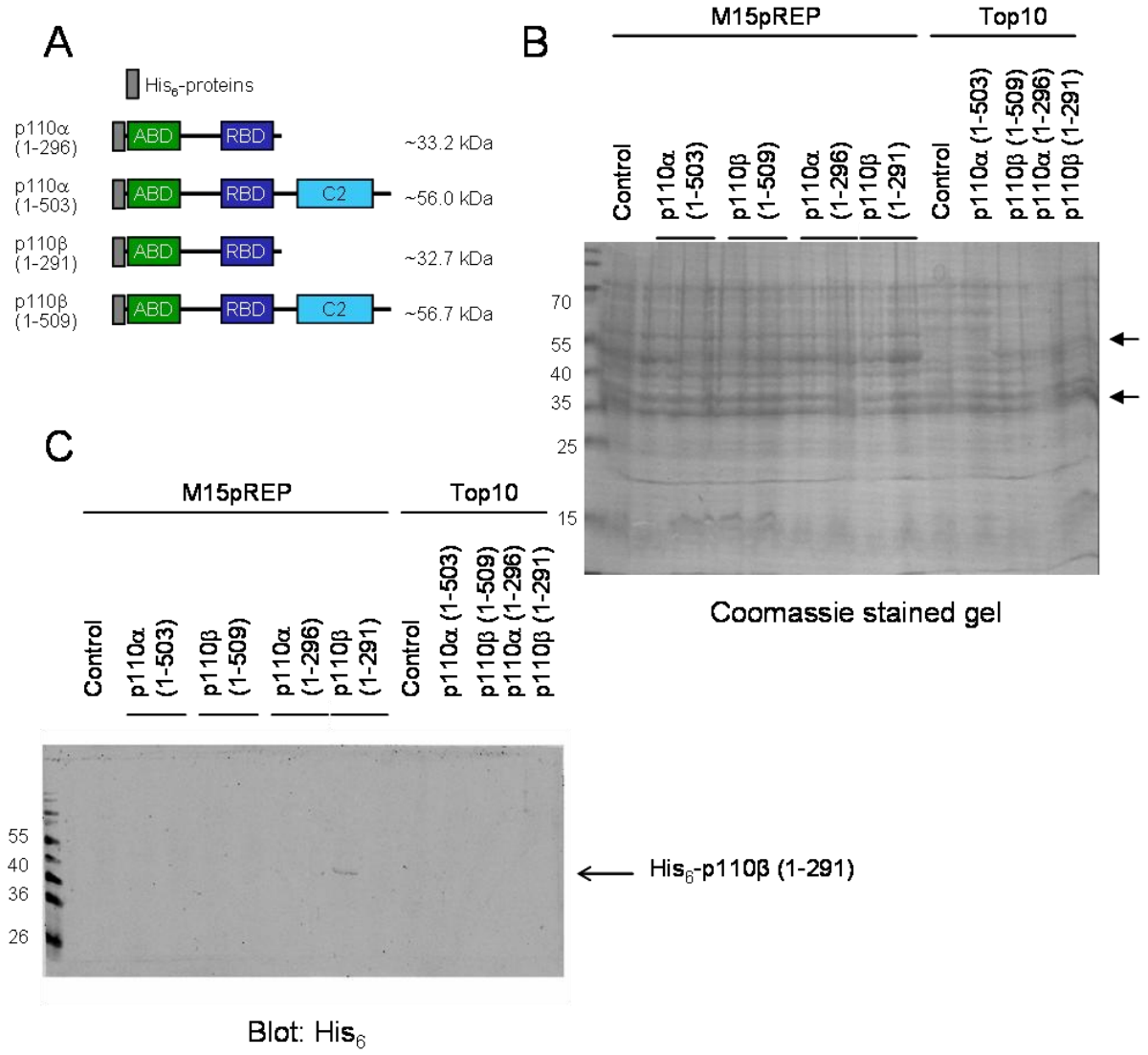

Figure 4.17 - Expression of His_6-p110 fragments. Several cell lines of either TOP10 or M15pREP strains of *E. coli* which had been transformed to express constructs of p110 were grown, induced with IPTG, and lysed with distilled water and SDS sample buffer. **A)** Schematic of the p110 fragments studied. Fragments used were derived from both p110α and p110β. All fragments included the p85-binding (ABD) and Ras-binding (RBD) domains, while two of the four also included the p110 C2 domain. **B)** Whole cell lysates were resolved using SDS-PAGE and visualized with Coomassie Blue stain. **C)** Whole cell lysates were resolved using SDS-PAGE and analyzed by Western blot with anti-His_6 tag antibodies to detect the His_6-p110 proteins.

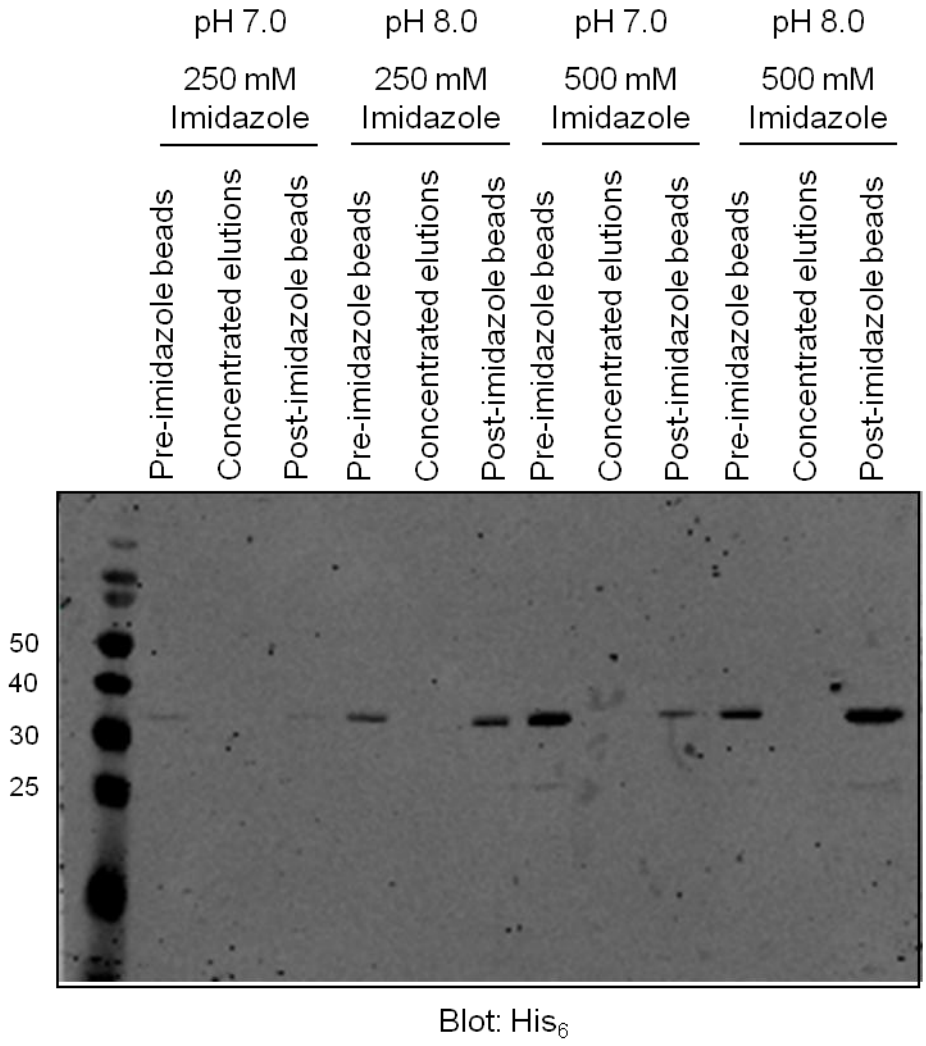

Figure 4.18 – His_6-p110β (1-291) has strong binding to TALON resin. p110β 1-291 was induced as per the standard protein induction and purification procedure for His_6-tagged proteins (3.2.4). Following collection of low quantities of solublized protein following bacterial lysis, the pellet was resolubilized using Sarkosyl sulfate. Resolubilized protein was recovered from solution using TALON resin. Two separate imidazole concentrations at two separate pHs were attempted to remove the resolubilized protein. Samples were resolved using 15% SDS-PAGE and analyzed by Western blot analysis against the His_6 tag.

5.0 Discussion

Previous studies performed in this laboratory have shown that p85 binds to Rab5, as well as acting as a Rab5GAP protein, a protein which stimulates the intrinsic GTP hydrolysis activity of Rab5 (Anderson and Chamberlain, 2005; Chamberlain and Anderson, 2005; Chamberlain *et al*., 2004; Chamberlain *et al*., 2008). However, while previous data have shown that these proteins do interact, the precise mechanism of interaction is still not well understood. The goal of this project was to measure the binding affinity of these two proteins, as well as to determine if the presence of activated PDGFR influences the binding affinity of p85 and Rab5 and/or the Rab5GAP activity of p85.

5.1 Interaction of Rab5 and p85

The interaction of the Rab5 and p85 proteins was analyzed using two different methods: SPR analysis to directly measure the binding affinity of p85 to Rab5 in different nucleotide-bound states, and GAP assays to analyze the effect that p85 has on Rab5 GTP hydrolysis.

5.1.1 Binding affinity of p85 to Rab5

In order to measure the binding affinities of p85 to Rab5 in different nucleotide bound states, Rab5 proteins were immobilized by amine coupling onto a BIAcore™ CM5 Sensor chip loaded with or without nucleotides. The immobilized Rab5 proteins were exposed to purified p85 samples which were flowed over the Rab5-immobilized flowcells at increasing concentrations. The net change of signal (measured in RU) was measured and converted into total theoretical saturation of the chip assuming 1:1 binding between the p85 and the Rab5 molecules. Maximum binding was plotted versus p85 concentration and non-linear regression curve fitting allowed binding affinities to be determined.

The data that was generated indicates that p85 has a binding affinity towards Rab5 between 1.1 and 2.2 μM with very little variation observed between the three Rab5 nucleotide-binding states: Rab5-NF, Rab5-GDP, and Rab5-GTP. However, while there was very little difference in the binding affinities, there were significant differences in the magnitude of binding of p85 to Rab5 in the three nucleotide binding states (Fig. 4.14). In all experiments, p85 showed the greatest total binding to Rab5 bound to the GTP analog GppCp, and the least

with Rab5-NF. However, there was a difference in total magnitude of binding between p85 binding to Rab5 associated with the GTP analogs GTPγS and GppCp.

Rab5-GDP appears to bind p85 with equal affinity as it does to Rab5-GTPγS, but not to Rab5-GppCp. It can be explained that the similarity between binding of p85 to Rab5-GDP and Rab5-GTPγS is due to the hydrolysis of the Rab5-GTPγS into GDP by Rab5, while GppCp cannot be hydrolyzed at all. This is due to the fact that the structure of GppCp contains a diester bond between the β and γ phosphate groups instead of the typical phosphate bond in GTP, preventing the hydrolysis of the nucleotide. Conversely, GTPγS contains a sulfur atom in place of the double-bonded oxygen atom on the γ-phosphate of GTP which reduces the rate of hydrolysis of the nucleotide. As GTPγS contains the same phosphoester bond as GTP it is easier to hydrolyze than GppCp, though it is hydrolyzed three orders of magnitude slower than GTP (Karim and Thompson, 1986).

When doing these experiments, it was presumed that all nucleotides were removed from the purified Rab5 by treating the protein with EDTA to remove its bound Mg^{2+}, and with it the associated nucleotide. It was later discovered after performing spectrophotometric analysis of the purified Rab5 samples that it was very difficult to remove bound nucleotide (likely GDP due to the GTPase activity of Rab5) from the Rab5 proteins. As such, the fraction of Rab5 that was nucleotide free or loaded with one of the GTP analogs (GTPγS and GppCp) was likely much less than originally believed. With the Rab5 proteins being persistently nucleotide-associated, it is entirely possible that the similarity of the binding affinities of p85 to Rab5 in all three nucleotide-bound conformations assayed was caused by the fact that approximately half of the Rab5 molecules retained a bound nucleotide (most likely GDP), even in samples treated to generate nucleotide-free and GTPγS- or GppCp-bound Rab5. It is possible that p85 does not associate with Rab5-NF and that the binding observed was simply a result of the presence of Rab5-GDP. However, it should be noted that the data does clearly indicate that p85 does bind better to Rab5 proteins which are nucleotide-associated and less well once the nucleotide has been removed from the Rab5.

5.2 p85 as a Rab5GAP

Previous studies performed by our lab have shown that p85 is a Rab5GAP (Chamberlain *et al*., 2004) using an assay developed in our lab (Anderson and Chamberlain, 2005). In order to analyze the effects of the activated PDGFR on the Rab5GAP activity of p85, these experiments were repeated. Early assays yielded results that were similar to those previously reported (Chamberlain *et al*., 2004) with GTP hydrolysis increased by 570- to 1700-fold upon p85 addition. However, as additional assays were performed it was noticed that there was increasing variation between the results of the assays. After performing several control experiments it was discovered that the p85 samples were hydrolyzing GTP in the absence of Rab5. Since p85 has been previously shown not to have any GTP hydrolysis activity (Chamberlain *et al*., 2004), this implies that this hydrolysis activity is due to some form of contamination in the purified p85 samples. It was also observed, as stated above (Section 5.1.1) that Rab5 was detected to be at least partially loaded with nucleotide prior to its loading with [α-^{32}P]GTP in the GAP assay. This would prevent the loading of the radiolabelled nucleotide into the Rab5 active site, thereby preventing the hydrolysis of GTP to GDP and lowering the observed overall activity of both Rab5 and the Rab5GAP activity of p85.

5.2.1 Influence of the PDGFR on p85 Rab5GAP Activity

PI3K is recruited to the plasma membrane by the activated, phosphorylated PDGFR where it phosphorylates phosphoinositol lipids. Following receptor internalization, PI3K remains associated with the active PDGFR so long as it retains tyrosine phosphorylated sites (Ogiso *et al*., 2002; Pawson and Scott, 2005; Schlessinger, 2000). As such, there is a period of time when p85 would be both PDGFR- and Rab5-associated when the endocytic vesicle is tethered to the early/sorting endosome. It has been observed that p85 undergoes a conformational change in its N-terminal SH2 domain when PDGFR-associated (Piccione *et al*., 1993; Shoelson *et al*., 1993). It was theorized that this observed conformational change may alter the Rab5GAP activity or binding affinity of p85 to Rab5.

To analyze the effects that the PDGFR had on p85:Rab5 dynamics, a synthetic peptide corresponding to the p85 binding site in both the inactive and active forms of the PDGFR were introduced into the GAP assays to measure their effects on p85 Rab5GAP activity. Similar peptides have been shown to elicit the same conformational change in p85 observed when it

binds to wild type phosphorylated PDGFR (Panayotou *et al*., 1992; Shoelson *et al*., 1993). It was verified that the phosphopeptide (ppPDGFR peptide), but not the non-phosphorylated peptide (PDGFR peptide) used did indeed compete with the wild type tyrosine phosphorylated PDGFR for p85 binding *in vitro*.

Neither of the PDGFR peptides altered the p85 Rab5GAP activity when added to the GAP assay. This is likely due to the fact that the observed conformational change is primarily in the N-terminal SH2 domain rather than the BH domain of p85 which is where the catalytic arginine finger important for p85 Rab5GAP activity is located. These results suggest that PDGFR-association and dissociation does not influence the p85 Rab5GAP activity.

5.2.2 p85 GAP Activity toward Rab4, Rab7, and Rab11

There are more than 60 human Rab proteins which have been identified, each of which has a separate function in relation to the trafficking of endosomes and vesicles in the cell (Barr and Lambright, 2010; Pereira-Leal and Seabra, 2000; Seabra and Wasmeier, 2004; Stenmark and Olkkonen, 2001). Previous experiments have shown that p85 has greater GAP activity towards Rab7 (Chamberlain, 2007) and equivalent GAP activity to Rab4 as Rab5. Also observed is that p85 appears to have little to no GAP activity towards Rab11 (Chamberlain *et al*., 2004).

The GAP activity of p85 was assayed towards Rab4, Rab7, and Rab11 to verify the previous results and to explore the possibility of using these proteins as positive and negative controls of p85 RabGAP activity. The resulting data, however, did not match the previous reported activity of p85 towards Rab11 with p85 having positive activity towards all of Rab4, Rab7, and Rab11. It was observed that p85 had lower GAP activity towards these three Rab proteins than observed towards Rab5. The reason for this divergent result of p85 towards Rab11 is not clear.

As with previously mentioned GAP assays, it was later noted that p85 samples displayed GTPase activity even in the absence of a Rab GTPase protein. While the GTP hydrolysis observed was much lower than that seen in the presence of Rab protein, this hydrolysis activity in the purified p85 preparations may be the cause of the discrepancy between the previously reported Rab11 data and the data reported in this study. This, however, is likely not the sole cause of the discrepancy as previous studies (Dielle Detillieux,

unpublished data) have shown that Rab11 does not bind p85 while this study showed GTP hydrolysis on par with that of Rab4 and Rab7, both of which have been reported to interact with p85. Not only that, but all three proteins (in the presence of p85) showed much greater GTP hydrolysis compared to p85 alone, suggesting that the Rab proteins were in fact contributing to the GTP hydrolysis activity.

5.3 Tau as a Rab5GAP

Tau proteins are microtubule-associated proteins which are involved in the stabilization of cytoskeleton in neuronal cells (Bhat and Setaluri, 2007; Lewis *et al*., 1988). There are six principle Tau isoforms which result from alternate mRNA splicing. Previous work in the lab of Dr. Nicole Leclerc at the Université de Montréal has shown that Tau proteins, specifically the 383 amino acid Tau4 isoform without the large Tau insert, was observed to associate with Rab5 and appeared to act as a Rab5GAP (Jenny Oberg, unpublished data). In an effort to identify the catalytic arginine finger which is common in many GAPs, a pair of mutants—TauR379A, and TauR349A—were generated. These, along with wild type Tau were assayed for GAP activity to identify if either of the two arginine residues that were mutated were the catalytically important arginine finger.

When assayed, it was found that neither of the two arginine mutants decreased the GAP activity of Tau towards Rab5. In fact, in both cases the mutant Tau proteins increased the relative Rab5GAP activity. This suggests that not only do the mutated arginines not participate in the GAP activity of the Tau protein, but they may even interfere with it. Further mutagenesis experiments are required to identify the catalytic arginine finger within the Tau protein and the significance of Rab5 regulation to the biological function of Tau.

5.4 Efforts to Remove Contamination

All of the experiments in this study suffered from issues caused by contamination, be it nucleotide or protein. Many different techniques were used to further purify these proteins and remove this contamination, most of which met with limited success.

5.4.1 Purification of p85

It was observed in many experiments that purified p85 preparations exhibited the ability to hydrolyse GTP independent of Rab5. This suggests that there was a contaminating GTPase protein which was not removed through purification.

5.4.1.1 Removal of Possible GTPase Contamination From p85 Samples

There are many GTPases present in *E. coli* cells, including the Obg/GTP1 subfamily of guanine nucleotide binding proteins. However, none of the known *E. coli* GTPases bear a great sequence similarity to Rab5, due in part that that bacteria lack the enzymatic machinery to prenylate Rab proteins (Elliott *et al*., 2001; Lei *et al*., 2000; Pylypenko *et al*., 2006; Selyunin *et al*., 2011; Shaw *et al*., 2005; Wout *et al*., 2004). This is supported by performing BLAST analysis of Rab5 against *E. coli* proteins. All of the ones queried had very high E-values (the lowest having an E-value of 0.02), implying that there was not a great deal of similarity. There are, however, functional similarities between several proteins, such as the membrane-trafficking protein ARF6, a member of the Ras superfamily (Elliott *et al*., 2001; Shaw *et al*., 2005). Because of this it was assumed that one such protein was pulled out along with the p85 protein.

The first technique used to increase the purity of the p85 samples involved alteration of the standard GST-fusion protein purification procedure. The first alteration consisted of changing the conditions of the lysis buffers used when harvesting the GST-p85 from BL21 cells. This, however, did not significantly affect the overall purity of p85. Increasing the ionic strength by more than doubling the concentration of NaCl, changing the detergent used from Triton X-100 to NP-40, and adding urea to the buffer did not appear to remove the GTPase contamination from p85 purifications. In addition, analysis of the purified p85 samples by Coomassie Blue stain SDS-PAGE gels did not reveal any obvious protein contaminants in any of the conditions attempted, including the basic purification procedure. This suggests that if there is a contaminating GTPase, it is present in very low concentrations in the purified p85 samples.

Our laboratory has also generated a dual-tagged p85 protein with both an N-terminal GST-tag and a C-terminal His_6-tag. This clone was designed to produce ultra-pure samples of p85 for purposes such as crystallography. While it was capable of producing ultra-pure p85

proteins, when tested in a GAP assay it proved to contain little or no Rab5GAP activity (data not shown). This result suggests that the C-terminal His_6-tag, or possibly the additional time and manipulations used during the additional purification steps or buffer negatively impacted the Rab5GAP activity of p85. As such, the use of this clone was discontinued for these studies.

The purified p85 samples were also subjected to anion-exchange chromatography. This process works by separating proteins based on their charges and ability to bind to positively charged media. This technique allows for the separation of proteins based on their relative charges at a specific pH. If there were a contaminating GTPase protein, even if it had the same pI as p85, would almost certainly elute off the anion exchange column at a different time than p85 due to its different amino acid composition. However, it was observed that post-anion exchange purified p85 showed similar GTP hydrolysis to the non-anion exchange purified p85 sample. This suggests that either there is no associated GTPase protein, or that it is bound so tightly to p85 that it cannot be removed easily.

It was observed using dynamic light scattering that p85 in a 50 mM sodium acetate buffer, pH 7.0, forms monomers and dimers based on the hydrodynamic radius in solution with a Polydispersity of 13.5% ± 1%. Polydispersity is a measurement of a sample to indicate the presence of multiple populations of different sizes within a sample. If a sample contains multiple populations of different hydrostatic radii it is said to be polydispersed and will have a higher Polydispersity. If the sample contains few individual populations, as represented by lower polydispersities the sample is said to be monomodal and has lower observed Polydispersity (typically below 20% Polydispersity). Using this information, it should be possible to separate out p85 using gel filtration chromatography in a similar buffer. Once isolated, the purified p85 samples could be analyzed using SDS-PAGE and silver staining for the presence of small G proteins that could not be identified by Coomassie Blue stain. Alternatively, mass spectrometry could be used to analyze the composition of the protein samples to analyze if there is a contaminating protein.

5.4.1.2 Possible Degradation of p85

Another explanation for the altered activity of p85 is that it was susceptible to proteolysis, thereby altering the physical and chemical properties and affinities of the protein. Resolving the purified p85 using SDS-PAGE and staining with Coomassie stain revealed in

most cases a purified protein band at approximately 83 kDa which corresponds to the size of purified p85 protein. However, it was also observed in many protein batches of p85 that there was a smaller quantity of a lower molecular weight protein product around 75 kDa in size (Sections 4.2.3). This smaller protein was resistant to separation from the full-length p85 by other means such as anion-exchange chromatography, suggesting that it may be a proteolysed form of p85.

In order to minimize the proteolytic degradation of proteins, all GST-fusion proteins were expressed in BL21 cells which lack the Lon protease which degrades abnormal bacterial proteins (such as mammalian proteins), and the ompT protease which is normally located in the outer membrane (Charette *et al*., 1981; Dervyn *et al*., 1990; Gottesman, 1989; Grodberg and Dunn, 1988). Coupled with the fact that the buffers used to lyse the bacteria contained three separate protease inhibitors (AEBSF, aprotinin, and leupeptin), proteolysis should be kept to a minimum. It should be noted, however, that the three protease inhibitors used only inhibit serine, cysteine, and threonine proteases, while the EDTA present in the bacterial lysis buffer which was used both to lyse the cells and store the proteins should inhibit metalloproteases, leaving the possibility that aspartate and glutamate proteases may still be present and uninhibited. This is ameliorated, however, by the fact that there are only few aspartate proteases that have been identified in prokaryotic systems (Bardy and Jarrell, 2003; LaPointe and Taylor, 2000; Ng *et al*., 2006).

5.4.2 Removal of Bound Nucleotides from Rab5

Rab5 is a small monomeric G protein. Like the similarly functional Ras proteins, there is an associated Mg^{2+} ion in its active site which is required for both binding to its cofactor—GDP or GTP—and for the hydrolysis of GTP into GDP (John *et al*., 1990; Simon *et al*., 1996). As this Mg^{2+} ion is required for the binding of the nucleotides, it is also theoretically the easiest way of removing those nucleotides. In many experiments it is important to load proteins with very specific cofactors or substrates in order to analyze the conformation of that product or its physical properties under that conformation. One of the objectives of this study was to analyze the difference in binding affinity of p85 to Rab5 under different nucleotide binding states. As such, a method of removing any residual bound nucleotide from the Rab5 protein and replacing it with a different one of our choosing was required.

The original method used for this was simply including 1 mM EDTA in the lysis and wash buffers. EDTA should chelate any metal ions in the solution, removing them and hopefully the bound nucleotide as well. Unfortunately, a spectrophotometric analysis of the UV spectrum showed that there was a significant absorption signal at 260 nm compared to what was expected for Rab5 proteins. This high absorption typically indicates the presence of contaminating nucleotides (Cavaluzzi and Borer, 2004; Tataurov *et al*., 2008). As Rab5 binds to both GTP and GDP, it stands to reason that this signal at 260 nm was caused by bound guanosine nucleotides. As such, it was determined that 1 mM EDTA was insufficient to remove the associated guanosine nucleotide in the active site. This observation is supported by other studies using Rab5 and the related Rho protein (John *et al*., 1990).

Later purifications were performed in 10 mM EDTA, but this also did not appear to remove the bound nucleotide to any great degree. Using a modified version of the technique pioneered by John *et al*., the Rab5 proteins were treated with alkaline phosphatase in the presence and absence of snake venom phosphodiesterase (John *et al*., 1990). When Rab5 is treated with these two enzymes in sequence, all the phosphate groups of the bound guanosine nucleotide should be removed, leaving the guanine, or at least a GMP, in its place. The resultant guanine nucleotide should then have a much lower binding affinity to the Rab5 protein, leading to its removal.

In all cases where the Rab5 protein itself was not significantly degraded, the trials ended with absorbance signals equivalent to the Rab5 samples which were not treated with the phosphate-removing enzymes. It is possible that the enzymes did, in fact, act upon the bound nucleotides to remove phosphate groups and that the continued signal was due to guanosine itself still associated with the protein as it is the nucleotide itself rather than the phosphate groups which provides the absorbance at 260 nm. If this were true, it should make it substantially easier to replace the associated nucleotides with the ones desired. Unfortunately, as spectrophotometric analysis is the primary means of detecting the presence of any bound nucleotide, it was not possible to measure whether or not these enzymes did in fact have an effect on the nature of the Rab5 bound nucleotide (i.e., GMP, GDP, or GTP).

Efforts to use ion-exchange chromatography to purify Rab5 also did not meet with positive results. It was also hoped that the nucleotide could be removed using cation-exchange chromatography, or alternatively, that the Rab5 proteins themselves could be separated by their

nucleotide binding states based on their charge differences. However, despite many attempts using different conditions, Rab5 would not bind to either a cation- or anion-exchange column. Because of this, the technique was not used for Rab5 purification.

It is presently not clear if the failure of the phosphatase/phosphodiesterase treatment was due to an inability of the enzymes to hydrolyze the bound nucleotides or if the hydrolyzed nucleotides simply exhibited similar affinity towards Rab5 in spite of their fewer phosphate groups. If the failure was in the availability of the phosphate group, a potential analysis would be to take aliquots of the purified protein sample and treat them with molybdate/malachite green or other phosphate-detection assays (Ekman and Jager, 1993; Harder *et al*., 1994; Maehama *et al*., 2000; Martin *et al*., 1985) to track the release of phosphate. Alternatively, a variation of a GAP assay could be performed where instead of measuring the increase in GTP hydrolysis with the presence of a GAP protein, you would measure the degradation of guanosine nucleotide phosphates using GTP- or GDP-specific antibodies. This technique, however, suffers from the same problem of not being able to replace the Rab5-associated nucleotide with an appropriate, radiolabelled nucleotide. Finally, it is possible to track the removal of phosphate and guanine via high-performance liquid chromatography (HPLC) (John *et al*., 1990).

An additional possibility for removing the associated GDP, or at least replacing it with GTP or one of its non-hydrolysable analogs, would be to treat the Rab5 protein with the desired nucleotide in the presence of a known GEF protein, such as Rin1 (Chen *et al*., 2009). The Rin1 would theoretically displace any bound GDP with the desired nucleotide (if one other than GDP is desired), though it is unknown if GEF proteins would displace GDP for GTP analogs such as GppCp or GTPγS as effectively as GTP. The issue with this is that Rin1 would have to be removed from the protein samples, and would need to be expressed as a tagged protein or introduced to Rab5 prior to the cleavage of its GST-tag.

5.5 Future Studies

In order for these experiments to be continued, more stringent purification procedures must be developed. It has been observed that the p85 protein appears to be associated with some sort of contaminating bacterial GTPase, even following multiple purification steps. One way to ameliorate this is to introduce additional purifications steps and to create a new dual-

tagged p85 protein. As the presence of the C-terminal His_6 tag was linked to ablation of p85 Rab5GAP activity, the new p85 fusion protein should be N-terminally tagged with His_6 and C-terminally tagged with GST to be cleaved off the fusion protein with a PreScission protease enzyme. With two tags, coupled with anion-exchange chromatography and gel filtration, it should be possible to remove any additional associated proteins. Additionally, purified p85 samples could be silver stained to better identify contaminating proteins, and those proteins could be analyzed by mass spectroscopy to identify if they are p85 degradation products or other, non-p85-derived proteins.

In terms of removing nucleotide contamination from Rab5 proteins, a more faithful repeat of the procedure pioneered by John *et al*. (John *et al*., 1990) involving tracking the degradation of GTP and GDP via HPLC will probably need to be pursued. This can be avoided in GAP assays if a GST-Rin1 fusion protein can be developed which could be added to the Rab5 mastermix in the reaction to replace any associated GDP with [α-^{32}P]GTP. This GST-Rin1 would be immobilized on glutathione Sepharose resin and removed after a brief (5 minute) incubation with the Rab5 by centrifugation. However, depending on the binding affinity of Rin1 to Rab5 and if it is only a transient association, this procedure may not be possible.

Following the increased purification procedure, the above studies should be repeated in order to ascertain more accurate data. With decreased nucleotide contaminating the Rab5 proteins, it will be possible to analyze if p85 does, in fact, associate with Rab5-NF or if the previous data to that effect were simply an artefact of the residual nucleotides already bound. Additionally, it will give a clearer image of the difference between Rab5:p85 binding in the Rab5-GDP and Rab5-GTP binding states.

The logical continuation of this study would be to analyze the effect of the activated PDGFR, by way of the ppPDGFR peptide, on Rab5:p85 binding. This can be accomplished simply by incubating the p85 samples with 10 to 100 µM of the ppPDGFR peptide. Though the conformational change in the SH2 domain did not alter the GAP activity of p85, it is possible that it may influence the ability of the protein to bind to Rab5, or possibly for it to bind greater or lesser affinity with different Rab5 nucleotide binding states.

The p110 catalytic subunit of PI3K also induces a conformational change when bound to p85. More importantly, it has been shown that the p85 subunit of PI3K has been shown not

to stabilize the switch regions of Rab5, one of the primary functions of GAPs (Scheffzek *et al*., 1998; Terzyan *et al*., 2004). Because p110 is present with p85 when p85 would normally interact with Rab5, and p110 can bind selectively to Rab5-GTP, it is theorized that p110 may stabilize these switch regions (Christoforidis *et al*., 1999; McBride *et al*., 1999; Mills *et al*., 1998; Rubino *et al*., 2000; Simonsen *et al*., 1998). Previous attempts to purify p110, either separately or coexpressed with p85, have not yielded stable proteins. However, one possible solution to this would be to form a p85-p110 chimeric protein, containing the p85 BH domain, N-terminal SH2 domain, and p110 binding domain linked to the p110 protein. If this chimeric protein was stable in solution, it should be able to provide the GAP activity of p85 via the BH domain while stabilizing the switch regions though the p110 protein domains (Chamberlain *et al*., 2004).

5.6 Conclusion

The objectives of this study were twofold: To analyze the effects of proteins accessory to p85 (specifically the activated PDGFR) on the Rab5GAP activity of p85, and to measure the effect that Rab5 nucleotide-binding state has on the binding affinity of p85 towards Rab5. While some avenues proved impractical or impossible to pursue, such as the analysis of the role of p110 on p85:Rab5 binding and on the Rab5GAP activity of p85, others proved far more successful. It was found that the PDGFR in both its active and inactive conformations did not significantly affect the Rab5GAP activity of p85. It was also found that the mutation of two arginines found in Tau, a putative Rab5GAP, to alanines did not confer any reduction in observed Rab5GAP activity from Tau.

For the second objective of this study, it was observed that while p85 binds to Rab5 with similar affinity regardless of observed Rab5 nucleotide binding state, the total magnitude of the two proteins is markedly increased in the presence of a nucleotide. This was likely due to the presence of nucleotide on at least a portion of the immobilized Rab5. As p85 showed noticeable binding to Rab5-GDP p85 may, in addition to its primary role involving p85:Rab5-GTP binding in p85 Rab5GAP regulation have an additional role in the regulation of Rab5-GDP, possibly as a Rab5GDF protein.

6.0 References

Albert, S., Will, E., and Gallwitz, D. (1999). Identification of the catalytic domains and their functionally critical arginine residues of two yeast GTPase-activating proteins specific for Ypt/Rab transport GTPases. EMBO J *18*, 5216-5225.

Alonso, A., Zaidi, T., Novak, M., Grundke-Iqbal, I., and Iqbal, K. (2001). Hyperphosphorylation induces self-assembly of tau into tangles of paired helical filaments/straight filaments. Proc Natl Acad Sci USA *98*, 6923-6928.

Alvarez, R.H., Kantarjian, H.M., and Cortes, J.E. (2006). Biology of platelet-derived growth factor and its involvement in disease. Mayo Clin Proc *81*, 1241-1257.

Anderson, D.H., and Chamberlain, M.D. (2005). Assay and stimulation of the Rab5 GTPase by the p85 alpha subunit of phosphatidylinositol 3'-kinase. Methods Enzymol *403*, 552-561.

Anderson, R.G. (1998). The caveolae membrane system. Annu Rev Biochem *67*, 199-225.

Arcaro, A., Zvelebil, M.J., Wallasch, C., Ullrich, A., Waterfield, M.D., and Domin, J. (2000). Class II phosphoinositide 3-kinases are downstream targets of activated polypeptide growth factor receptors. Mol Cell Biol *20*, 3817-3830.

Arikan, M.C., Memmott, J., Broderick, J.A., Lafyatis, R., Screaton, G., Stamm, S., and Andreadis, A. (2002). Modulation of the membrane-binding projection domain of tau protein: splicing regulation of exon 3. Brain Res Mol Brain Res *101*, 109-121.

Armstrong, J. (2000). How do Rab proteins function in membrane traffic? Int J Biochem Cell Biol *32*, 303-307.

Augustinack, J.C., Schneider, A., Mandelkow, E.M., and Hyman, B.T. (2002). Specific tau phosphorylation sites correlate with severity of neuronal cytopathology in Alzheimer's disease. Acta Neuropathol *103*, 26-35.

Backmann, N., Zahnd, C., Huber, F., Bietsch, A., Pluckthun, A., Lang, H.P., Guntherodt, H.J., Hegner, M., and Gerber, C. (2005). A label-free immunosensor array using single-chain antibody fragments. Proc Natl Acad Sci USA *102*, 14587-14592.

Barbieri, M.A., Fernandez-Pol, S., Hunker, C., Horazdovsky, B.H., and Stahl, P.D. (2004). Role of rab5 in EGF receptor-mediated signal transduction. Eur J Cell Biol *83*, 305-314.

Barbieri, M.A., Kong, C., Chen, P.I., Horazdovsky, B.F., and Stahl, P.D. (2003). The SRC homology 2 domain of Rin1 mediates its binding to the epidermal growth factor receptor and regulates receptor endocytosis. J Biol Chem *278*, 32027-32036.

Bardy, S.L., and Jarrell, K.F. (2003). Cleavage of preflagellins by an aspartic acid signal peptidase is essential for flagellation in the archaeon Methanococcus voltae. Mol Microbiol *50*, 1339-1347.

Barr, F., and Lambright, D.G. (2010). Rab GEFs and GAPs. Curr Opin Cell Biol *22*, 461-470.

Bernards, A. (2003). GAPs galore! A survey of putative Ras superfamily GTPase activating proteins in man and Drosophila. Biochim Biophys Acta *1603*, 47-82.

Bertrand, J., Plouffe, V., Senechal, P., and Leclerc, N. (2010). The pattern of human tau phosphorylation is the result of priming and feedback events in primary hippocampal neurons. Neuroscience *168*, 323-334.

Bhat, K.M., and Setaluri, V. (2007). Microtubule-associated proteins as targets in cancer chemotherapy. Clin Cancer Res *13*, 2849-2854.

Biarc, J., Chalkley, R.J., Burlingame, A.L., and Bradshaw, R.A. (2011). Receptor tyrosine kinase signaling--a proteomic perspective. Adv Enzyme Regul *51*, 293-305.

Bokoch, G.M., Vlahos, C.J., Wang, Y., Knaus, U.G., and Traynor-Kaplan, A.E. (1996). Rac GTPase interacts specifically with phosphatidylinositol 3'-kinase. Biochem J *315*, 775-779.

Booker, G.W., Gout, I., Downing, A.K., Driscoll, P.C., Boyd, J., Waterfield, M.D., and Campbell, I.D. (1993). Solution structure and ligand-binding site of the SH3 domain of the p85 alpha subunit of phosphatidylinositol 3'-kinase. Cell *73*, 813-822.

Bradshaw, J.M., and Waksman, G. (2002). Molecular recognition by SH2 domains. Adv Protein Chem *61*, 161-210.

Burnett, G., and Kennedy, E.P. (1954). The enzymatic phosphorylation of proteins. J Biol Chem *211*, 969-980.

Cantor, C.R., Warshaw, M.M., and Shapiro, H. (1970). Oligonucleotide interactions. 3. Circular dichroism studies of the conformation of deoxyoligonucleotides. Biopolymers *9*, 1059-1077.

Carpenter, C.L., and Cantley, L.C. (1996). Phosphoinositide kinases. Curr Opin Cell Biol *8*, 153-158.

Cavaluzzi, M.J., and Borer, P.N. (2004). Revised UV extinction coefficients for nucleoside-5'-monophosphates and unpaired DNA and RNA. Nucl. Acids Res *32*, e13.

Chamberlain, M.D. (2007). The interaction of the p85 subunit of PI3K with Rab proteins. Ph.D thesis in Department of Biochemistry, College of Medicine (Saskatoon, SK, University of Saskatchewan), p. 150.

Chamberlain, M.D., and Anderson, D.H. (2005). Measurement of the interaction of the p85alpha subunit of phosphatidylinositol 3'-kinase with Rab5. Meth. Enzymol *403*, 541-552.

Chamberlain, M.D., Berry, T.R., Pastor, M.C., and Anderson, D.H. (2004). The p85alpha subunit of phosphatidylinositol 3'-kinase binds to and stimulates the GTPase activity of Rab proteins. J Biol Chem *279*, 48607-48614.

Chamberlain, M.D., Chan, T., Oberg, J.C., Hawrysh, A.D., James, K.M., Saxena, A., Xiang, J., and Anderson, D.H. (2008). Disrupted RabGAP function of the p85 subunit of phosphatidylinositol 3'-kinase results in cell transformation. J Biol Chem *283*, 15861-15868.

Chamberlain, M.D., Oberg, J.C., Furber, L.A., Poland, S.F., Hawrysh, A.D., Knafelc, S.M., McBride, H.M., and Anderson, D.H. (2010). Deregulation of Rab5 and Rab4 proteins in p85R274A-expressing cells alters PDGFR trafficking. Cell Signal *22*, 1562-1575.

Charette, M.F., Henderson, G.W., and Markovitz, A. (1981). ATP hydrolysis-dependent protease activity of the lon (capR) protein of Escherichia coli K-12. Proc Natl Acad Sci USA *78*, 4728-4732.

Chen, P.I., Kong, C., Su, X., and Stahl, P.D. (2009). Rab5 isoforms differentially regulate the trafficking and degradation of epidermal growth factor receptors. J Biol Chem *284*, 30328-30338.

Chin, Y.R., and Toker, A. (2009). Function of Akt/PKB signaling to cell motility, invasion and the tumor stroma in cancer. Cell Signal *21*, 470-476.

Christoforidis, S., McBride, H.M., Burgoyne, R.D., and Zerial, M. (1999). The Rab5 effector EEA1 is a core component of endosome docking. Nature *397*, 621-625.

Citri, A., and Yarden, Y. (2006). EGF-ERBB signalling: towards the systems level. Nat Rev Mol Cell Biol *7*, 505-516.

Cozzone, A.J. (1988). Protein phosphorylation in prokaryotes. Annu Rev Microbiol *42*, 97-125.

Cunningham, C.C., Leclerc, N., Flanagan, L.A., Lu, M., Janmey, P.A., and Kosik, K.S. (1997). Microtubule-associated protein 2c reorganizes both microtubules and microfilaments into distinct cytological structures in an actin-binding protein-280-deficient melanoma cell line. J Cell Biol *136*, 845-857.

Dervyn, E., Canceill, D., and Huisman, O. (1990). Saturation and specificity of the Lon protease of Escherichia coli. J Bacteriol *172*, 7098-7103.

Desai, A., and Mitchison, T.J. (1997). Microtubule polymerization dynamics. Annu Rev Cell Dev Biol *13*, 83-117.

Doherty, G.J., and McMahon, H.T. (2009). Mechanisms of endocytosis. Annu Rev Biochem *78*, 857-902.

Domin, J., Pages, F., Volinia, S., Rittenhouse, S.E., Zvelebil, M.J., Stein, R.C., and Waterfield, M.D. (1997). Cloning of a human phosphoinositide 3-kinase with a C2 domain that displays reduced sensitivity to the inhibitor wortmannin. Biochem J *326*, 139-147.

Drubin, D.G., and Kirschner, M.W. (1986). Tau protein function in living cells. J Cell Biol *103*, 2739-2746.

Dumas, J.J., Zhu, Z., Connolly, J.L., and Lambright, D.G. (1999). Structural basis of activation and GTP hydrolysis in Rab proteins. Structure *7*, 413-423.

Edelhoch, H. (1967). Spectroscopic determination of tryptophan and tyrosine in proteins. Biochemistry *6*, 1948-1954.

Edeling, M.A., Smith, C., and Owen, D. (2006). Life of a clathrin coat: insights from clathrin and AP structures. Nat Rev Mol Cell Biol *7*, 32-44.

Ekman, P., and Jager, O. (1993). Quantification of subnanomolar amounts of phosphate bound to seryl and threonyl residues in phosphoproteins using alkaline hydrolysis and malachite green. Anal Biochem *214*, 138-141.

Elliott, S.J., Krejany, E.O., Mellies, J.L., Robins-Browne, R.M., Sasakawa, C., and Kaper, J.B. (2001). EspG, a novel type III system-secreted protein from enteropathogenic Escherichia coli with similarities to VirA of Shigella flexneri. Infect Immun *69*, 4027-4033.

Engelman, J.A., Luo, J., and Cantley, L.C. (2006). The evolution of phosphatidylinositol 3'-kinases as regulators of growth and metabolism. Nat Rev Genet *7*, 606-619.

Ferguson, K.M. (2008). Structure-based view of epidermal growth factor receptor regulation. Annu Rev Biophys *37*, 353-373.

Fidyk, N.J., and Cerione, R.A. (2002). Understanding the catalytic mechanism of GTPase-activating proteins: demonstration of the importance of switch domain stabilization in the stimulation of GTP hydrolysis. Biochemistry *41*, 15644-15653.

Flanagan, L.A., Cunningham, C.C., Chen, J., Prestwich, G.D., Kosik, K.S., and Janmey, P.A. (1997). The structure of divalent cation-induced aggregates of PIP2 and their alteration by gelsolin and tau. Biophys J *73*, 1440-1447.

Friedhoff, P., von Bergen, M., Mandelkow, E.M., and Mandelkow, E. (2000). Structure of tau protein and assembly into paired helical filaments. Biochim Biophys Acta *1502*, 122-132.

Fruman, D.A. (2010). Regulatory subunits of class IA PI3K. Curr Top Microbiol Immunol *346*, 225-244.

Fruman, D.A., Meyers, R.E., and Cantley, L.C. (1998). Phosphoinositide kinases. Annu Rev Biochem *67*, 481-507.

Garrett, T.P., McKern, N.M., Lou, M., Frenkel, M.J., Bentley, J.D., Lovrecz, G.O., Elleman, T.C., Cosgrove, L.J., and Ward, C.W. (1998). Crystal structure of the first three domains of the type-1 insulin-like growth factor receptor. Nature *394*, 395-399.

Gearing, A.J. (2007). Targeting toll-like receptors for drug development: a summary of commercial approaches. Immunol Cell Biol *85*, 490-494.

Glasel, J.A. (1995). Validity of nucleic acid purities monitored by 260nm/280nm absorbance ratios. Biotechniques *18*, 62-63.

Goedert, M., Crowther, R.A., and Garner, C.C. (1991). Molecular characterization of microtubule-associated proteins tau and MAP2. Trends Neurosci *14*, 193-199.

Goedert, M., Spillantini, M.G., and Crowther, R.A. (1992). Cloning of a big tau microtubule-associated protein characteristic of the peripheral nervous system. Proc Natl Acad Sci USA *89*, 1983-1987.

Goedert, M., Spillantini, M.G., Jakes, R., Rutherford, D., and Crowther, R.A. (1989). Multiple isoforms of human microtubule-associated protein tau: sequences and localization in neurofibrillary tangles of Alzheimer's disease. Neuron *3*, 519-526.

Gottesman, S. (1989). Genetics of proteolysis in Escherichia coli*. Annu Rev Genet *23*, 163-198.

Gout, I., Dhand, R., Hiles, I.D., Fry, M.J., Panayotou, G., Das, P., Truong, O., Totty, N.F., Hsuan, J., Booker, G.W., *et al.* (1993). The GTPase dynamin binds to and is activated by a subset of SH3 domains. Cell *75*, 25-36.

Grodberg, J., and Dunn, J.J. (1988). ompT encodes the Escherichia coli outer membrane protease that cleaves T7 RNA polymerase during purification. J Bacteriol *170*, 1245-1253.

Grucza, R.A., Bradshaw, J.M., Futterer, K., and Waksman, G. (1999). SH2 domains: from structure to energetics, a dual approach to the study of structure-function relationships. Med Res Rev *19*, 273-293.

Guinebault, C., Payrastre, B., Racaud-Sultan, C., Mazarguil, H., Breton, M., Mauco, G., Plantavid, M., and Chap, H. (1995). Integrin-dependent translocation of phosphoinositide 3-kinase to the cytoskeleton of thrombin-activated platelets involves specific interactions of p85 alpha with actin filaments and focal adhesion kinase. J Cell Biol *129*, 831-842.

Gupta, R.C., Randerath, E., and Randerath, K. (1976). An improved separation procedure for nucleoside monophosphates on polyethyleneimine-(PEI-)cellulose thin layers. Nucleic Acids Res *3*, 2915-2921.

Harder, K.W., Owen, P., Wong, L.K., Aebersold, R., Clark-Lewis, I., and Jirik, F.R. (1994). Characterization and kinetic analysis of the intracellular domain of human protein tyrosine phosphatase beta (HPTP beta) using synthetic phosphopeptides. Biochem J *298 (Pt 2)*, 395-401.

Harpur, A.G., Layton, M.J., Das, P., Bottomley, M.J., Panayotou, G., Driscoll, P.C., and Waterfield, M.D. (1999). Intermolecular interactions of the p85alpha regulatory subunit of phosphatidylinositol 3'-kinase. J Biol Chem *274*, 12323-12332.

Heasman, S.J., and Ridley, A.J. (2008). Mammalian Rho GTPases: new insights into their functions from in vivo studies. Nat Rev Mol Cell Biol *9*, 690-701.

Herman, P.K., and Emr, S.D. (1990). Characterization of VPS34, a gene required for vacuolar protein sorting and vacuole segregation in Saccharomyces cerevisiae. Mol Cell Biol *10*, 6742-6754.

Huang, C.H., Mandelker, D., Schmidt-Kittler, O., Samuels, Y., Velculescu, V.E., Kinzler, K.W., Vogelstein, B., Gabelli, S.B., and Amzel, L.M. (2007). The structure of a human p110alpha/p85alpha complex elucidates the effects of oncogenic PI3Kalpha mutations. Science *318*, 1744-1748.

Hunter, S., Koch, B.L., and Anderson, S.M. (1997). Phosphorylation of cbl after stimulation of Nb2 cells with prolactin and its association with phosphatidylinositol 3'-kinase. Mol Endocrinol *11*, 1213-1222.

Hutagalung, A.H., and Novick, P.J. (2011). Role of Rab GTPases in membrane traffic and cell physiology. Physiol Rev *91*, 119-149.

Ilic, N., and Roberts, T.M. (2010). Comparing the roles of the p110alpha and p110beta isoforms of PI3K in signaling and cancer. Curr Top Microbiol Immunol *347*, 55-77.

Itzen, A., and Goody, R.S. (2011). GTPases involved in vesicular trafficking: structures and mechanisms. Semin Cell Dev Biol *22*, 48-56.

Jenkins, S.M., and Johnson, G.V. (1998). Tau complexes with phospholipase C-gamma in situ. Neuroreport *9*, 67-71.

John, J., Sohmen, R., Feuerstein, J., Linke, R., Wittinghofer, A., and Goody, R.S. (1990). Kinetics of interaction of nucleotides with nucleotide-free H-ras p21. Biochemistry *29*, 6058-6065.

Johnsson, B., Lofas, S., and Lindquist, G. (1991). Immobilization of proteins to a carboxymethyldextran-modified gold surface for biospecific interaction analysis in surface plasmon resonance sensors. Anal Biochem *198*, 268-277.

Jonsson, U., Fagerstam, L., Ivarsson, B., Johnsson, B., Karlsson, R., Lundh, K., Lofas, S., Persson, B., Roos, H., Ronnberg, I., *et al.* (1991). Real-time biospecific interaction analysis using surface plasmon resonance and a sensor chip technology. Biotechniques *11*, 620-627.

Kapeller, R., Prasad, K.V., Janssen, O., Hou, W., Schaffhausen, B.S., Rudd, C.E., and Cantley, L.C. (1994). Identification of two SH3-binding motifs in the regulatory subunit of phosphatidylinositol 3'-kinase. J Biol Chem *269*, 1927-1933.

Karim, A.M., and Thompson, R.C. (1986). Guanosine 5'-O-(3-thiotriphosphate) as an analog of GTP in protein biosynthesis. The effects of temperature and polycations on the accuracy of initial recognition of aminoacyl-tRNA ternary complexes by ribosomes. J Biol Chem *261*, 3238-3243.

Kimura, T., Ono, T., Takamatsu, J., Yamamoto, H., Ikegami, K., Kondo, A., Hasegawa, M., Ihara, Y., Miyamoto, E., and Miyakawa, T. (1996). Sequential changes of tau-site-specific phosphorylation during development of paired helical filaments. Dementia *7*, 177-181.

Kinchen, J.M., and Ravichandran, K.S. (2010). Identification of two evolutionarily conserved genes regulating processing of engulfed apoptotic cells. Nature *464*, 778-782.

Kong, C., Su, X., Chen, P.I., and Stahl, P.D. (2007). Rin1 interacts with signal-transducing adaptor molecule (STAM) and mediates epidermal growth factor receptor trafficking and degradation. J Biol Chem *282*, 15294-15301.

Laemmli, U.K. (1970). Cleavage of structural proteins during the assembly of the head of bacteriophage T4. Nature *227*, 680-685.

LaPointe, C.F., and Taylor, R.K. (2000). The type 4 prepilin peptidases comprise a novel family of aspartic acid proteases. J Biol Chem *275*, 1502-1510.

Leevers, S.J., Vanhaesebroeck, B., and Waterfield, M.D. (1999). Signalling through phosphoinositide 3-kinases: the lipids take centre stage. Curr Opin Cell Biol *11*, 219-225.

Lei, M., Lu, W., Meng, W., Parrini, M.C., Eck, M.J., Mayer, B.J., and Harrison, S.C. (2000). Structure of PAK1 in an autoinhibited conformation reveals a multistage activation switch. Cell *102*, 387-397.

Lewis, S.A., Wang, D.H., and Cowan, N.J. (1988). Microtubule-associated protein MAP2 shares a microtubule binding motif with tau protein. Science *242*, 936-939.

Li, H., DeRosier, D.J., Nicholson, W.V., Nogales, E., and Downing, K.H. (2002). Microtubule structure at 8 A resolution. Structure *10*, 1317-1328.

Li, X.A., Everson, W.V., and Smart, E.J. (2005). Caveolae, lipid rafts, and vascular disease. Trends Cardiovasc Med *15*, 92-96.

Maehama, T., Taylor, G.S., Slama, J.T., and Dixon, J.E. (2000). A sensitive assay for phosphoinositide phosphatases. Anal Biochem *279*, 248-250.

Mandelkow, E.M., and Mandelkow, E. (1998). Tau in Alzheimer's disease. Trends Cell Biol *8*, 425-427.

Marsh, M., and McMahon, H.T. (1999). The structural era of endocytosis. Science *285*, 215-220.

Martin, B., Pallen, C.J., Wang, J.H., and Graves, D.J. (1985). Use of fluorinated tyrosine phosphates to probe the substrate specificity of the low molecular weight phosphatase activity of calcineurin. J Biol Chem *260*, 14932-14937.

Mayer, B.J. (2001). SH3 domains: complexity in moderation. J Cell Sci *114*, 1253-1263.

McBride, H.M., Rybin, V., Murphy, C., Giner, A., Teasdale, R., and Zerial, M. (1999). Oligomeric complexes link Rab5 effectors with NSF and drive membrane fusion via interactions between EEA1 and syntaxin 13. Cell *98*, 377-386.

Miaczynska, M., and Zerial, M. (2002). Mosaic organization of the endocytic pathway. Exp Cell Res *272*, 8-14.

Miled, N., Yan, Y., Hon, W.C., Perisic, O., Zvelebil, M., Inbar, Y., Schneidman-Duhovny, D., Wolfson, H.J., Backer, J.M., and Williams, R.L. (2007). Mechanism of two classes of cancer mutations in the phosphoinositide 3-kinase catalytic subunit. Science *317*, 239-242.

Mills, I.G., Jones, A.T., and Clague, M.J. (1998). Involvement of the endosomal autoantigen EEA1 in homotypic fusion of early endosomes. Curr Biol *8*, 881-884.

Mills, I.G., Jones, A.T., and Clague, M.J. (1999). Regulation of endosome fusion. Mol Membr Biol *16*, 73-79.

Mitra, S., Cheng, K.W., and Mills, G.B. (2011). Rab GTPases implicated in inherited and acquired disorders. Semin Cell Dev Biol *22*, 57-68.

Mohrmann, K., and van der Sluijs, P. (1999). Regulation of membrane transport through the endocytic pathway by rabGTPases. Mol Membr Biol *16*, 81-87.

Mukherjee, S., Ghosh, R.N., and Maxfield, F.R. (1997). Endocytosis. Physiol Rev *77*, 759-803.

Neuwald, A.F. (2009). The glycine brace: a component of Rab, Rho, and Ran GTPases associated with hinge regions of guanine- and phosphate-binding loops. BMC Struct Biol *9*, 11.

Ng, S.Y., Chaban, B., and Jarrell, K.F. (2006). Archaeal flagella, bacterial flagella and type IV pili: a comparison of genes and posttranslational modifications. J Mol Microbiol Biotechnol *11*, 167-191.

Nuoffer, C., and Balch, W.E. (1994). GTPases: multifunctional molecular switches regulating vesicular traffic. Annu Rev Biochem *63*, 949-990.

Odai, H., Sasaki, K., Iwamatsu, A., Hanazono, Y., Tanaka, T., Mitani, K., Yazaki, Y., and Hirai, H. (1995). The proto-oncogene product c-Cbl becomes tyrosine phosphorylated by stimulation with GM-CSF or Epo and constitutively binds to the SH3 domain of Grb2/Ash in human hematopoietic cells. J Biol Chem *270*, 10800-10805.

Ogiso, H., Ishitani, R., Nureki, O., Fukai, S., Yamanaka, M., Kim, J.H., Saito, K., Sakamoto, A., Inoue, M., Shirouzu, M., *et al.* (2002). Crystal structure of the complex of human epidermal growth factor and receptor extracellular domains. Cell *110*, 775-787.

Olsen, J.V., Blagoev, B., Gnad, F., Macek, B., Kumar, C., Mortensen, P., and Mann, M. (2006). Global, in vivo, and site-specific phosphorylation dynamics in signaling networks. Cell *127*, 635-648.

Pace, C.N., Vajdos, F., Fee, L., Grimsley, G., and Gray, T. (1995). How to measure and predict the molar absorption coefficient of a protein. Protein Sci *4*, 2411-2423.

Pan, J.Y., Sanford, J.C., and Wessling-Resnick, M. (1996). Influence of Mg2+ on the structure and function of Rab5. J Biol Chem *271*, 1322-1328.

Panayotou, G., Bax, B., Gout, I., Federwisch, M., Wroblowski, B., Dhand, R., Fry, M.J., Blundell, T.L., Wollmer, A., and Waterfield, M.D. (1992). Interaction of the p85 subunit of PI 3-kinase and its N-terminal SH2 domain with a PDGF receptor phosphorylation site: structural features and analysis of conformational changes. EMBO J *11*, 4261-4272.

Pawson, T., and Scott, J.D. (2005). Protein phosphorylation in signaling--50 years and counting. Trends Biochem Sci *30*, 286-290.

Pereira-Leal, J.B., and Seabra, M.C. (2000). The mammalian Rab family of small GTPases: definition of family and subfamily sequence motifs suggests a mechanism for functional specificity in the Ras superfamily. J Mol Biol *301*, 1077-1087.

Pfeffer, S., and Aivazian, D. (2004). Targeting Rab GTPases to distinct membrane compartments. Nat Rev Mol Cell Biol *5*, 886-896.

Phizicky, E.M., and Fields, S. (1995). Protein-protein interactions: methods for detection and analysis. Microbiol Rev *59*, 94-123.

Piccione, E., Case, R.D., Domchek, S.M., Hu, P., Chaudhuri, M., Backer, J.M., Schlessinger, J., and Shoelson, S.E. (1993). Phosphatidylinositol 3'-kinase p85 SH2 domain specificity defined by direct phosphopeptide/SH2 domain binding. Biochemistry *32*, 3197-3202.

Pleiman, C.M., Hertz, W.M., and Cambier, J.C. (1994). Activation of phosphatidylinositol-3' kinase by Src-family kinase SH3 binding to the p85 subunit. Science *263*, 1609-1612.

Pylypenko, O., Rak, A., Durek, T., Kushnir, S., Dursina, B.E., Thomae, N.H., Constantinescu, A.T., Brunsveld, L., Watzke, A., Waldmann, H., *et al.* (2006). Structure of doubly prenylated Ypt1:GDI complex and the mechanism of GDI-mediated Rab recycling. EMBO J *25*, 13-23.

Reyes, P. (1972). PEI-cellulose thin-layer chromatography: a highly versatile system for separating purine and pyrimidine nucleotides from nucleosides and free bases. Anal Biochem *50*, 35-39.

Robinson, D.R., Wu, Y.M., and Lin, S.F. (2000). The protein tyrosine kinase family of the human genome. Oncogene *19*, 5548-5557.

Roos, H., Karlsson, R., Nilshans, H., and Persson, A. (1998). Thermodynamic analysis of protein interactions with biosensor technology. J Mol Recognit *11*, 204-210.

Rosenfeld, M.E., Bowen-Pope, D.F., and Ross, R. (1984). Platelet-derived growth factor: morphologic and biochemical studies of binding, internalization, and degradation. J Cell Physiol *121*, 263-274.

Rossman, K.L., Der, C.J., and Sondek, J. (2005). GEF means go: turning on RHO GTPases with guanine nucleotide-exchange factors. Nat Rev Mol Cell Biol *6*, 167-180.

Rubino, M., Miaczynska, M., Lippe, R., and Zerial, M. (2000). Selective membrane recruitment of EEA1 suggests a role in directional transport of clathrin-coated vesicles to early endosomes. J Biol Chem *275*, 3745-3748.

Scheffzek, K., Ahmadian, M.R., Kabsch, W., Wiesmuller, L., Lautwein, A., Schmitz, F., and Wittinghofer, A. (1997). The Ras-RasGAP complex: structural basis for GTPase activation and its loss in oncogenic Ras mutants. Science *277*, 333-338.

Scheffzek, K., Ahmadian, M.R., and Wittinghofer, A. (1998). GTPase-activating proteins: helping hands to complement an active site. Trends Biochem Sci *23*, 257-262.

Schlessinger, J. (2000). Cell signaling by receptor tyrosine kinases. Cell *103*, 211-225.

Schu, P.V., Takegawa, K., Fry, M.J., Stack, J.H., Waterfield, M.D., and Emr, S.D. (1993). Phosphatidylinositol 3'-kinase encoded by yeast VPS34 gene essential for protein sorting. Science *260*, 88-91.

Schuller, H.M. (1991). The signal transduction model of carcinogenesis. Biochem Pharmacol *42*, 1511-1523.

Seabra, M.C., and Wasmeier, C. (2004). Controlling the location and activation of Rab GTPases. Curr Opin Cell Biol *16*, 451-457.

Selyunin, A.S., Sutton, S.E., Weigele, B.A., Reddick, L.E., Orchard, R.C., Bresson, S.M., Tomchick, D.R., and Alto, N.M. (2011). The assembly of a GTPase-kinase signalling complex by a bacterial catalytic scaffold. Nature *469*, 107-111.

Shaw, R.K., Smollett, K., Cleary, J., Garmendia, J., Straatman-Iwanowska, A., Frankel, G., and Knutton, S. (2005). Enteropathogenic Escherichia coli type III effectors EspG and EspG2 disrupt the microtubule network of intestinal epithelial cells. Infect Immun *73*, 4385-4390.

Shin, H.W., Hayashi, M., Christoforidis, S., Lacas-Gervais, S., Hoepfner, S., Wenk, M.R., Modregger, J., Uttenweiler-Joseph, S., Wilm, M., Nystuen, A., *et al.* (2005). An enzymatic cascade of Rab5 effectors regulates phosphoinositide turnover in the endocytic pathway. J Cell Biol *170*, 607-618.

Shoelson, S.E., Sivaraja, M., Williams, K.P., Hu, P., Schlessinger, J., and Weiss, M.A. (1993). Specific phosphopeptide binding regulates a conformational change in the PI 3-kinase SH2 domain associated with enzyme activation. EMBO J *12*, 795-802.

Simon, I., Zerial, M., and Goody, R.S. (1996). Kinetics of interaction of Rab5 and Rab7 with nucleotides and magnesium ions. J Biol Chem *271*, 20470-20478.

Simonsen, A., Lippe, R., Christoforidis, S., Gaullier, J.M., Brech, A., Callaghan, J., Toh, B.H., Murphy, C., Zerial, M., and Stenmark, H. (1998). EEA1 links PI(3)K function to Rab5 regulation of endosome fusion. Nature *394*, 494-498.

Somsel Rodman, J., and Wandinger-Ness, A. (2000). Rab GTPases coordinate endocytosis. J Cell Sci *113 Pt 2*, 183-192.

Sorkin, A., and von Zastrow, M. (2009). Endocytosis and signalling: intertwining molecular networks. Nat Rev Mol Cell Biol *10*, 609-622.

Stenmark, H. (2009). Rab GTPases as coordinators of vesicle traffic. Nat Rev Mol Cell Biol *10*, 513-525.

Stenmark, H., and Olkkonen, V.M. (2001). The Rab GTPase family. Genome Biol *2*, REVIEWS3007.

Strom, M., Vollmer, P., Tan, T.J., and Gallwitz, D. (1993). A yeast GTPase-activating protein that interacts specifically with a member of the Ypt/Rab family. Nature *361*, 736-739.

Tall, G.G., Barbieri, M.A., Stahl, P.D., and Horazdovsky, B.F. (2001). Ras-activated endocytosis is mediated by the Rab5 guanine nucleotide exchange activity of RIN1. Dev Cell *1*, 73-82.

Tao, H., Liu, W., Simmons, B.N., Harris, H.K., Cox, T.C., and Massiah, M.A. (2010). Purifying natively folded proteins from inclusion bodies using sarkosyl, Triton X-100, and CHAPS. Biotechniques *48*, 61-64.

Tataurov, A.V., You, Y., and Owczarzy, R. (2008). Predicting ultraviolet spectrum of single stranded and double stranded deoxyribonucleic acids. Biophys Chem *133*, 66-70.

Terzyan, S., Zhu, G., Li, G., and Zhang, X.C. (2004). Refinement of the structure of human Rab5a GTPase domain at 1.05 A resolution. Acta Crystallogr D Biol Crystallogr *60*, 54-60.

Touchot, N., Chardin, P., and Tavitian, A. (1987). Four additional members of the ras gene superfamily isolated by an oligonucleotide strategy: molecular cloning of YPT-related cDNAs from a rat brain library. Proc Natl Acad Sci USA *84*, 8210-8214.

Ueki, K., Fruman, D.A., Brachmann, S.M., Tseng, Y.H., Cantley, L.C., and Kahn, C.R. (2002). Molecular balance between the regulatory and catalytic subunits of phosphoinositide 3-kinase regulates cell signaling and survival. Mol Cell Biol *22*, 965-977.

Ullrich, O., Horiuchi, H., Bucci, C., and Zerial, M. (1994). Membrane association of Rab5 mediated by GDP-dissociation inhibitor and accompanied by GDP/GTP exchange. Nature *368*, 157-160.

Vanhaesebroeck, B., and Waterfield, M.D. (1999). Signaling by distinct classes of phosphoinositide 3-kinases. Exp Cell Res *253*, 239-254.

Vetter, I.R., and Wittinghofer, A. (2001). The guanine nucleotide-binding switch in three dimensions. Science *294*, 1299-1304.

Volinia, S., Dhand, R., Vanhaesebroeck, B., MacDougall, L.K., Stein, R., Zvelebil, M.J., Domin, J., Panaretou, C., and Waterfield, M.D. (1995). A human phosphatidylinositol 3'-kinase complex related to the yeast Vps34p-Vps15p protein sorting system. EMBO J *14*, 3339-3348.

Wetlaufer, D.B., Edsall, J.T., and Hollingworth, B.R. (1958). Ultraviolet difference spectra of tyrosine groups in proteins and amino acids. J Biol Chem *233*, 1421-1428.

Wout, P., Pu, K., Sullivan, S.M., Reese, V., Zhou, S., Lin, B., and Maddock, J.R. (2004). The Escherichia coli GTPase CgtAE cofractionates with the 50S ribosomal subunit and interacts with SpoT, a ppGpp synthetase/hydrolase. J Bacteriol *186*, 5249-5257.

Yang, X.J., and Seto, E. (2008). Lysine acetylation: codified crosstalk with other posttranslational modifications. Mol Cell *31*, 449-461.

Yu, J., Wjasow, C., and Backer, J.M. (1998). Regulation of the p85/p110alpha phosphatidylinositol 3'-kinase. Distinct roles for the n-terminal and c-terminal SH2 domains. J Biol Chem *273*, 30199-30203.

Zhao, L., and Vogt, P.K. (2008). Helical domain and kinase domain mutations in p110alpha of phosphatidylinositol 3-kinase induce gain of function by different mechanisms. Proc Natl Acad Sci U S A *105*, 2652-2657.

Zheng, Y., Bagrodia, S., and Cerione, R.A. (1994). Activation of phosphoinositide 3-kinase activity by Cdc42Hs binding to p85. J Biol Chem *269*, 18727-18730.

Zhou, H.X., Rivas, G., and Minton, A.P. (2008). Macromolecular crowding and confinement: biochemical, biophysical, and potential physiological consequences. Annu Rev Biophys *37*, 375-397.

Zhu, G., Liu, J., Terzyan, S., Zhai, P., Li, G., and Zhang, X.C. (2003). High resolution crystal structures of human Rab5a and five mutants with substitutions in the catalytically important phosphate-binding loop. J Biol Chem *278*, 2452-2460.

Zwick, E., Bange, J., and Ullrich, A. (2001). Receptor tyrosine kinase signalling as a target for cancer intervention strategies. Endocr Relat Cancer *8*, 161-173.